SANDIA REPORT

SAND2014-3341
Unlimited Release
Printed April 2014

Relationship between Metrics Used to Represent Displacement Damage in Materials

Patrick J. Griffin

Prepared by
Sandia National Laboratories
Albuquerque, New Mexico 87185 and Livermore, California 94550

Sandia National Laboratories is a multi-program laboratory managed and operated by Sandia Corporation, a wholly owned subsidiary of Lockheed Martin Corporation, for the U.S. Department of Energy's National Nuclear Security Administration under contract DE-AC04-94AL85000.

Issued by Sandia National Laboratories, operated for the United States Department of Energy by Sandia Corporation.

Available to DOE and DOE contractors from
U.S. Department of Energy
Office of Scientific and Technical Information
P.O. Box 62
Oak Ridge, TN 37831

Telephone: (865) 576-8401
Facsimile: (865) 576-5728
E-Mail: reports@adonis.osti.gov
Online ordering: http://www.osti.gov/bridge

Available to the public from
U.S. Department of Commerce
National Technical Information Service
5285 Port Royal Rd.
Springfield, VA 22161

Telephone: (800) 553-6847
Facsimile: (703) 605-6900
E-Mail: orders@ntis.fedworld.gov
Online order: http://www.ntis.gov/help/ordermethods.asp?loc=7-4-0#online

SAND2014-3341
Printed April 2014

Relationship between Metrics Used to Represent Displacement Damage in Materials

Patrick J. Griffin
Radiation Effects Sciences & Applications Department

Sandia National Laboratories
P.O. Box 5800
Albuquerque, New Mexico 87185-MS1146

Abstract

This report provides a set of consistent definitions for metrics relevant to the modeling of displacement damage in materials. The limitations/approximations built into the various metrics are discussed as is the intended application that gave rise to community use of the metric. Recommended sources for numerical tabulations of the neutron displacement kerma and the charged particle non-ionizing energy loss in some important semiconductor materials are also provided.

ACKNOWLEDGMENTS

The author wishes to express his appreciation to the reviewers of this document. Their input has helped ensure that the accuracy and completeness of this material. In particular, Emeritus Professor John Williams, University of Arizona, provided many helpful comments that permitted me to improve this presentation and clarify the relationship of terms used with those found in other community standards. Excellent constructive review comments were also received from Dr. Craig Heimbach (NIST, retired), Dr. Doug Selby (ORNL), and Dr. K. Russell DePriest (SNL).

CONTENTS

FIGURES

TABLES

NOMENCLATURE

ACRR	Annular Core Research Reactor
arc	athermal recombination-corrected
BCA	binary collision approximation
cema	Converted Energy per unit Mass
CPE	charged particle equilibrium
CSDA	continuous slowing down approximation
CSEWG	Cross Section Evaluation Working Group
DFT	density functional theory
ENDF	Evaluated Nuclear Data File
GGA	generalized gradient approximation
HF	Hartree-Fock
ICRU	International Commission on Radiation Units
IV	interstitial-vacancy
kerma	Kinetic Energy Released per unit MAss
KP	Kinchin-Pease
LDA	local density approximation
LET	linear energy transfer
LSS	Lindhard, Scharff, Schiott
MCNP	Monte Carlo N-Particle
MD	molecular dynamics
NIEL	non-ionizing energy loss
NRT	Norgett-Robinson-Torrens
PKA	primary knock-on atom
rpa	replacement per atom
SIA	self-interstitial atom
terma	total energy released per unit mass
ZBL	Zeigler, Biersack, Littmark

1. PURPOSE

The radiation effects community has long used a quantity called displacement kerma [Ro71, Ro68] as a metric to characterize neutron damage in electronics that is produced by effects that are proportional to the introduction of defects in the lattice of crystalline materials. The term displacement dose has also been used [A170, He93]. In more recent times the radiation effects community has been concerned about relating displacement damage induced by neutrons to that induced by charged particles, typically heavy ions [A521]. The metric used to correlate the damage has been the non-ionizing energy loss (NIEL) [Ak01, Ak06, Bo09, Xap, Me01, Me03, Ju04]. The purpose of this document is to clarify the definitions for these various terms and to provide reference sources for baseline data that can be used to characterize the displacement damage from neutrons, protons, alpha particles, and primary knock-on atoms (PKA) in materials. Particular attention is given to damage in silicon (Si) and gallium arsenide (GaAs), two materials of significant interest to the modern semiconductor community.

2. DEFINITIONS

We start out by establishing the definitions for some basic quantities. We look to international standards, such as the ICRU [ICRU60, ICRU85], to support the establishment of clear and accepted definitions for some basic quantities that will underpin our later discussion (Section 4) of displacement kerma and NIEL.

2.1 Particle Number

Particle number, *N*, is the number of the particles that are emitted, transferred or received.

Unit: 1

See ICRU 60, Section 2.1.1.
See ICRU 85, Section 3.1.1.

The particle number, *N*, represents an integral/sum over particles of various energies. d*N* is defined as the number of particles of energy between E and E+dE.

The distribution, N_E, of the particle with respect to energy is given by:

$$N_E = dN/dE \qquad \text{Eqn. 1}$$

Since the particle distribution, N_E, has an energy dependence for the particles, this dependence is sometimes made explicit by using the notation N_E(E).

Many in the nuclear physics community use the notation $n(E)$ for the energy-dependent particle number distribution rather than N_E. This notation, however, is not what is used in ICRU 85.

2.2 Radiant Energy

Radiant energy, R, is the energy, excluding rest energy, of the particles that are emitted, transferred or received.

Unit: J

See ICRU 60, Section 2.1.1.
See ICRU 85, Section 3.1.1.

The distribution, R_E, of the radiant energy with respect to energy is given by:

$$R_E = dR/dE \qquad \text{Eqn. 2}$$

The distributions, with respect to energy, of the particle number and the radiant energy are related as:

$$R_E = E \cdot N_E \qquad \text{Eqn. 3}$$

2.3 Fluence

Fluence, Φ, is the quotient of dN by d*a*, where dN is the number of particles incident on a sphere of cross-sectional area d*a*, thus:

$$\Phi = {dN}/{da} \qquad \text{Eqn. 4}$$

Unit: m^{-2}

See ICRU 60, Section 2.1.3.
See ICRU 85, Section 3.1.3.

The fluence, Φ, represents an integral/sum over particles of various energies. dΦ is defined as the fluence of particles of energy between E and E+dE.

2.3.1 Fluence Distribution

The distribution, Φ_E, of the fluence with respect to energy is given by:

$$\Phi_E = {d\Phi}/{dE} \qquad \text{Eqn. 5}$$

where dΦ is the fluence of particles with energy between E and E+dE.

See ICRU 60, Section 2.1.3.
See ICRU 85, Section 3.1.3.

Since the fluence distribution, Φ_E, has an energy dependence for the particles, this dependence is sometimes made explicit by using the notation $\Phi_E(E)$.

Many in the nuclear physics community use the notation φ(*E)* for the energy-dependent derivative of the fluence rather than Φ_E. This notation, however, is not what is used in ICRU 85.

2.4 Energy Fluence

Energy fluence, ψ, is the quotient of dR by d*a*, where dR is the radiant energy incident on a sphere of cross-sectional area d*a*, thus:

$$\psi = dR / da \qquad \text{Eqn. 6}$$

Unit: J m^{-2}

See ICRU 60, Section 2.1.3.
See ICRU 85, Section 3.1.3.

The energy fluence, ψ, represents an integral/sum over particles of various energies.

2.4.1 Energy Fluence Distribution

The distribution, ψ_E, of the energy fluence with respect to energy is given by:

$$\psi_E = d\psi / dE \qquad \text{Eqn. 7}$$

where dψ is the energy fluence of particles with energy between E and E+dE.

See ICRU 60, Section 2.1.3.
See ICRU 85, Section 3.1.3.

Since the fluence distribution, ψ_E, has an energy dependence for the particles, this dependence is sometimes made explicit by using the notation $\psi_E(E)$.

Note that the fluence distribution and the energy fluence distribution are related as:

$$\psi_E = E \cdot \Phi_E \qquad \text{Eqn. 8}$$

2.5 Fluence Rate

Fluence rate, $\dot{\Phi}$, is the quotient of dΦ by d*t*, where dΦ is the increment of the fluence in the time interval d*t*, thus:

$$\dot{\Phi} = d\Phi / dt \qquad \text{Eqn. 9}$$

Unit: m^{-2} s^{-1}

See ICRU 60, Section 2.1.4.
See ICRU 85, Section 3.1.4.

Since the fluence rate, $\dot{\Phi}$, has an energy dependence for the particles, this dependence is sometimes made explicit by using the notation , $\dot{\Phi}(E)$.

In some communities the term "flux" has been applied to this quantity of fluence rate, however the ICRU defines flux in a different manner. Section 2.1.2 of the ICRU document states that "this usage is discouraged because of the possible confusion with the … definition of flux" that is endorsed by the ICRU.

2.6 Cross Section

Cross section of a target entity and for a particular interaction (or any explicitly defined set of interactions) produced by an incident charged or uncharged particle) is the quotient of P by Φ where P is the probability of interactions for a single target entity when subjected to the particle fluence, Φ, thus

$$\sigma = P \big/ \Phi \qquad \text{Eqn. 10}$$

Unit: m^2

See ICRU 60, Section 3.1.
See ICRU 85, Section 4.1.

Since the cross section, σ, has an energy dependence for the particles, this dependence is sometimes made explicit by using the notation $\sigma(E)$.

2.6.1 Microscopic Cross Section

Microscopic cross section is another term for the cross section, σ, but it is typically quoted in units of a barn, where 1 barn = 10^{-24} cm^2 = 10^{-28} m^2. The symbol "b" can be used as an abbreviation for the unit barn.

Unit: barn

2.6.2 Macroscopic Cross Section

Macroscopic cross section is the microscopic cross section multiplied by the target particle number density, N_o, thus:

$$\Sigma = N_o \cdot \sigma \qquad \text{Eqn. 11}$$

Unit: cm^{-1}

N_o has units of $volume^{-1}$.

When a material is composed of more than one element/isotope, the macroscopic cross section is expressed as:

$$\Sigma = \sum_i N_i \cdot \sigma_i \qquad \text{Eqn. 12}$$

where the summation index "i" is over the isotopes in the material composition and N_i represents the number density of that isotope in units of nuclei per volume.

2.7 Stopping Power

2.7.1 Mass Stopping Power

Mass stopping power, S/ρ, (of a material and for charged particles of a given type and energy) is the quotient of dE by ρd*l* where dE is the energy lost by a charged particle in traversing a distance d*l* in the material of density ρ, thus:

$$S/\rho = 1/\rho \cdot dE/dl \qquad \text{Eqn. 13}$$

Unit: J m^2 kg^{-1}

See ICRU 60, section 3.4.
See ICRU 85, section 4.4.

The mass stopping power can be expressed as the sum of the following components:

- Mass electronic (or collisional) stopping power due to collisions with electrons, $(S/\rho)_{el}$.
- Mass radiative stopping power due to emission of bremsstrahlung in the electric field of atomic nuclei or atomic electrons, $(S/\rho)_{rad}$.
- Mass nuclear stopping power due to elastic Coulomb collisions in which recoil is imparted to atoms, $(S/\rho)_{nuc}$. Note that this term "mass nuclear stopping power" can be confusing since it does not refer to nuclear interactions. In fact, ICRU 60 refers to the use of the term "nuclear" in this context as a "misnomer".
  It is important that a user understands that "true" nuclear interactions are not included in this stopping power term. This means that explicit actions must be taken, when necessary, to address secondary particles that are generated by "true" nuclear processes. This is discussed later in Section 5 for the WinNIEL treatment of energy deposition from high energy ions.

The separate mass stopping power components can be expressed in terms of a cross section, for example, the mass electronic stopping power for an atom can be expressed as:

$$\left(S/\rho\right)_{el} = \frac{N_A}{M} \cdot Z \int \varepsilon \cdot \frac{d\sigma}{d\varepsilon} d\varepsilon \qquad \text{Eqn. 14}$$

where N_A is the Avogadro constant, $6.02214129 \times 10^{23}$ mol^{-1}; M the molar mass of the atom; Z the atomic number of the atom; $d\sigma/d\varepsilon$ the differential cross section (per unit atomic electron) for interactions; and ε is the energy loss.

In application to radiation damage in materials, the mass stopping power is often used with units of $keV \cdot cm^2/mg$.

Figure 1 shows the energy-dependence of the range of different ions in silicon. Figure 2 shows the electronic stopping power for protons and Si ions in silicon. The proton stopping power in this figure is given in units of 10^{-15} $eV \cdot cm/atom$, which is equivalent to 0.02144 $MeV \cdot cm^2/mg$. The left-hand portion of the figure shows a peak proton stopping power of ~0.536 $MeV \cdot cm^2/mg$ at ~ 100 keV. The Si ion range is given in units of $MeV \cdot cm^2/mg$. The right-hand portion of the figure shows a peak silicon ion stopping power in elemental silicon of ~14 $MeV \cdot cm^2/mg$ at ~1-MeV/nucleon. Figure 3 shows the relative magnitudes of the electronic and nuclear stopping power for protons and Si ions in a silicon lattice. For protons, the electronic stopping power always dominates. For incident Si ions in a silicon lattice, the nuclear stopping power dominates for low ion energies. Note that the stopping power is a metric for the energy loss at a particular ion energy and is not an integral metric over the complete ion track as the silicon ion slows down in a material. The partition of the stopping power into its electronic and nuclear/collisional terms should not be confused with the LSS energy partition (to be discussed later in Section 3.7.1) which is a metric that applies to the division between electronic and nuclear/collisional losses as integrated over a complete ion track and any evolved cascade of secondary ions that may be displaced from the lattice.

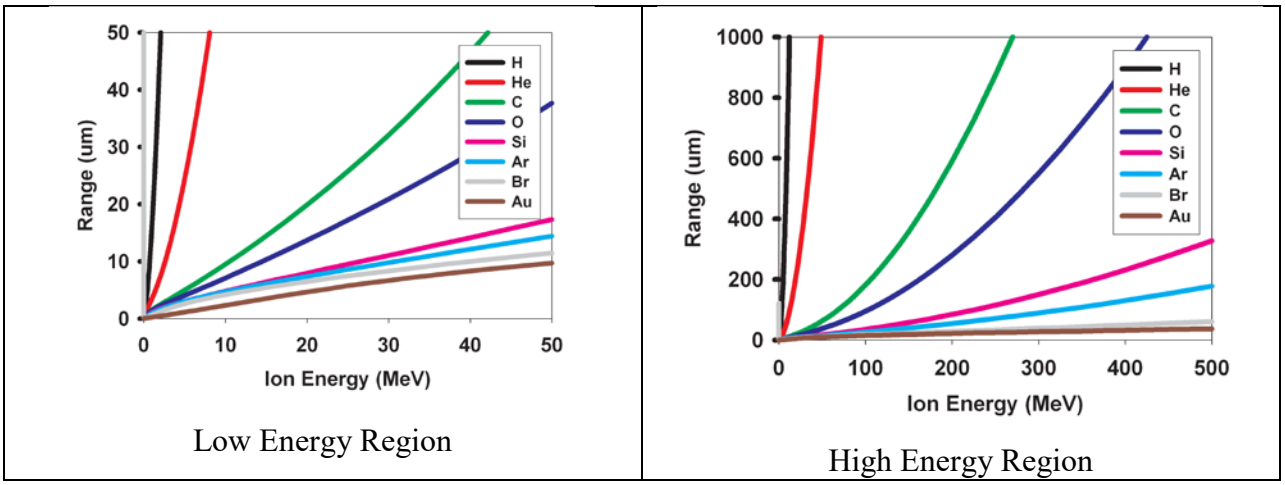

Figure 1: Range of Ions in Silicon

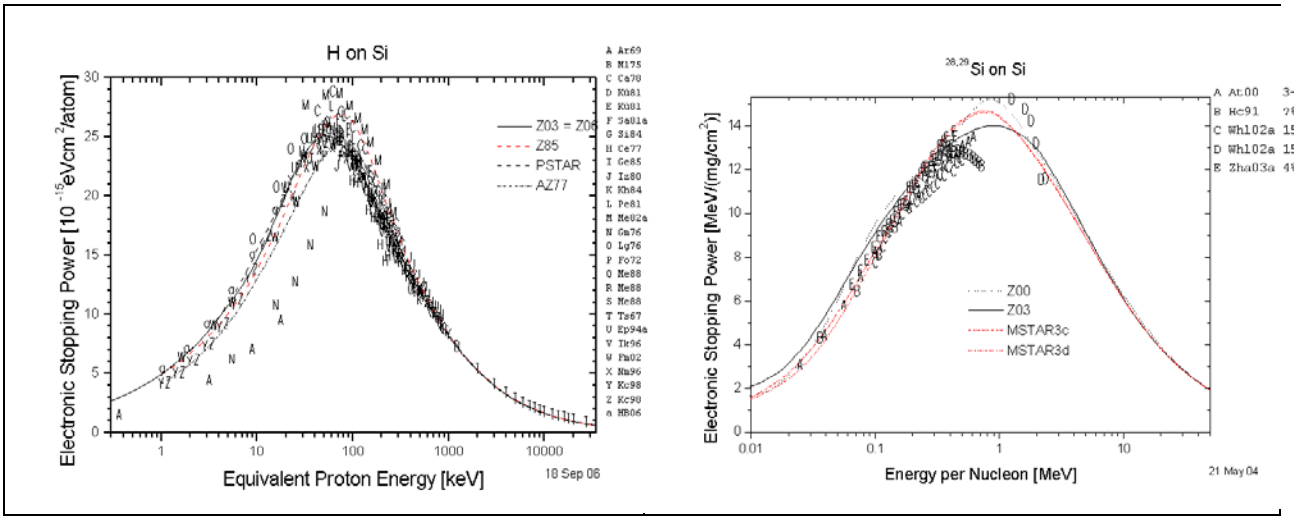

Figure 2: Energy-dependent Stopping Power in Silicon

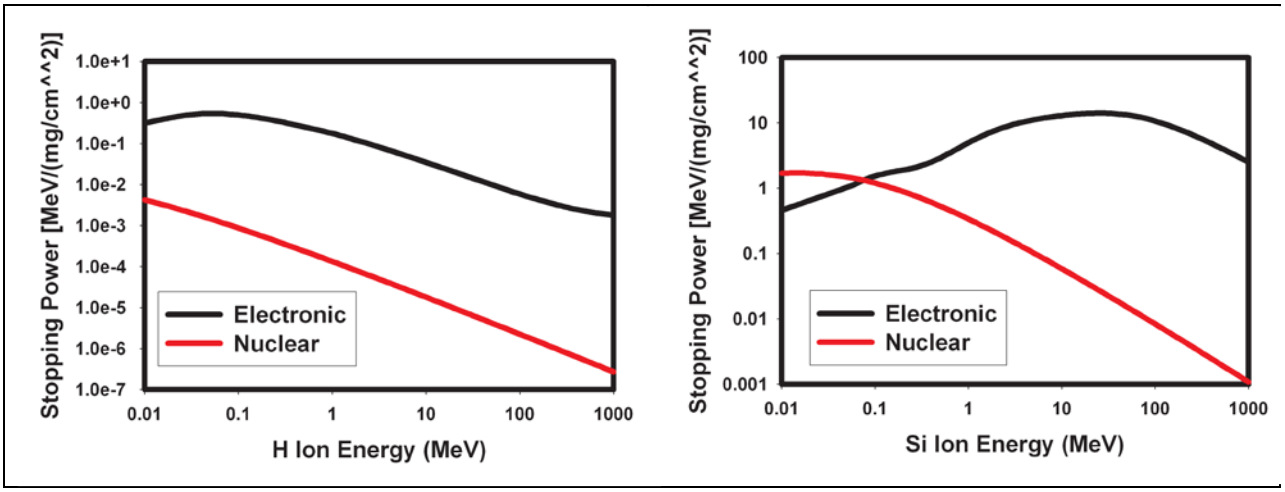

Figure 3: Comparison of Electronic and Nuclear Stopping Power in Silicon

2.7.2 Linear Stopping Power

Linear stopping power, S, (of a material and for charged particles) is the quotient of the material density and the mass stopping power, thus:

$$S = dE/dl \qquad \text{Eqn. 15}$$

Unit: J m^{-1}

As with the mass stopping power, this term can be divided into three components, electronic, radiative, and nuclear, which are notated as S_{el}, S_{rad}, and S_{nuc}.

Note, the symbol for the linear stopping power is S, not L. L is used below to refer to the linear energy transfer, which is addressed in Section 2.8.

2.8 Linear Energy Transfer (LET)

Linear energy transfer, or restricted linear electronic stopping power, L_Δ, (of a material and for charged particles of a given type and energy) is the quotient of dE_Δ by dl, where dE_Δ is the mean energy lost by a charged particle due to electronic collisions in traversing a distance dl, minus the mean sum of the kinetic energies of all the electrons released with kinetic energies in excess of Δ, thus:

$$L_\Delta = dE_\Delta/dl \qquad \text{Eqn. 16}$$

Unit: J m^{-1}

See ICRU 60, section 3.5.
See ICRU 85, section 4.5.

Note that the linear energy transfer only considers the energy loss from electronic collisions. Thus L_∞ is equal to S_{el}. The term L_∞ is often notated as L and is termed the unrestricted linear energy transfer.

The linear energy transfer can also be expressed as:

$$L_\Delta = S_{el} - dE_{ke,\Delta}/dl \qquad \text{Eqn. 17}$$

where $dE_{ke,\Delta}$ refers to the sum of the kinetic energies of all the electrons released with kinetic energies in excess of Δ.

Figure 4 shows the unrestricted LET for some typical ions in silicon.

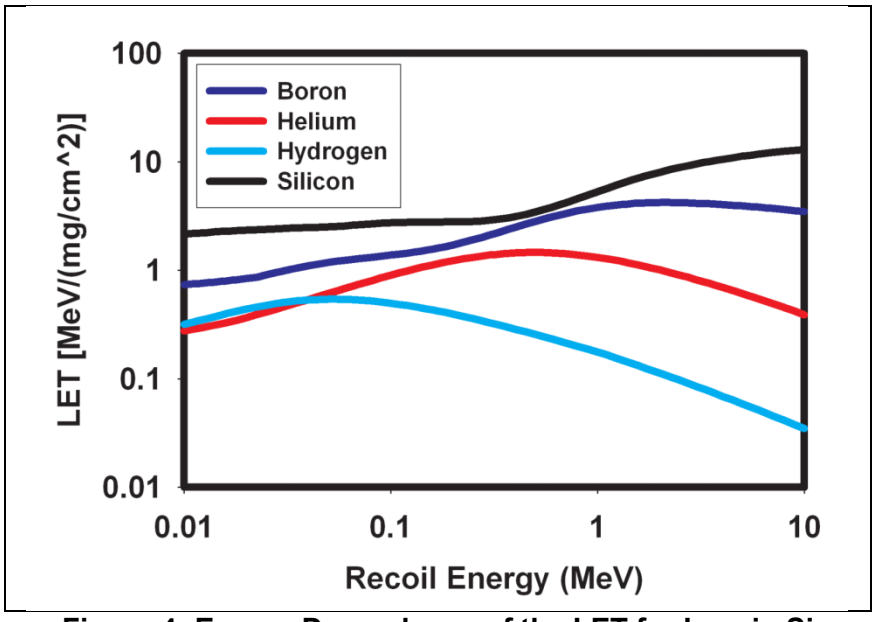

Figure 4: Energy Dependence of the LET for Ions in Si

2.9 Mass Energy Transfer Coefficient

Mass energy transfer coefficient, μ_{tr}/ρ, (for uncharged particles of a given type and energy) is the quotient of $\{dR_{tr} / R\}$ by ρdl, where dR_{tr} is the mean energy that is transferred to kinetic energy of charged particles by interactions of the uncharged particles of incident radiant energy, R, in traversing a distance dl in a material of density ρ:

$$\frac{\mu_{tr}}{\rho} = \frac{1}{\rho \cdot dl}\frac{dR_{tr}}{R} \qquad \text{Eqn. 18}$$

The binding energies of the liberated charged particles are not included in dR_{tr}.

Unit: J kg^{-1}

See ICRU 85, section 4.3.
See ICRU 60, section 3.3.

2.10 Mass Energy Absorption Coefficient

Mass energy absorption coefficient, μ_{en}/ρ, (for uncharged particles of a given type and energy) is the product of μ_{tr}/ρ and (1-g), where g is the fraction of kinetic energy transferred to charged particles that is subsequently lost, on average, in radiative processes (bremsstrahlung, in-flight annihilation, and fluorescence radiations) as the charged particles slow to rest in the material. Thus:

$$\frac{\mu_{en}}{\rho} = \frac{\mu_{tr}}{\rho} \cdot (1 - g) \qquad \text{Eqn. 19}$$

2.11 Kerma

Kerma, K, (for ionizing uncharged particles) is the quotient of dE_{tr} by dm, where dE_{tr} is the mean sum of the initial kinetic energies of all charged particles liberated in a mass dm of a material by the uncharged particle incident on a mass dm of a material, thus:

$$K = dE_{tr} \Big/ dm \qquad \text{Eqn. 20}$$

The term dE_{tr} includes the kinetic energy of the charged particles emitted in the decay of excited atoms/molecules or in nuclear de-excitation or disintegrations.

Unit: J kg^{-1}
The special name of the unit of kerma is gray (Gy).

See ICRU 85, section 5.1.1.
See ICRU 60, section 4.1.1.

Kerma is an acronym for "kinetic energy released per unit mass".

For a fluence, Φ, of uncharged particles of energy E, the kerma, K, in a specific material is given by:

$$K = \Phi \cdot E \cdot \frac{\mu_{tr}}{\rho} \qquad \text{Eqn. 21}$$

The kerma per fluence, K/Φ, is termed the kerma coefficient for uncharged particles of energy E in a specified material.

In dosimetry applications, the kerma, K, is often expressed in terms of the distribution, Φ_E, of the uncharged particle fluence with respect to energy. Thus:

$$K = \int \Phi_E(E) \cdot E \cdot \frac{\mu_{tr}}{\rho} dE \qquad \text{Eqn. 22}$$

There are some apparent ambiguities in the above Equations 21 and 22 in that:

- it uses μ_{tr} rather than μ_{en}, i.e. energy transfer rather than energy absorption, thus it includes the energy radiated as uncharged particles from charged particle emission, e.g. bremsstrahlung from liberated electrons (see Equation 19),
- yet the definition addresses energy liberated as a sum "over all charged particles" emitted, and hence does not include photons emitted directly from primary neutron interactions;

and

- it includes kinetic energy of secondary charged particle emission from the decay of excited atoms,

- yet the definition addresses only including the sum of "initial" kinetic energies from all charged particles.

While the above facts can be properly taken into account in calculating the kerma, one has to be very careful to reconcile the definitions for terms.

Although kerma is a quantity that addresses the initial transfer of energy to matter, it is sometimes used as an approximation to absorbed dose. The numerical value of the kerma approaches the absorbed dose to the degree that 1) charged particle equilibrium exists; 2) radiative losses are negligible; 3) and the kinetic energy of the uncharged particles is large compared with the binding energy of the liberated particles. When radiative losses are not negligible, a quantity termed the collision kerma is a good approximation to the absorbed dose. The definition of the collision kerma, K_{col}, is similar to that for kerma but has μ_{tr} replaced by μ_{en} in Equations 21 and 22.

2.12 Terma

Terma, *T*, (for ionizing uncharged particles) is the total energy released per unit mass. This quantity is defined in a manner similar to what is seen in the right-hand-side of Equations 21 and 22 except that μ_{tr} is replaced by μ. Terma includes energy loss that is either local or at a distance.

2.13 Cema

Cema, C, (for ionizing charged particles) is the quotient of dE_{el} by dm, where dE_{el} is the mean energy lost in electronic interactions in a mass dm of a material by charged particles, except secondary electrons, incident on dm, thus:

$$C = dE_{el} / dm \qquad \text{Eqn. 23}$$

Unit: J kg^{-1}
The special name of the unit of cema is gray (Gy).

See ICRU 85, section 5.1.5.
See ICRU 60, section 4.1.5.

Cema is a non-stochastic quantity. Cema applies to directly ionizing radiation, such as electrons and protons, while kerma applies to uncharged particles.

Cema is an acronym for "converted energy per unit mass".

Cema describes the energy transfer from primary charged particles to secondary charged particle, i.e. electrons.

For a distribution of charged particles, cema can be written as:

$$C = \int \Phi_E(E) \cdot \frac{S_{el}}{\rho} dE = \int \Phi_E(E) \cdot \frac{L_\infty}{\rho} dE \qquad \text{Eqn. 24}$$

Comparing Equations 22 and 24, one often hears that kerma and cema are parallel quantities, kerma applying to uncharged particles and cema applying to charged particles. There is a significant issue with the above definition, taken from the ICRU, when one tries to treat cema and kerma as "parallel quantities", one for charged particles and the other for uncharged particles. The issue is that the definition clearly states that cema only includes energy deposition from "electronic interactions". This is clearly seen in Equation 24 where only the electronic stopping power is used. In the case of kerma, energy deposition from non-electronic processes is included.

The literature often states that, as in the case of kerma, "cema is the same as dose when a condition of electron equilibrium exists." This is not correct if left only as stated in this previous sentence. What would be correct is to say that "cema is the same as ionizing dose when electron equilibrium exists." In the literature, some have neglected to properly distinguish between "total dose" and "ionizing dose". The need for this distinction is clear from the inclusion of only the electronic stopping power in Equation 24. The ICRU 85 correctly makes the statement that cema can be used as an approximation to absorbed dose from charged particles to the degree that 1) secondary charged particle equilibrium exists and 2) that radiative losses and those due to elastic nuclear interactions are negligible.

This document is attempting to address displacement damage metrics in a way that supports a comparison between damage resulting from neutrons and that from charged particles, especially protons and heavy ions [A521, A693]. In order to preserve a discussion in this document that can address cema and kerma as "parallel quantities" while not misusing community standard terms, and for the purposes only of facilitating a discussion within this document, we will define a new quantity, "augmented cema" which uses the same form as Equation 24 but uses the total stopping power, i.e. the sum of the electronic/collisional, "nuclear", and radiative stopping powers. The purpose of this definition is to include the energy deposited from the "nuclear" stopping power. Note that the radiative stopping power is also included here since it is include in the Equation 20 parallel definition of kerma. That is done despite the fact that the radiated bremsstrahlung energy does not represent liberated "charged particles", but comes from secondary emission from liberated electrons.

This "augmented cema" can then be partitioned into three types of "augmented cema" based on the partition of the implied stopping power: an "augmented electronic", "augmented nuclear" and "augmented radiative" cema. The "augmented electronic cema" is then identical to the ICRU-defined term cema. While defining new quantities is not a desirable approach, it will permit the discussion of damage metrics to proceed until a better path forward is found.

2.14 Absorbed Dose

Absorbed dose, D, is the quotient of dε by d*m*, where dε is the mean energy imparted by ionizing radiation to matter mass d*m*, thus:

$$D = d\varepsilon / dm \qquad \text{Eqn. 25}$$

Unit: J kg^{-1}
The special name of the unit of absorbed dose is gray (Gy).

See ICRU 85, section 5.2.5.
See ICRU 60, section 4.2.5.

The definition of absorbed dose makes no assumptions regarding the existence of electron or charged particle equilibrium.

2.15 Charged Particle Equilibrium

Charged particle equilibrium exists at a point if the distribution of the charged-particle radiance with respect to energy is constant within distances equal to the maximum charged particle range.

See ICRU 85, section 5.1.1.
See ICRU 60, section 4.1.1.

Charged particle equilibrium obviously implies a condition of electron equilibrium, since an electron is one type of charged particle.

While a condition of electron equilibrium does not, in principle, have to imply a condition of charged particle equilibrium for all ion species, since heavy (ion) charged particles are so strongly ionizing it is not easy to realize a state where electron equilibrium exists without also having equilibrium for the heavier charged particles.

3. TERMINOLOGY FOR MATERIAL DISPLACEMENT DAMAGE

While Section 2 addressed community-accepted definitions for dosimetry quantities, this section defines some commonly used damage metrics used in the radiation community when they address displacement damage in materials.

3.1 Displacements per Atom

Displacements per atom, dpa, is the mean number of times each atom of a solid is displaced from its lattice site during an exposure to displacing radiation.

See ASTM E170.

A related quantity is displacement dose.

3.2 Lattice Energy Transfer Cross Section

Lattice energy transfer cross section, $\sigma_{en}^{lattice}(E \to T)$, characterizes the energy imparted to the lattice by neutron-nucleus reactions [He93] and can be defined as:

$$\sigma_{en}^{lattice}(E \to T) = \sum_i \sigma_i(E) \cdot K_i^{recoil}(E \to T) \qquad \text{Eqn. 26}$$

where:

$\sigma_i(E)$ is the neutron energy-dependent cross section for the ith reaction channel;
$K_i^{recoil}(E \to T)$ is the probability density that a reacting neutron with energy E will produce a recoil of energy T in the laboratory system;
$\sigma_{en}^{lattice}(E \to T)$ is a microscopic differential cross section for a neutron with energy E producing a recoil ion with energy T.

Unit: m^2/J or b/eV

3.3 Displacement Dose

Displacements dose, D_d, is the quotient of $d\varepsilon_d$ by d*m*, where $d\varepsilon_d$ is the mean energy imparted by radiation to matter which produces displacements (that is, excluding the part that produces ionization and excitation of electrons) in a volume element d*m*, thus,

$$D_d = {d\varepsilon_d}/{dm} \qquad \text{Eqn. 27}$$

Unit: J kg^{-1}
The special name of the unit of dose is gray (Gy).

See ASTM E170. A related quantity is displacement per atom (dpa).

3.4 Damage Energy

The definition of damage energy, T_{dam}, is not entirely consistent throughout the range of applications. To clarify the issue, we distinguish two separate types of damage energy, one for neutrons and one for ions.

The complexity that requires the use of two terms is that the concept of damage energy only includes the energy imparted by a single neutron interaction (including neutron elastic scattering events), but it includes the energy imparted by a charged particle integrated over its complete slowing down process. There may be different ways to define this term without forcing the definition of the two separate quantities, such as by defining the energy deposition to take place within the "local" region, but it is felt that this two-term definition is clearer than other approaches.

When the symbol T_{dam} is used in this document, it is assumed that it can apply equally to either the neutron-induced damage energy, ${}^{n}T_{dam,}$ or the charged particle-induced damage energy, ${}^{ion}T_{dam}$. Thus the T_{dam} notation is used in conjunction with an energy argument that refers to the energy of either an incident neutron or charged particle.

3.4.1 Charged Particle Damage Energy

The damage energy for a charged particle, ${}^{ion}T_{dam}(T)$, is the total energy imparted to the lattice by an incident ion of energy T as it slows down in a lattice of infinite homogeneous extent. Note that the ion slowing down process involves many different ion-atom interactions and that the energy imparted to the lattice over this total slowing down process is summed over the infinite volume. When an ion-atom collision displaces a lattice atom, the subsequent energy imparted by this displaced lattice atom is also included in the sum.

The damage energy for a charged particle can be divided into two components, that due to the stopping or radiation of the principal ion, ${}^{ion}T_{dam}^{rad}(T)$, and that due to any subsequent transmutation and spallation reactions induced by the principal ion, ${}^{ion}T_{dam}^{trans}(T)$. Thus:

$$ {}^{ion}T_{dam}(T) = {}^{ion}T_{dam}^{rad}(T) + {}^{ion}T_{dam}^{trans}(T) \qquad \text{Eqn. 28} $$

The first term on the right-hand side of this expression relates back to the definition of the stopping power of an ion as presented in Section 2.7.1 which, by definition, includes only Coulombic interactions – even though it includes a term that has traditionally been referred to as a "nuclear stopping power" but actually refers to ion-lattice atom Coulombic interactions. The second term on the right-hand side of the expression above represents the true "nuclear" component. The WinNIEL code, discussed in Section 5.2, is one of the few codes that address the kinetic energy transfer (in the rest frame) from any actual ion-atom nuclear transmutation reaction, that is, ion-induced transmutation reactions and spallation reactions, and it addresses this term in the context of the non-ionizing energy loss (NIEL), as discussed in Section 4.4, rather than from the perspective of a damage energy.

Note that the ion damage energy is a good metric for the local energy deposition to the lattice only if there is a local equilibrium for the induced charged particles. It should be noted that, due to attenuation of the incident source particles, local charged particle equilibrium may not be attainable in a physically meaning scenario if the extent of the range of the induced charged particles is not small with respect to the mean free path for interactions of the source particle.

Figure 5, taken from Reference [La08], shows the displacement energy as a function of the incident ion energy for carbon ions in carbon; silicon ions in silicon; and germanium ions in germanium. The energy going into displacements first increases with increasing ion energy and then saturates. The saturation reflects the behavior of the stopping power and its partition between nuclear and ionization contributions as shown in Figures 2 and 3.

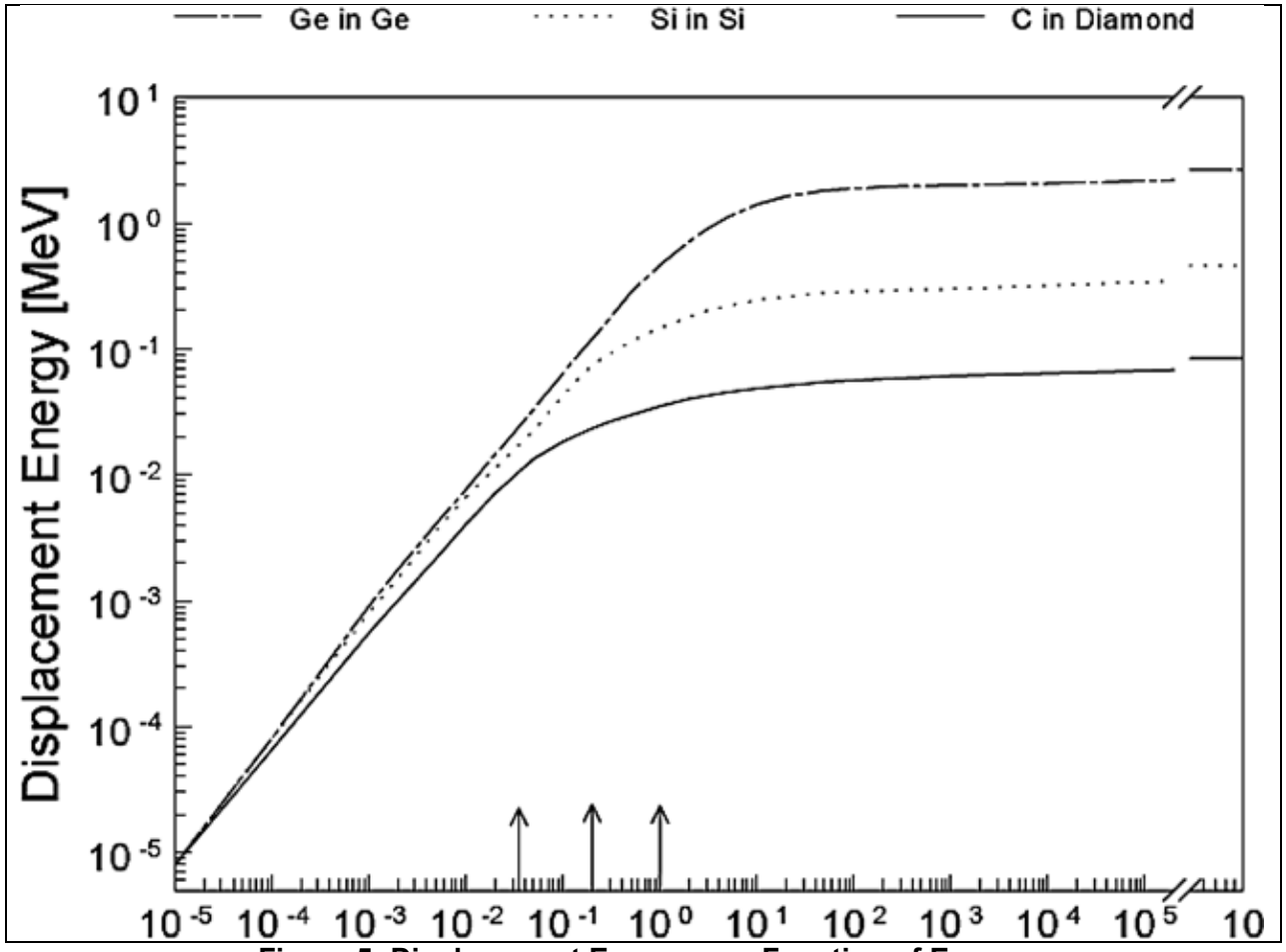

Figure 5: Displacement Energy as a Function of Energy

3.4.2 Neutron Damage Energy

The damage energy[1], ${}^{n}T_{dam}(E)$, is the total energy imparted to the lattice by an incident neutron of energy E in a single neutron-nucleus reaction, including the imparted energy to the lattice that comes from subsequent collisions by any of the secondary charged particles that are generated (but not including the effects from any secondary gammas emitted[2]). For small feature sizes, especially in semiconductors, the condition of local charged particle equilibrium may not exist even for neutron source particles due to differing neutron interaction probabilities with the variation of materials within the range of the secondary charged particles. While the ion damage energy, and by implication the neutron damage energy, is still a well-defined quantity in the absence of this local secondary charged particle equilibrium, this lack of correlation with the "local" energy imparted to the lattice may impact the correlation of some damage metrics with experimentally observed damage effects.

3.5 Neutron Damage Energy Cross Section

The neutron damage energy cross section[3], ${}^{n}\sigma_{dam}$, is the sum, over all open neutron-induced reaction channels indexed with the subscript "i", and all emitted particles within a channel "i" as indexed with the subscript "j_i", of the cross section for that channel multiplied by the energy transfer distribution for that channel and the damage energy for the resulting charged particles and can be written as:

$$ {}^{n}\sigma_{dam}(E) = \sum_{i,j_i} \int \sigma_{i,j_i}(E) \cdot K_{i,j_i}^{recoil}\left(E \rightarrow T_{j_i}\right) \cdot {}^{ion}T_{dam}(T_{j_i}) \cdot dT_{j_i} \qquad \text{Eqn. 29} $$

and

$$ {}^{n}T_{dam}(E) = \frac{{}^{n}\sigma_{dam}(E)}{\sigma(E)} \qquad \text{Eqn. 30} $$

where σ(E) is the total neutron cross section.

The notation adopted here for a neutron-induced reaction is:

$$ {}^{1}_{0}\mathrm{n} + {}^{A}_{Z}\mathrm{T} \rightarrow {}^{A\text{-}a+1}_{Z\text{-}z}\mathrm{R} + {}^{a}_{z}\mathrm{r} $$

This notation captures both the atomic weight and atomic number of the various nuclei. In this notation: "n" is the incident neutron, "T" is the target element with atomic weight "A" and

[1] Units for "damage energy" are the same as those for "energy",i.e. the SI accepted unit is the joule (J).

[2] Secondary gammas are omitted here because they have a long range, i.e. they do not deposit their energy locally in the lattice. Photons can cause various modes of damage, even inducing lattice displacements through their generation of high energy electrons, see Section 3.9. Any locally gamma radiation needs to be treated separately, quantified with respect to fluence and spectrum and the deposited energy due to gammas needs to be addressed as a separate contributor to the damage metric, e.g. see Reference [Re93].

[3] The units for a "damage cross section" are the same as for "cross section" as defined in Section 2.6, i.e. with SI-accepted units of m^2.

atomic number "Z"; "R" is the primary residual nucleus; and "r" is the light isotope in the residual channel. In this notation, "A-a+1" is greater than "a". The attribute "primary" for the "R" nucleus in the outgoing reaction channel denotes that it is the heavy particle in this channel. This residual nucleus is often referred to as the primary "knock-on" atom (PKA).

It should be noted that, while some analysis/codes only treat the damage energy from the primary residual atom, the definition of damage energy requires that the damage from all emitted particles be considered. This underscores the warning given in the beginning of Section 3.4 that the "definition of damage energy … is not entirely consistent throughout the range of applications."

In cases where a neutron-induced residual reaction product is emitted in an excited state that subsequently decays with the emission of a different ion, the damage energy from the subsequent decay products should also be include in the neutron damage energy. The SPECTER code [Gr85] includes this consideration for some cases of interest to the pressure vessel embrittlement community, e.g. beta decay of ^{28}Al.

3.6 Neutron DPA Cross Section

Neutron DPA cross section, ${}^{n}\sigma_{dpa}(E)$, characterizes the production of Frenkel pairs, i.e. lattice vacancy-hole combinations, produced in the lattice by neutron-nucleus reactions [He93] and can be defined as:

$$ {}^{n}\sigma_{dpa}(E) = \int \sigma\left(E \to T\right) \cdot \nu_d \left[{}^{ion}T_{dam}(T) \right] \cdot dT \qquad \text{Eqn. 31} $$

where $\nu_d(T)$ is defined as the number of Frenkel pairs created by an ion with damage energy T. There is an implied summation/integration over all of the open cross section channels and all emitted particles in each open channel. There are various possible formulations for the term $\nu_d(T)$. This topic is addressed in section 3.9 on displacement models.

This term is an adjunct to the neutron damage energy cross section defined above in Section 3.5.

3.7 Energy Partition Function

Section 2.6.1 definition of the mass stopping power showed that, in addition to energy being lost due to radiative processes, energy deposited from a particle interaction can come about due to electronic process or nuclear processes. Recall that the word "nuclear", in the context of a stopping power, does not apply to a "true nuclear process" but rather refers energy deposited in lattice atoms by elastic Coulomb collisions, including the screened Coulombic interactions. A "true nuclear processes" refers to any interaction due to the strong or weak nuclear forces, and thus, for an incident proton or light ion, would include true nuclear elastic scattering, e.g. of the proton (or light ion) from the individual nucleons in the lattice atoms. "True nuclear processes" also includes spallation reactions induced by the incident particle. When there is a danger of confusion in the usage of the term "nuclear" in this report we will use the words "radiative nuclear" and "transmutation nuclear" to distinguish the processes. When the term "nuclear" is

used without qualification, it should be considered to include both the radiative and transmutation nuclear components. Most previous work in the area of displacement damage energy in materials has only considered the radiative nuclear processes. The WinNIEL code, discussed in Section 5.2, is an exception in that it does address the "true nuclear" or "transmutation nuclear" displacement component.

In the context of a stopping power, the "radiative nuclear" or (lattice) displacement component of the deposited energy can go into overcoming the binding energy of displaced lattice atoms, or into phonons within the crystal structure that eventually are reflected in bulk material heating. The non-nuclear energy deposition represents energy imparted to electrons by ionization or excitation. The concept of an energy partition function is used to divide the energy of an ion, or of the recoil atom from a neutron-induced reaction, into its ionization and "nuclear" (including both radiative and transmutation) components. This allows the damage energy, T_{dam}, within a material to be determined from the initial ion/recoil-atom energy and a definition of the lattice material (atomic mass, atomic number, and, in some partition models, even the crystal structure) where it originates.

In general, the deposited energy can be "partitioned" into any set of processes and this need not be a binary division. In practice, the most important partition is into two categories that are referred to as "ionization" and "displacement" processes. In this nomenclature, the word "displacement" is more properly termed "non-ionizing" since many types of energy deposition, such as energy going into lattice phonons, are typically binned in the "displacement" category. Properly, only the lattice atom binding energy would go into this "displacement" partition.

Note that the energy partition function, as defined in this document, yields the amount of energy that goes into the lattice and does not represent the fraction of this energy. When most sources plot the energy partition function, they are plotting the ratio of (what is defined here as) the energy partition function, T_{dam}, and the ion energy, T_R.

Various representations of the displacement energy partition function are addressed in the following subsections. Note that there is considerable ambiguity/variation in the treatment of the energy partition function for energies below the displacement threshold energy, E_d. While the conventional analytical representations, as addressed below for the Robinson and Akkerman models, produce a numerical value for ion energies less than E_d, by definition no lattice atom displacements can take place for ion energies less than E_d. However, for energies less than E_d, the energy imparted to a lattice atom does go into phonons – and hence should be accounted as part of the non-ionizing portion of the damage even if it does not result in any lattice atom displacements. Many implementations of these analytical functions, such as the implementation of the Robinson energy partition in the NJOY-2012 code, assume that the energy partition is zero below E_d. In Robinsons initial work [Ro71, Ro75, Ro77] he notes that, for electrons, it is customary to set the damage energy to zero below a certain energy (his equation 3), but, in defining the damage energy for neutrons, he uses a lower integration bound of zero for the recoil atom energy while employing an integrand containing his analytic formulation for the energy partition function (his equation 17). With respect to the implementation in the MARLOWE BCA code, Robinson notes [Ro83]:

"The damage energy appears in MARLOWE as the sum of three terms.

a) The kinetic energy transferred in quasielastic collisions to target atoms which are not displaced (each contribution < E_d).

b) The energy expended by displaced particles in overcoming binding (each contribution = E_b).

c) The final kinetic energy of each recoil which stops within the target (each contribution < E_c)."

Thus MARLOW includes the energy less than E_d in its definition of the "damage energy". In the above quote, E_b is the binding energy and E_c is the cut-off energy below which the ion is not tracked [Ro92].

3.7.1 LSS

The classical treatment of the energy partition into ionization and displacement components comes from the work by Lindhard, Scharff, and Schiott [Li63] in 1963 and is referred to as the LSS energy partition [Do72]. The LSS partition of energy into the lattice from an ion with energy T_R is notated as $T^{LSS}_{dam}(T_R)$. This approach is based upon the continuous slowing down treatment of the primary and secondary recoil atoms. The LSS approach used a Thomas-Fermi screening function over the Coulomb potential to model the elastic interactions and a non-local free uniform electron gas model for the inelastic electronic scattering.

The LSS model assumes the local density approximation (LDA); that is, material can be represented as a "structureless" solid, referred to as a "lattice gas". Thus the LSS theory does not account for any crystal effects upon the lattice displacement nor does it account for any complications due to the cascade development [He93].

The Lindhard model is limited to energies, T_R, less than about $24.8*Z^{4/3}*A$ (in keV) [No75, Ro71] where A is the atomic mass of the incident ion and Z is the atomic number of the incident ion. In iron this limitation translated to a maximum permissible ion energy of 107 MeV. In silicon, the limitation translates to a maximum permissible ion energy of 23 MeV. These limitations are relevant when considering the equivalence of charged particle induced damage and neutron-induced damage. This energy limitation is related to the LSS assumption that the stopping power is related to the ion velocity and, for collisions that impart more than the Bohr velocity, to the lattice recoils, $e^2/\hbar$ = ~25 keV/amu, this assumption is violated [Mo12, Zi99].

It must be noted that while the above energy limitation applies to the Lindhard LSS model, codes such as MARLOWE that incorporate the LSS model often are augmented to also use the semi-empirical Ziegler potential to address "the transition from the Lindhard to the Bethe regime governed by Rutherford scattering" [Hou19] through the use of this "heavy ion scaling rule" to capture the stopping poser of atoms with energies greater than 25 keV per amu. In MARLOWE, this has been implemented by several different people and is typically accomplished by augmenting the MARLOWE code with new interaction potentials based on the ZBL potential [ZBL85, Hou10].

3.7.2 Robinson

Robinson and Torrens [Ro74, Ro96] have compared the LSS approach with a detailed simulation using the Firsov theory for inelastic energy loss. Robinson [Ro71] showed that the LSS energy partition function can be approximated by a displacement damage energy, ${}^{ion}T_{dam}^{Robinson}(T_R)$, given by:

$$ {}^{ion}T_{dam}^{Robinson}(T_R) = \frac{T_R}{\left[1 + k_L \cdot g\left(T_R / E_L\right)\right]} \qquad \text{Eqn. 32} $$

where:

- ${}^{ion}T_{dam}^{Robinson}(T_R)$ is the energy that is imparted to the lattice, i.e. the non-ionizing component of the deposited energy, from an ion with energy T_R
- T_R is the initial energy of the incident ion, in the case of a neutron interaction this is the neutron-induced primary recoil atom
- Z_R is the atomic number of the recoil atom
- Z_L is the atomic number of the lattice atom
- A_R is the atomic weight of the recoil atom
- A_L is the atomic weight of the lattice atom

k_L, g(ε), and E_L are defined as:

$$ k_L = \frac{0.0793 \cdot Z_R^{2/3} \cdot Z_L^{1/2} \cdot \left(A_R + A_L\right)^{3/2}}{\left(Z_R^{2/3} + Z_L^{2/3}\right)^{3/4} \cdot A_R^{3/2} \cdot A_L^{1/2}} \qquad \text{Eqn. 33} $$

$$ g(\varepsilon) = 3.4008 \cdot \varepsilon^{1/6} + 0.40244 \cdot \varepsilon^{3/4} + \varepsilon \qquad \text{Eqn. 34} $$

$$ E_L = 30.724 \cdot Z_R \cdot Z_L \cdot \left(Z_R^{2/3} + Z_L^{2/3}\right)^{1/2} \cdot \frac{\left(A_R + A_L\right)}{A_L} \qquad \text{Eqn. 35} $$

Note, with respect to the above equations, while the NJOY-2012 code properly implements the above formulae, the NJOY-2012 code manual [NJ2012] Equation 198 incorrectly reports the exponent of the combined mass term in the numerator of the quantity k_L, in Equation 33 above, as 2/3 rather than the correct value of 3/2. In the NJOY manual this term is labeled as F_L.

For cases where the recoil atom is the same as the lattice atoms, i.e. $A_R = A_L$ and $Z_R = Z_L$, the k_L and E_L terms correspond to parameters in the original Lindhard theory:

$$k_L = \frac{0.133745 \cdot Z^{2/3}}{A^{1/2}}$$ Eqn. 36

$$E_L = 86.931 \cdot Z^{7/3} \quad (eV)$$ Eqn. 37

Note that the Robinson fit to the LSS energy partition is limited (by the nature of its empirical derivation) to cases where the recoil atom is close in atomic number and atomic weight to the lattice atoms. To quote from Section 5 of Reference [No75]:

> "Some limitations of this model must be pointed out. The Lindhard formulation of eqs (5)-(9) applies strictly only to monatomic systems (i.e. Z1=Z2) and to energies less (perhaps much less) than about 25*Z1^4/3*A1 (keV). The former limitation should not be too serious as long as the ratio Z1/Z2 does not differ too much from unity. If necessary, it could be relaxed by repeating the Lindhard calculation for other cases"

This means that the Robinson fit to the LSS partition function should not be used to capture the displacement energy from low mass secondary particles, e.g. protons and alpha, that result from neutron-induced reactions. The damage from the low mass secondary particles should still be considered and is modeled in the general LSS approach; it is only that the Robinson fit to the energy partition may not be accurate to address these cases where the mass of the residual ion is much less than that of the lattice atoms. Analysis tools such as the HEATR module of the NJOY-2012 code, addressed in Section 5.1, use the Robinson fit to the energy partition but only address the displacement kerma due to the primary residual particle and ignore the displacement kerma from lighter secondary protons and alpha particles. This is usually an adequate approximation, but should be considered in an application-specific context. . Clearly, when the damage partition is being used to establish a correlation with an observed level of damage, the energy from all secondary particles should be taken into consideration, as should any relevant deposited energy from the time-dependent decay of any emitted metastable secondary particles, as discussed in Section 3.5.

For elastic scattering in a silicon-28 lattice, Figure 6 shows the fraction of energy imparted to recoil atoms (phonons and displacements, i.e. the non-ionizing energy fraction). Figure 6 shows that, for low energy recoils, most of the energy goes into the lattice as opposed to ionization. As the lattice atom recoil energy increases, more and more of the energy goes into ionization. For a low recoil energy of 20 eV for a silicon atom in a silicon lattice, 91% of the energy, or 18.2 eV, goes into the lattice.

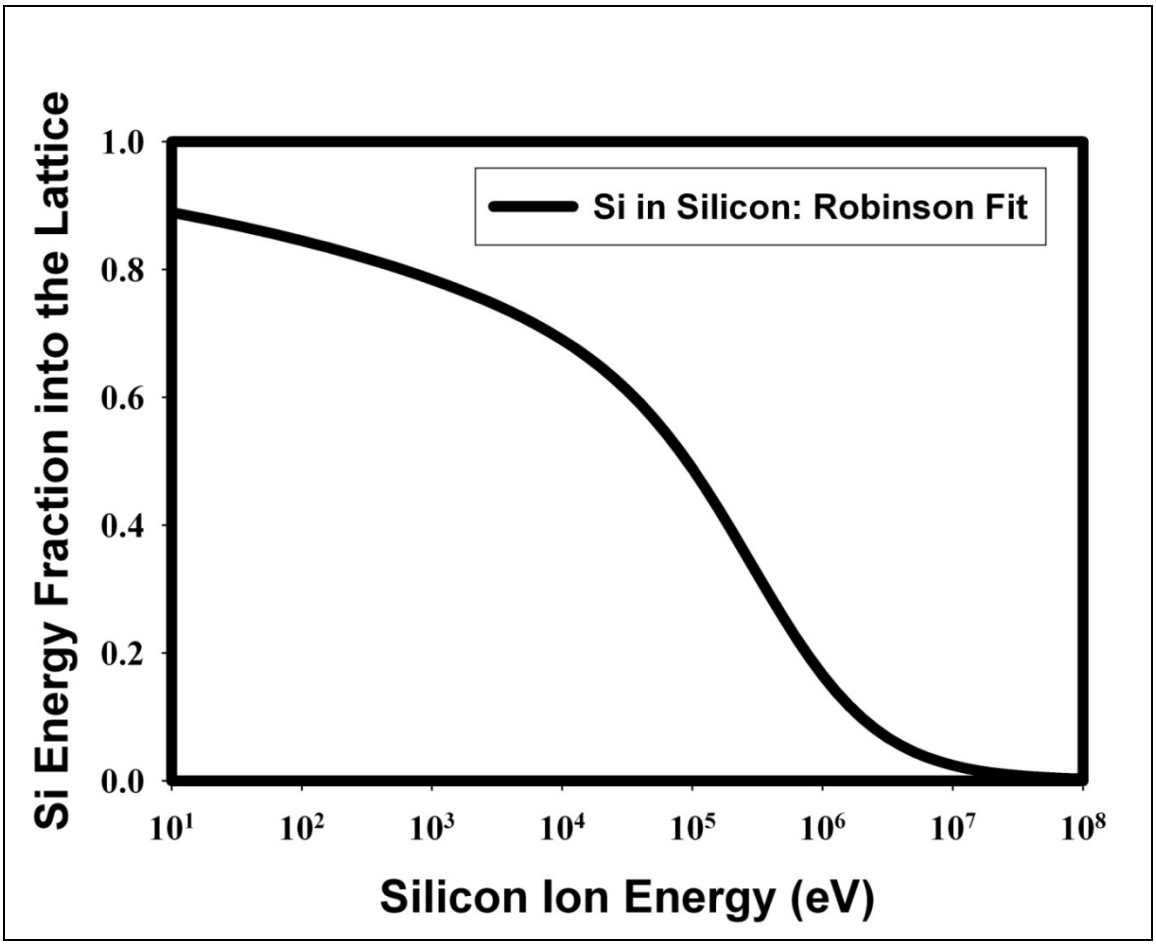

Figure 6: Fraction of Recoil Energy from a Si Ion Imparted to the Lattice in a Silicon Crystal

3.7.3 Akkerman

Recent work by Akkerman [Ak06], has used updated potentials for silicon to derive a new energy partition in silicon valid for for ion energies < 500 keV. Akkerman used the Ziegler, Biersack, and Littmark (ZBL) [ZBL85] potential for the elastic Coulomb scattering and used a combination of a local (impact parameter dependent) model and a non-local model for the inelastic ion-atom scattering. Their results used a displacement threshold energy of 21 eV for silicon.

The Akkerman damage partition model, ${}^{ion}T_{dam}^{Akkerman-Si}$, uses the same functional representation as was adopted by the Robinson methodology, but they defined a different g-function. We label the Akkerman g-function as $g_{Akkerman}(\varepsilon)$. Its functional form is:

$$g_{Akkerman}(\varepsilon) = 0.74422 \cdot \varepsilon + 1.6812 \cdot \varepsilon^{3/4} + 0.90565 \cdot \varepsilon^{1/6} \qquad \text{Eqn. 38}$$

The Akkerman damage partition is then given by:

$$ {}^{ion}T_{dam}^{Akkerman}(T_R) = \frac{T_R}{\left[1 + k_L \cdot g_{Akkerman}\left(T_R / E_L\right)\right]} \qquad \text{Eqn. 39} $$

In Reference [Ak06] the authors report that, for protons on the silicon lattice, "the presence of a significant part of low energy particles in the recoil spectrum where the new partition function is significantly larger than Lindhard's result". In the conclusion to Reference [Ak06] the authors note that"

> "for protons .. the new partition factor increases significantly the calculated NIEL, up to 15% relative to those calculated with Lindhard's factor. However, this difference decreases with increasing proton energy and becomes negligible when approaching 10 MeV."

and

> "The use of the new partition factor increases NIEL for electrons with energy from 0.3 MeV to 100 MeV by 12% to 15% compared to the data calculated with Lindhard's partition factor."

It is not clear if the author comments above regarding the energy partition comparisons for protons and alpha particles were made using the LSS methodology or if they used the Robinson fit to the LSS work. It must be noted that the original Robinson work clearly stated that their fit to the LSS work is only valid when the incident particle was similar in Z and A to the lattice. Clearly use of the Robinson damage partition for protons in a silicon lattice violates this caution concerning the fit.

Figure 7 compares the Akkerman and Robinson energy partition functions for a silicon ion incident on a silicon lattice. The agreement is seen to be consistent with the above comments from the authors regarding the observed differences for incident protons and alpha particles in the silicon lattice, i.e. the agreement is within about 15% for low energy incident silicon ions and decreases to a negligible difference for high energy incident ions. As was noted for protons and alpha particles, the Akkerman partition function results in about a 15% high lattice displacement damage component for low energy incident particles. At high energy the difference between the Akkerman and Robinson energy partition functions is not clearly depicted in Figure 7 due to the small values of the damage energy. To clarify the comparison, Figure 8 shows the ratio between the two damage partition functions. The figure shows that the Akkerman partition results tend to smaller damage energies, with an 8% lower value for 2 MeV incident silicon ions, and then tend higher again with the damage energy being about 8% higher for 100 MeV incident silicon ions.

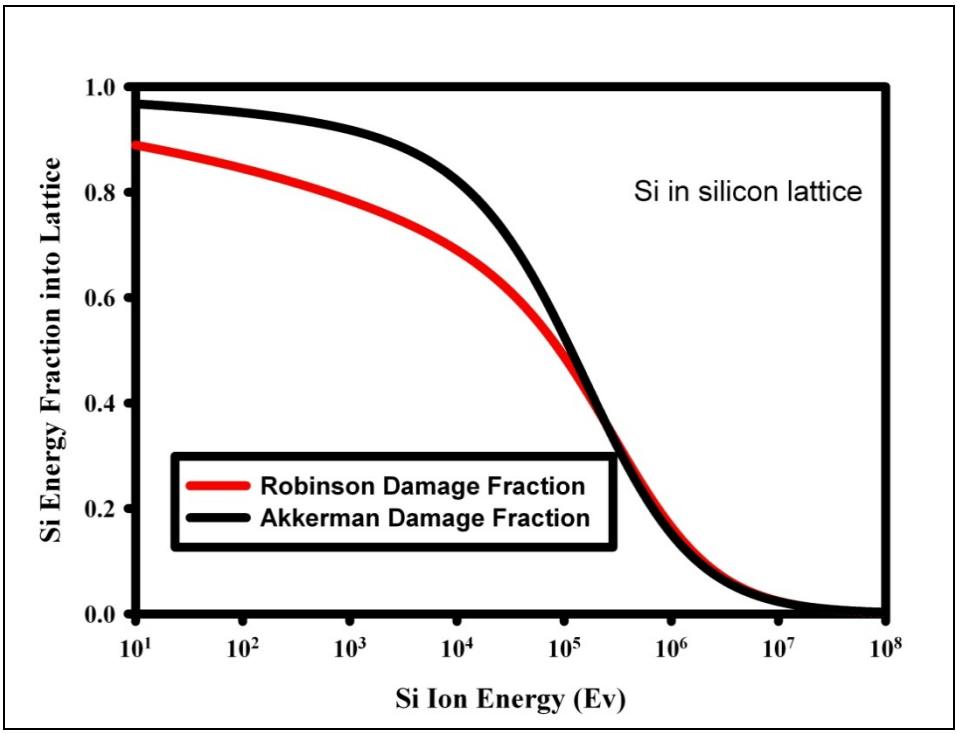

Figure 7: Comparison of the Robinson and Akkerman Damage Partition Functions for a Si Ion in a Silicon Crystal

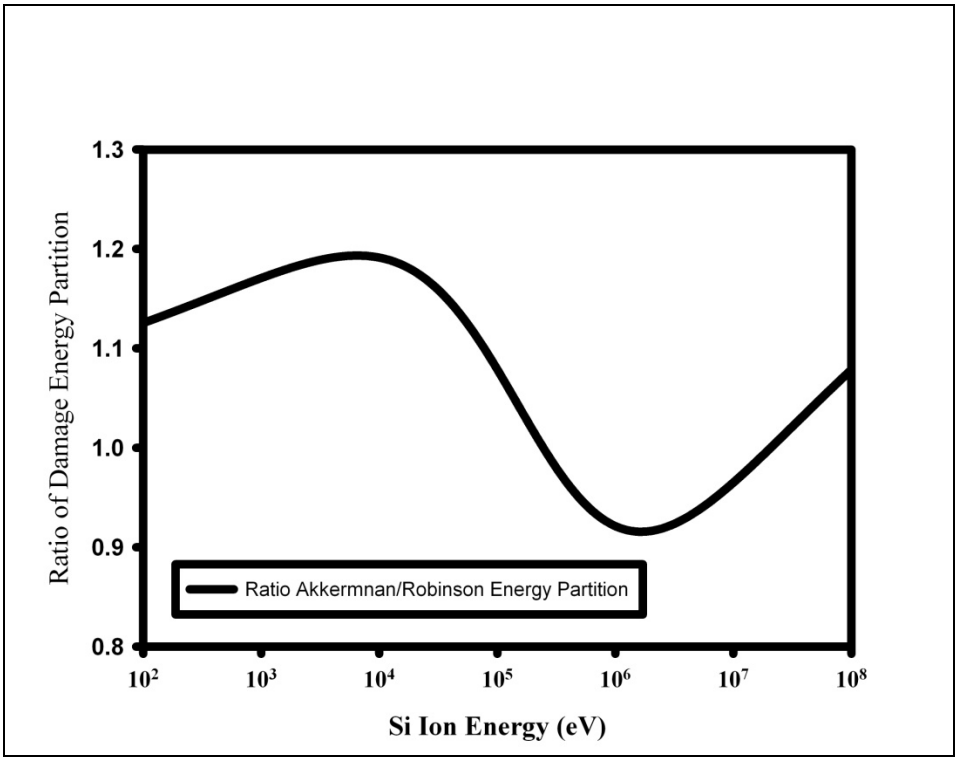

Figure 8: Ratio of Akkerman-to-Robinson Damage Energy Partition Function

3.7.4 BCA

Some investigators have used binary collision approximation (BCA) codes, such as MARLOWE, to determine the partition of energy into ionization and lattice deposition components, ${}^{ion}T^{BCA}_{code\text{-}potential}$. The use of a BCA model permits the user to specify the electronic (elastic and inelastic ion-electron) and nuclear (ion-atom) potentials used in the Monte Carlo simulation of the ion slowing down process and while tracking the various sources of energy deposition. Since there are a wide variety of BCA codes, this damage energy term is notated in the format (with subscripts) in order to clearly identify both the "code" and "potential" that were used in defining the energy partition.

The MARLOWE code supports dividing the energy loss into:

- Inelastic energy loss
- Binding loss (displacements)
- Binding loss (replacement)
- Binding loss (non-lattice)
- Sub-threshold loss (lattice)
- Sub-threshold Loss (non-lattice)
- Remaining kinetic energy
- Available for damage
- In replacement sequences
- Carried by focusons
- Replacement threshold
- Focuson threshold
- Carried through front surface
- Binding loss (front surface)
- Remaining kinetic (front adatoms)

The SRIM code divides the energy into

- Electronic/ionization
    - from source ions
    - from recoil ions
- Phonons (includes all energies less than the displacement threshold energy)
    - from source ion
    - from recoil ions
- Vacancies, i.e. binding energy (loss to the target through creation of vacancies or replacement collisions)
    - from source ions
    - from recoil ions

3.7.5 Influence of the Interaction Potential on the Energy Partition

Table 1 compares the percent of the kerma that is ionizing for a Si recoil atom in a silicon lattice as computed using some of the Robinson fit to the LSS methodologies produced by various potentials in the MARLOWE BCA code. While the form of the potential can affect the energy partition, this is not seen to be a large effect.

Table 1: Comparison of Various Damage Partition Methodologies in Silicon

Si Ion Energy (keV)	MARLOWE BCA Code Using:		LSS
	Moliere Potential	ZBL Potential	
30 keV	29.1	32.9	38.5
50 keV	35.1	38.9	43.3
100 keV	44.0	47.8	52.
500 keV	72.0	72.9	74.5
1 MeV	82.7	82.7	83.5
10 MeV	94.7	95.0	97.6

3.8 Displacement Threshold Energy

Displacement threshold energy, E_d, is the minimum energy imparted to the primary recoil atom as a result of a neutron-induced reaction that will result in a displacement of the resulting lattice atom (identical to the target lattice atom in the case of an elastic or inelastic event).

3.8.1 E_d Value in Crystalline Silicon

For silicon, the traditional displacement threshold energy for silicon is 25 eV. This is the default values used in some codes such as NJOY [NJ2012] and reported in previous computations of the silicon displacement kerma. The ASTM E722-94 standard [A722] also uses a recommended value of 25 eV. Other codes, such as SRIM [Zi10], use a value of 15 eV. The value of 15 eV is supported by circa 1995 molecular dynamics simulation results discussed in Section 3.8.1.2 below. Other work, such as the results of Akkerman [Ak06] and the WinNIEL code [Xap, Xa04] use a value of 21 eV.

3.8.1.1 Experimental Data

The status of experimental data is succinctly captured in Reference [Ho08]:

> "E_d is poorly known in the material (Silicon). Experimental methods show a widely varying scale of results for E_d in the range of 10 – 30 eV."

The range of the experiment data can be seen in References [Bo76, Lo58, Co65, He69, Ma94, Smit]. The minimum displacement threshold energy in the <111> direction in silicon has been measured as 13 eV [Lof58, Co66]. This value has been matched by DFT MD calculations [Ho08]. The Reference [Co65] value is an indirect measure of the average measured over all crystal directions. A good baseline experimental value of 20.5 +/- 1 eV comes from the Reference [Bo76] and was derived from capacitance-voltage measurements on gold-silicon Schottky diodes using electron irradiation.

3.8.1.2 Molecular Dynamics Circa 1995

Molecular dynamics calculations by L. Miller et al. [Mi94] indicate that the silicon displacement threshold energy varies from 10 - 15 eV. Their conclusion was:

> "For our computational cell size of 576 atoms, a PKA kinetic energy of 15 eV results in a temperature of approximately 100-150 K (the lower value corresponds to a displaced atom with a formation energy of approximately 6 eV; the higher energy corresponds to no displacement."

An important consideration is the working definition of a displacement. The authors of the above work [Mi94] provide some insight to this:

> "A simple working definition ... (is) ... that the primary knock-on atom (PKA) in the silicon lattice is considered displaced when it exits the tetrahedron formed by the nearest neighbor atoms and comes into quasithermal equilibrium with the surrounding lattice before recombination can occur. (By quasithermal equilibrium we mean that the total available kinetic energy is more or less randomly distributed over all atoms in the computational cell.). ...
>
> The definition of a displacement event was also found to be dependent upon the time scale over which the Frenkel pair exerts it influence over the property being measured."

The authors [Mi94] present molecular dynamics calculations that show that the displacement threshold energy is dependent upon the direction of the recoil and upon the distance from the original lattice location that is set as the criteria for declaring the existence of a displacement. For closely separated Frenkel pairs, there is a strong probability for recombination. For displacements only outside the nearest-neighbor tetrahedron, the displacement threshold energies range from 10.1 to 18.3 eV. For displacements beyond three quarters of a cubic unit-cell width (with a lattice spacing constant of 5.4 Angstroms), the displacement threshold energies range from 11.5 to 22 eV.

If one uses a definition of a displacement that corresponds to a lattice displacement that is only just outside the nearest neighbor tetrahedron, the result is a displacement threshold energy that is about half that seen from radiation damage experimental studies using electrons [Bo76, He68]. This difference is attributed to the most probable separation distance between the members of the Frenkel pair and the fact that only widely separated Frenkel pairs persist for sufficient time to contribute to the observed electron damage. At temperatures of 80K, close Frenkel pairs, as defined here, may only exist for about 0.2 μs [Mi94. He70]. More stable defects are introduced when the vacancy-interstitial separations are at least 4.5 Angstroms (or greater than about 3/4 of a lattice constant).

Miller et al. [Mi94] give analytic expressions for the angle dependent displacement threshold energy. Fits to the equations in the <111> direction give:

$$E_d = 10.6 + 64.1 \cdot (\sin\theta)^2 - 4.54 \cdot (\sin\theta)^3 \cdot (\cos 3\theta) - 126.9 \cdot (\sin\theta)^4 \qquad \text{Eqn. 40}$$

and in the <100> direction:

$$E_d = 17.4 + 20.9 \cdot (\sin\theta)^2 - 15.6 \cdot (\sin\theta)^2 \cdot (\cos 2\theta) \qquad \text{Eqn. 41}$$

These expressions give an average bulk displacement energy of 17.5 eV in the <111> direction and 12.2 eV in the <100> unit cell direction. The formalism typically implemented in processing codes such as NJOY is not capable of handling an angle-dependent displacement threshold energy - so one must select a single average displacement threshold energy. Based on the molecular dynamics calculations and the comparisons to experimental observations, this MD modeling effort would suggest an energy of 15 eV. This corresponds to the value of the displacement threshold energy implemented by Zeigler in the SRIM code.

Different values could be selected for particular applications of the resulting displacement kerma reflecting different assumptions on the relevant time for observation of a phenomenon, and hence on the time at which the Frenkel pair exists. For an application with electronic lifetime degradation, where the late-time recombination is expected to be important, kinetic Monte Carlo or other defect annealing treatments should be used to transform this early-time displacement metric into a relevant late-time metric. Other treatments have been used by the material damage community to address the difference between close and distant Frenkel pairs.

3.8.1.3 DFT Calculations Circa 2008

Work in 2008 [Ho08] studied the displacement threshold energy in silicon using density functional theory (DFT) and molecular dynamics simulations. Consistent results were found using both the local density approximation (LDA) and the generalized gradient approximation (GGA). The DTF and Hartree-Fock (HF) methods "provided repulsive potentials which are significantly improved compared to the standard universal ZBL potential" [No97]. The average threshold energy, over all lattice directions, for the creation of stable Frenkel pairs was found to be 36 +/- 2 eV; in the <100> direction it was 20 +/- 2 eV; in the <111> direction it was found to be 12.5 +/- 1.5 eV. This work also found that there was a bond defect complex with a lower

threshold than a Frenkel pair [La09]. The average threshold energy for producing this bond defect or a Frenkel pair was found to be 24 eV +/- 2 eV. Reference [Ho08] notes that "The common usage of 13 and 15 eV for the value of the parameter (displacement threshold energy) is highly inappropriate, as from our calculations it is clear that the actual value is over a factor of two higher."

3.8.1.4 Displacement Modeling Considerations for BCA Modeling in Silicon

The application of the E_d in binary collision approximation codes was studied in Reference [Bu13]. They observed:

> "The displacement threshold energy is the energy that a target atom needs to leave its lattice site and form a stable interstitial. Its values given in the literature range from ~9 to 35 eV for silicon … A 13 eV displacement threshold energy was adopted in our simulations for amorphous Si, 20 eV for crystalline Si ... In our BCA simulations we assumed the surface binding energy to be … 4.7 eV for Si. … In our simulations we chose the bulk cut-off energy and the cut-off energy in the surface layer to be 3 and 1 eV, respectively, for all three target materials."

In this work [Bu13], MD and BCA simulation results for crystalline silicon were found to have some differences at small displacements, less than 5 Å, "due to displacements in amorphous pockets". They concluded, for silicon, that "the discrepancy between BCA and MD results is reduced but still significant for impacts on crystalline Si, which becomes partly amorphous during irradiations."

It should be noted that in BCA codes, such as MARLOWE, the relevant parameter in modeling the physics of the interactions may not be the displacement threshold energy, E_d, but the surface binding energies (one for a lattice site and one for atoms near the surface) and the model cut-off energy below which a recoil atom is not tracked. Section 3.7 of this report defines some of the energy terms used in the MARLOWE code. Reference [Ro92] notes that: "It must be emphasized that the only explicit displacement threshold energy (in) MARLOWE is $E_c + E_b$." This reference notes an example of this for Cu where the E_d is ~58 eV while the relevant MARLOWE input parameter $E_c + E_b$ is 7.02 eV. Thus there is a big difference between the displacement threshold energy and the relevant input parameters in MARLOWE BCA code models.

3.8.1.5 Recommended E_d Value in Silicon

For comparison of 1-MeV displacement damage in silicon, the recommendation, at this time, for the value of E_d is to be consistent with that found in the ASTM E722-94 standard, which is 25 eV. This is motivated by the need for a community consensus in the comparison of 1-MeV(Si) damage reported by damage simulation facilities and that used in analysis activities.

In light of the best experimental values [Bo76], 20.5 +/- 1 eV, and the latest high fidelity DFT-MD modeling [Ho08] value, 24 +/- 2 eV, and recent comparisons between BCA and MD modeling, which recommend using 20 eV, the community should consider revisiting the ASTM E722 recommended silicon damage function and the 1-MeV(Si) reference value.

If a new value for E_d is adopted by the radiation effects community, taking into account experimental and calculational results, a value of 20.5 eV is the recommended value for future analysis. Results from Section 5.1 show that the effect of this change in the displacement threshold energy on the displacement kerma for silicon is very small.

3.8.2 E_d Value in for Other Semiconductors

A compilation of results on other semiconductor materials can be found in Reference [OECD14].

In Ge, the minimum displacement threshold energy is similar to that seen in silicon, 14 eV [Co66]. Average threshold values of 18 eV [Lof58], 20 +/- 5 eV [Pou80], and 80 eV [Vit77] have been reported. DTF simulations have given values of 23 eV for the Frenkel pairs and 21 eV when one considers the IV pairs as well as the Frenkel pairs.

In GaAs experiments indicate minimum threshold displacement energy of 10 eV on both the Ga and As lattices [Leh93, Hau96]. Classical MD simulation indicate a minimum of 15 eV can produce antisite defects.

In GaN there is a large mass difference in the lattice atoms. Experiments report an average threshold displacement energy of 41 eV for the Ga sublattice [Wen03]. MD simulations give values of 45 eV and 110 eV for the Ga and N sublattices [Nor02] while DFT MD calculations give very different values of 73 eV and 32 eV.

3.9 Displacement Model

The displacement model relates the number of displaced atoms, ν_d, to the ion damage energy. Several models are used by the community. These models are discussed in the following subsections.

High energy photon radiation (> ~500 keV) can generate electrons that then can displace lattice atoms [Oen67, Fu03]. For irradiations in mixed photon/neutron environments produced by reactors, the photon displacement contribution can often be ignored, but exception can occur for well shielded locations where there is significant down-scattering of the neutrons and generation of high levels of secondary gamma radiation. Studies on material embrittlement at the HIFR reactor have shown that the photon displacement component cannot always be ignored [Re93].

In addition to direct photon-induced displacement, ionization can affect the evolution of defects and observed defect-related damage metrics. Charge injection can result in defect annealing in semiconductors such as Si and GaAs. Another example where ionizing radiation can have an effect is on the diffusivity of point defects that can be found in some materials, such as ceramic insulators [OECD14, Bo73, Mu11]. This can lead to a different microstructure and defect self-healing if higher ionization levels are present in irradiated materials. Annealing of defects can occur under ion beam analysis [Zin97, Zin97a].

Models for displaced atoms, which are addressed in the following subsections, do not cover the total range of ways that "defects" can be introduced into materials through irradiation. All "defects" introduced into materials cannot necessarily be attributed to displaced lattice ions. As noted for silicon, broken bond pairs can result in electrically active defects in silicon. Traps in TLDs are an example of ionization-related defect introduction in materials. Defect production from ionization has also been observed in insulating materials such as SiO_2 [De92, To12]. This observation complicates attempts to correlate observed defect production metrics with calculated quantities using non-ionizing energy deposition. In silicon semiconductors, trapped charge in the insulating SiO_2 can result in electric fields that affect the gain in bipolar semiconductors and complicate the interpretation of minority carrier lifetime changes due to the introduction of defects from displaced atoms, for example divacancies and vacancy-phosphorus (VP) defects that evolve from the primary Frenkel pair damage.

3.9.1 Kinchin-Pease

The material damage community has long recognized that closely spaced Frenkel pairs have a high probability for recombining. The community-standard approach has been to apply a weighting function for very closely spaced Frenkel pairs. For a displacement energy less than that required to displace a stable Frenkel pair, there are no displaced atoms created. For an energy up to the energy required to produce two defect pairs, only one defect pair is created.

The original Kinchin-Pease model [Ro68, Ki55, Si69, Od76] relates the number of defects, $\nu_d(E)$, to the primary recoil atom energy. It was derived for hard spheres and an isotropic threshold displacement energy and had the functional form:

$$ {}^{K\&P}\nu_d\left({}^{ion}T_{dam}\right) = \begin{pmatrix} 0 & 0 \le {}^{ion}T_{dam} < E_d \\ 1 & E_d \le {}^{ion}T_{dam} < E_I \\ {}^{ion}T_{dam} \Big/ \left(2 \cdot E_d\right) & E_I \le {}^{ion}T_{dam} < \infty \end{pmatrix} \qquad \text{Eqn. 42} $$

where E_I corresponds to a breakpoint energy above which knock-on atoms only lose energy by electron collisions, below which they lose energy by hard-sphere elastic scattering. E_I is greater that $2E_d$.

3.9.2 Norgett-Robinson-Torrens (NRT)

After the original Kinchin-Pease formulation, the radiation damage community did additional theoretical work and computer simulations. A group of experts at an IAEA Specialist's meeting on radiation damage units adopted a modified formulation for the number of displacements. This approach is called the Norgett, Robinson, and Torrens (NRT) Frenkel pair model and is given by:

$$ {}^{NRT}\nu_d\left({}^{ion}T_{dam}\right) = \begin{pmatrix} 0 & 0 \le {}^{ion}T_{dam} < E_d \\ 1 & E_d \le {}^{ion}T_{dam} < {2 \cdot E_d}/{\beta} \\ {\beta \cdot {}^{ion}T_{dam}}/{\left(2 \cdot E_d\right)} & {2 \cdot E_d}/{\beta} \le {}^{ion}T_{dam} < \infty \end{pmatrix} \qquad \text{Eqn. 43} $$

where β is an atomic scattering correction and is taken to be 0.8.

Robinson and Oen [Ro82] published a correction to Equation 43 to account for energy dissipated in sub-threshold displacements, however, the above form the equation is what is used in most analysis and what is built into codes such as NJOY [NJ2012].

3.9.3 Athermal Recombination-corrected Displacement (arc-dpa)

The NRT-dpa model in Equation 43 has the number of defects being, essentially, proportional to the radiation energy deposited per volume. This model is known to over-estimate the production of Frenkel pairs in metals under energetic ion displacement cascade conditions [OECD14]. Figure 9, extracted from Reference [OECD14], shows the defect production efficiency for ions in the metal copper.

To address short-comings in the NRT-dpa model, an athermal recombination-corrected (arc) dpa equation was developed [OECD14]. The arc-dpa model is given by

$$ {}^{arc-dpa}\nu_d\left({}^{ion}T_{dam}\right) = \begin{pmatrix} 0 & 0 \le {}^{ion}T_{dam} < E_d \\ 1 & E_d \le {}^{ion}T_{dam} < {2 \cdot E_d}/{\beta} \\ {\beta \cdot {}^{ion}T_{dam} \cdot \xi_{dpa}\left({}^{ion}T_{dam}\right)}/{\left(2 \cdot E_d\right)} & {2 \cdot E_d}/{\beta} \le {}^{ion}T_{dam} < \infty \end{pmatrix} \qquad \text{Eqn. 44} $$

where $\xi_{dpa}\left({}^{ion}T_{dam}\right)$ is an efficiency factor intended to represent the ratio of the number of true defects divided by the number of defects as defined by the NRT formalism in Equation 42. The efficiency factor should, based on experimental evidence and molecular dynamic modeling, be close to the NRT value at the threshold displacement energy, have a power law form at low

displacement energies, and saturate at a high displacement energy. This efficiency factor has the form:

$$\xi_{dpa}\left(T_R\right) = \frac{1 - c_{arc-dpa}}{\left(2 \cdot E_d \big/ 0.8\right)^b} \cdot T_R^{b_{arc-dpa}} + c_{arc-dpa} \qquad \text{Eqn. 45}$$

where T_R is the damage energy, E_d is the displacement threshold energy, and b and $c_{arc\text{-}dpa}$ are two unitless fitting parameters designed to match experimentally derived data with a physical meaning that is discussed in Reference [OECD14]. In this formulation, a fitting constraint is applied so that:

$$\xi(2E_d/0.8) = a_{arc\text{-}dpa} \cdot (2E_d/0.8)^b + c_{arc\text{-}dpa} = 1$$

and continuity is maintained at the boundaries of the functional description. The parameter "b" has the physical interpretation that it gives the point where there is a transition from a power law behavior, E^c, into a linear behavior that corresponding to where cascades split into subcascades. $c_{arc\text{-}dpa}$ can be physically interpreted as related to how efficiently interstitials are transported to the outer periphery of the displacement cascade, and it corresponds to the saturation level at high energy, and hence is ~ 0.3.

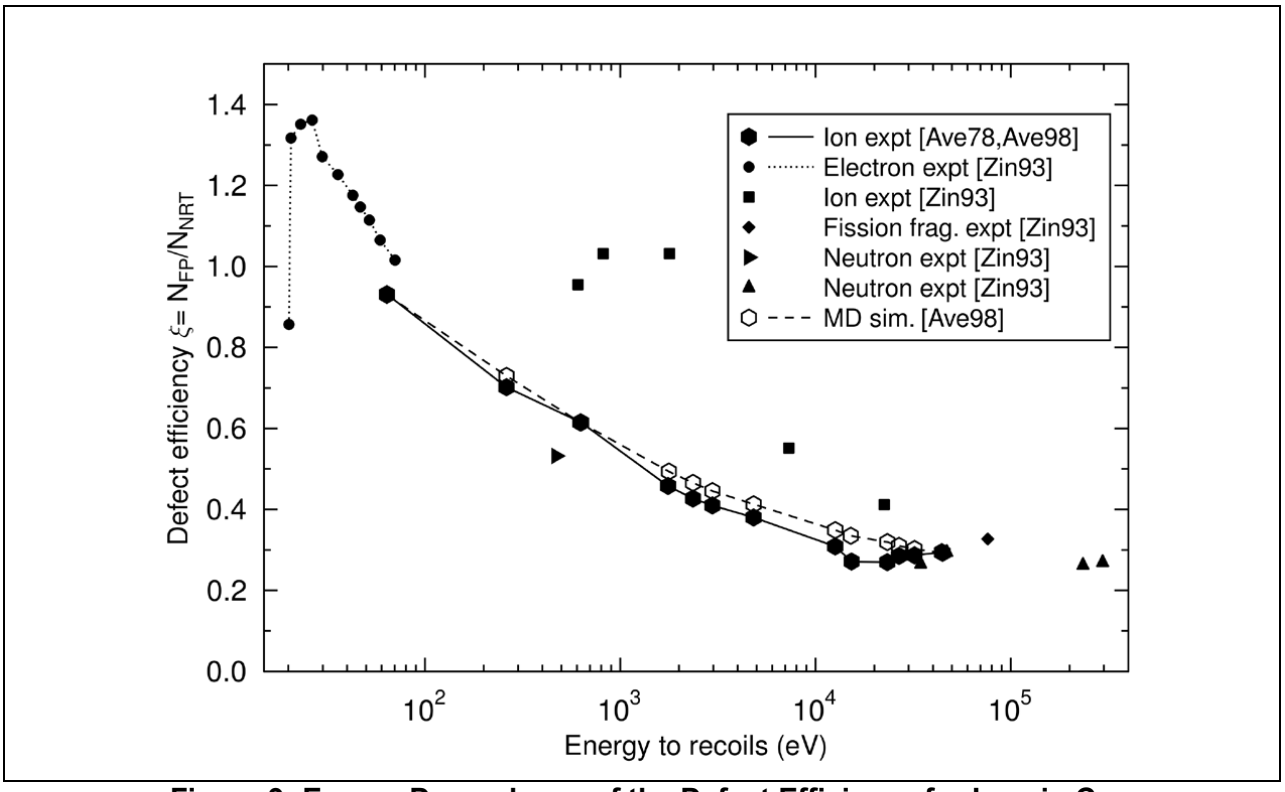

Figure 9: Energy Dependence of the Defect Efficiency for Ions in Cu

3.9.4 Replacement-per-atom (rpa)

In many materials, atom mixing is an important phenomenon and damage metrics can depend upon the number of atom replacements in a collision cascade. A major component in atom mixing comes from the heat spike in a collisional cascade [Gad95, Nor98a, Nor98b]. In this replacement model, the actual number of atoms that are displaced from the initial lattice site and end up in another site can significantly exceed the number of residual Frenkel pairs predicted in BCA models. This rpa model is presented in reference [OECD14]. The rpa model is given by:

$$ {}^{rpa}\nu_d\left({}^{ion}T_{dam}\right) = \begin{pmatrix} 0 & 0 \le {}^{ion}T_{dam} < E_d \\ 1 & E_d \le {}^{ion}T_{dam} < {2 \cdot E_d}/{\beta} \\ \beta \cdot {}^{ion}T_{dam} \cdot \xi_{rpa}\left({}^{ion}T_{dam}\right)/\left(2 \cdot E_d\right) & {2 \cdot E_d}/{\beta} \le {}^{ion}T_{dam} < \infty \end{pmatrix} \quad \text{Eqn. 46} $$

where $\xi_{rpa}\left({}^{ion}T_{dam}\right)$ is an efficiency factor given by the functional form:

$$ \xi_{rpa}(T_R) = \left[\frac{b_{rpa}^{c_{rpa}}}{\left(2 \cdot E_d / 0.8\right)^{c_{rpa}}} + 1 \right] \cdot \frac{T_R^{c_{rpa}}}{b_{rpa}^{c_{rpa}} + T_R^{c_{rpa}}} \quad \text{Eqn. 47} $$

T_R is the damage energy, and b_{rpa} and c_{rpa} are two unitless fitting parameters designed to match experimentally derived data with a physical meaning that is discussed in Reference [OECD14].

Figure 10, taken from Reference [OECD14], shows the results of the replacement-per-atom efficiency factors that result from MD calculations and the results of fitting the data to the function form used in Equation 46. Unlike for the arc-dpa efficiency factors from Equation 44, the rpa efficiency factors can be much greater than unity.

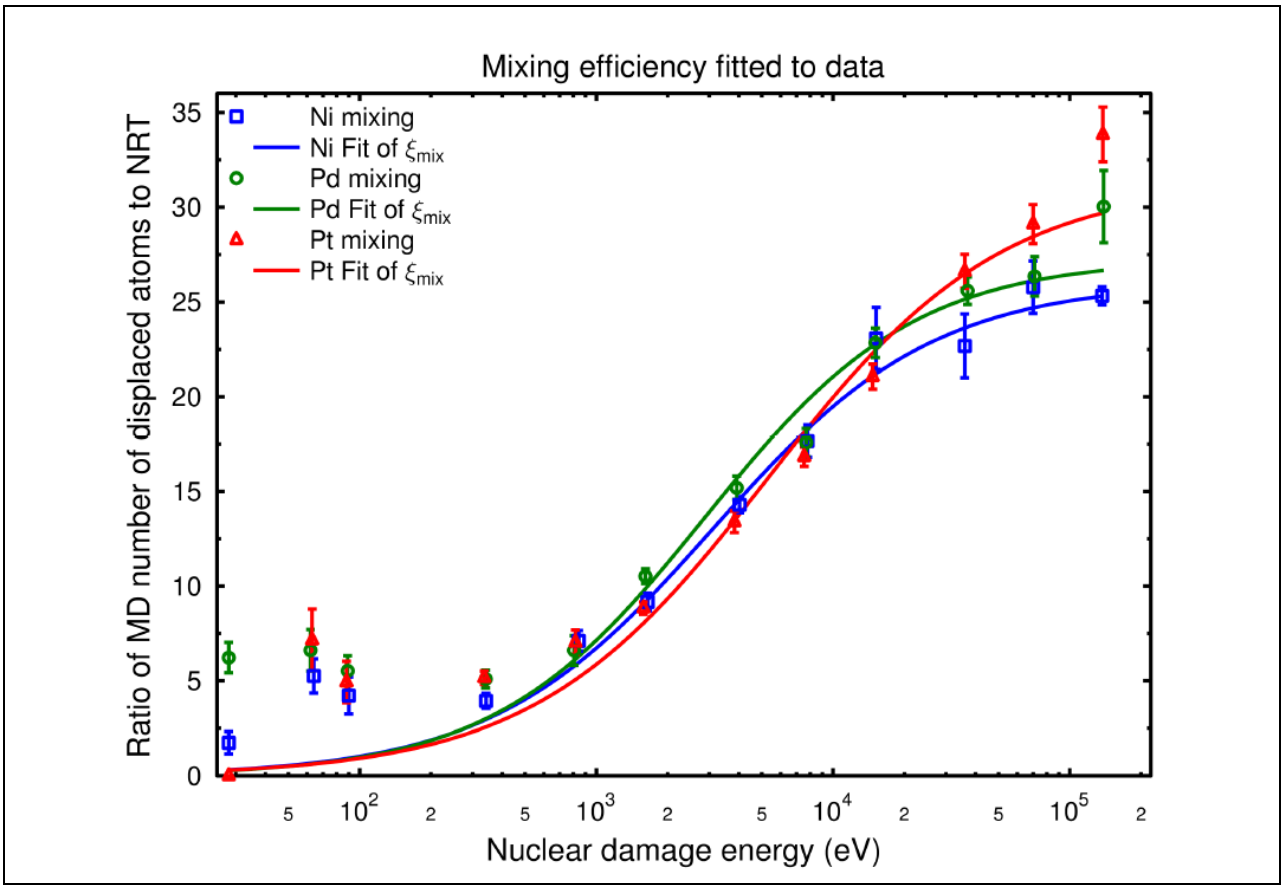

Figure 10: Calculated rpa Efficiency Factors and Fits in Ion Beam Mixing for Metals

4. DAMAGE METRICS

While Section 2 addressed community-accepted definitions for dosimetry quantities and Section 3 developed the terminology that is more specific to describing material damage, this section addresses the terminology used to describe material damage.

4.1 Displacement Cema

Displacement cema, C^{dpa}, is defined for charged particles to be the product of the augmented cema, C, for an ion of a given type and energy and the appropriate damage partition factor, ${}^{ion}T_{dam}$.

4.2 Usage of the Term Displacement Kerma

4.2.1 Microscopic Displacement Kerma Factor

Microscopic displacement kerma factor, κ^{dpa}, can be written as:

$$\kappa^{dpa}(E) = \sum_{i,j_i} \sigma_{i,j_i}(E) \int_0^{\infty} dT_{R,j_i} \int_{-1}^{1} d\mu \cdot f_{i,j_i}\left(E, \mu, T_{R,j_i}\right) \cdot {}^{ion}T_{dam}\left(T_{R,j_i}\right) \qquad \text{Eqn. 48}$$

where:

- the summation is over all open neutron-induced reaction channels, *i*
- the summation is over all emitted particles in the i^{th} channel, j_i
- $\sigma_{i,ji}(E)$ is the cross section for the j_i particle in the i^{th} reaction channel
- $f_{i,ji}(E,\mu,T_{R,ji})$ is the energy distribution for resulting charged particles which are emitted with:
    - an energy $T_{R,ji}$
    - at an angle characterized by μ
    - that result from the j_i particle in the i^{th} reaction channel
    - and are induced by the incident neutron energy with energy E.
- ${}^{ion}T_{dam}(T_{R,ji})$ is the displacement partition function for the emitted ion j_i in the i^{th} open channel with energy $T_{R,ji}$.

For neutrons, a code such as NJOY-2012 is often used in conjunction with a nuclear data evaluation to find the displacement kerma, κ^{dpa}. NJOY first calculates the reaction-specific total kerma induced by neutron interactions and identifies the recoil energy distribution for all of the reaction products. The recoil atom energy distribution for each reaction is then partitioned into a displacement component using the Robinson fit to the LSS theory. Figure 11 shows representative plots of the primary recoil energy distribution for 1-keV, 1-MeV, and 14-MeV neutrons interactions in silicon. The average recoil energy from the 1-keV neutron reactions is 70 eV; from the 1 MeV neutron 41-keV, and from the 14-MeV neutrons 569 keV for the primary recoil atom. Since the 14-MeV neutrons can open (n,α) interaction channels, there can also be a high energy emitted alpha particle. For a 14-MeV neutron the average energy of the alpha particles is 5.58 MeV. The recoil spectrum from low energy neutron interactions shows an abrupt drop in the high energy side of the distribution. This is due to the fact that the elastic interaction

channel is the dominant reaction at low energies and conservation of momentum and energy for each interaction results in a maximum energy transfer to a lattice atom. For elastic scattering, the maximum recoil energy for a lattice atom, E_{recoil}, is given by:

$$E_{recoil} = \frac{4 \cdot A \cdot E_n}{(A+1)^2} \qquad \text{Eqn. 49}$$

where E_n is the energy of the incident neutron and A is the atomic weight of the lattice atom.

Figure 12 shows the variation in the average primary recoil atom energy as a function of the incident neutron energy on a silicon lattice.

4.2.2 Displacement Kerma

Displacement kerma, K^{dpa}, is the microscopic kerma factor multiplied by number of atoms per unit mass in the target material and the incident particle fluence.

As with dose, kerma and cema, this quantity is specific to a material and the material is sometimes indicated in a subscript.

4.3 Ionization Kerma

Ionization kerma, K^{ion}, is obtained by subtracting the displacement kerma. K^{dpa}, from the total kerma, K.

This is the approach used for both ions and for neutrons. Figures 13 and 14 compare the energy-dependent fraction of energy, for neutrons with energy less than 20 MeV, which goes into ionization for ions and for neutrons in silicon and carbon, respectively. The left-hand plots show results for carbon and silicon ions in a lattice of the same material. The right-hand plots show the fraction of energy that goes into ionization from neutrons in silicon and carbon lattices. Because of the complex set of reactions that neutrons can induce in the material, and the subsequent complex distribution of recoil ion energies, the neutron energy-dependent shape shows much more structure.

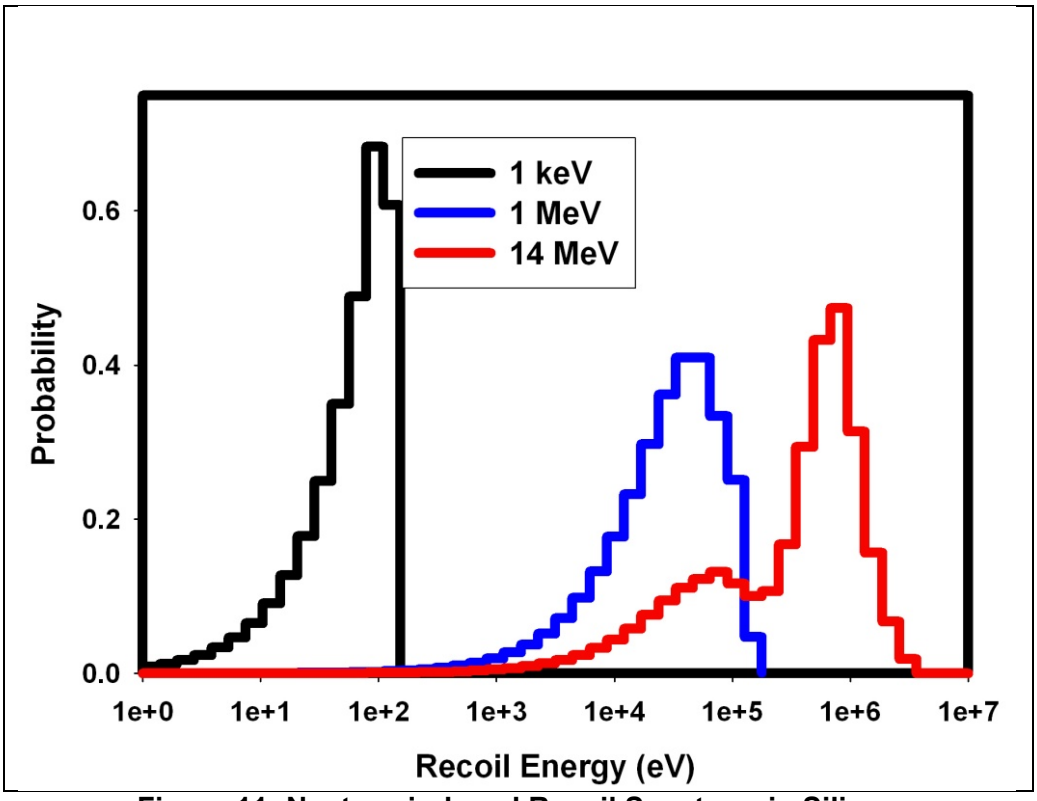

Figure 11: Neutron-induced Recoil Spectrum in Silicon

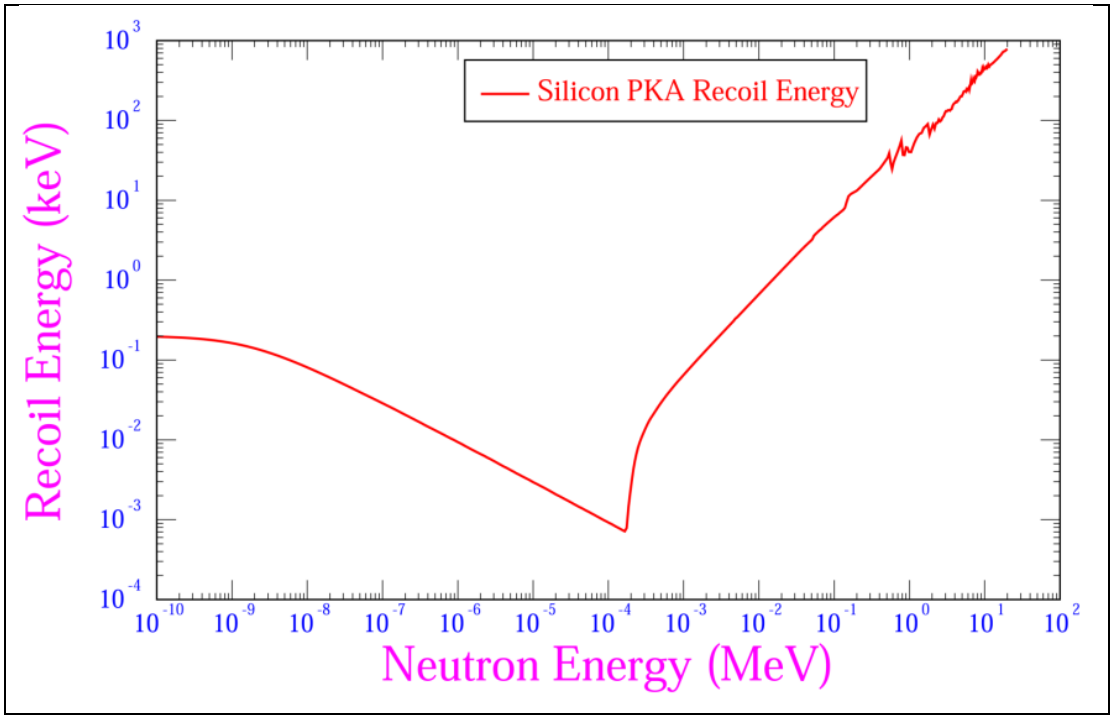

Figure 12: Average Recoil Energy from Neutron Interactions in Silicon

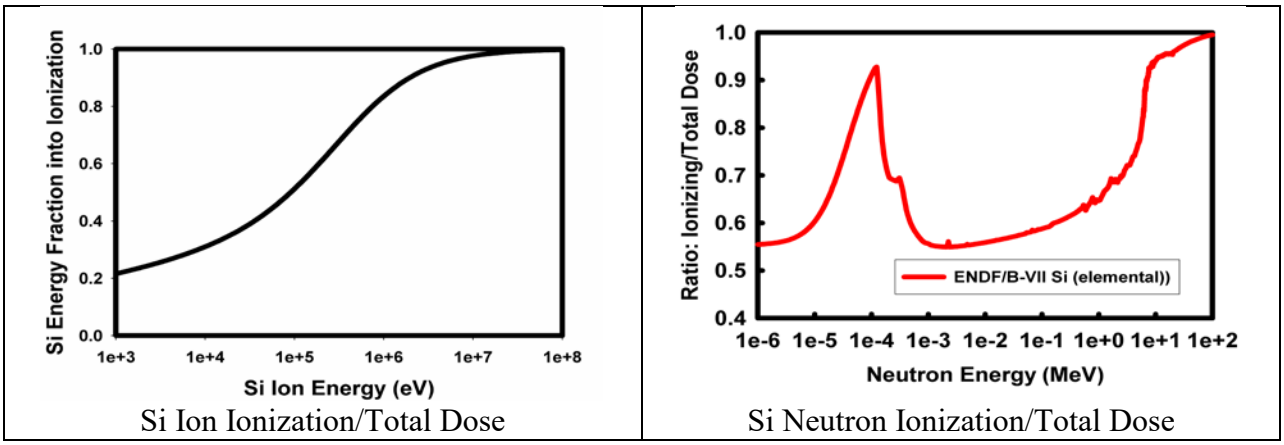

Si Ion Ionization/Total Dose | Si Neutron Ionization/Total Dose

Figure 13: Neutron and Ion Energy Partition in Silicon Lattice

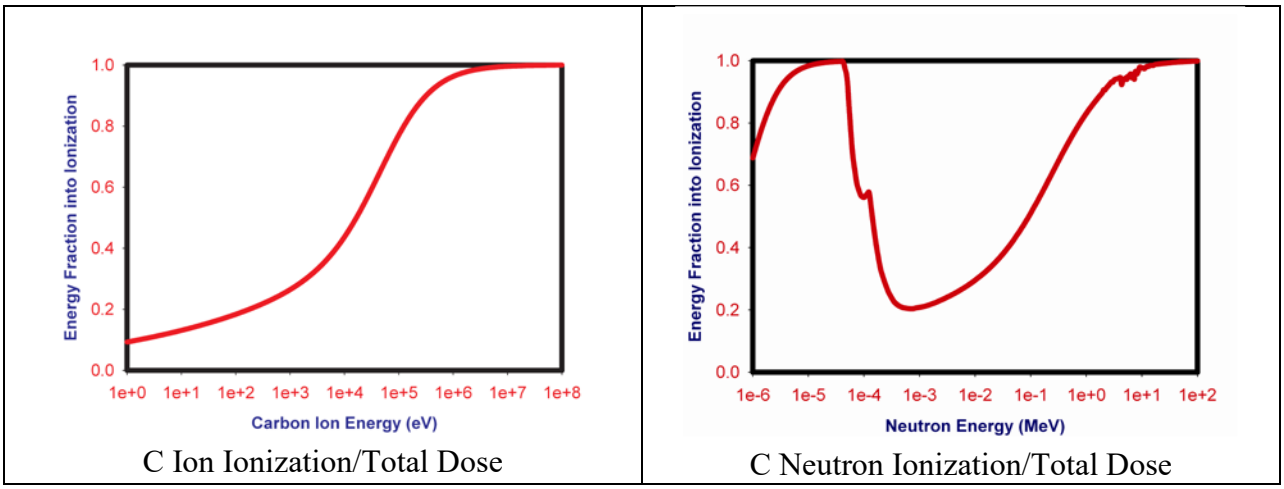

C Ion Ionization/Total Dose | C Neutron Ionization/Total Dose

Figure 14: Neutron and Ion Energy Partition in Carbon/Diamond Lattice

4.4 NIEL – Non-ionizing Energy Loss

Non-ionizing energy loss, NIEL(E), is given by:

$$NIEL(E) = \frac{N_A}{A_L} \cdot \sum_i \sigma_i(E) \cdot \int_{T_{min}}^{\infty} dT_R \int_{-1}^{1} d\mu \cdot f_i(E, \mu, T_R) \cdot {}^{ion}T_{dam}(T_R) \qquad \text{Eqn. 50}$$

where N_A is Avogadro's number of particles per mole and A_L is the molar mass of the lattice atoms.

Units are typically keV·cm^2/g or MeV·cm^2/g.

The lower bound for the integral, T_{min} is defined differently by various authors. Some authors set T_{min} to zero, others [Ak01, Bo09, Xap] use the displacement threshold energy, E_d. Based on the physics of the collision, for cases where the energy transfer is less that E_d, the lattice atom stays

in its lattice position but energy does go into phonons – and, hence, is part of the non-ionizing component. The importance of this difference is obscured somewhat by the fact that some models for the damage energy partition define the damage energy to be zero below the displacement threshold energy – which makes the lower integration bound irrelevant, or at least a coupled consideration.

Reference [La08] provides some analytical approximations for NIEL and observes that NIEL is the "rate at which energy of the incoming particle is lost per unit length in the material, in nonionizing processes. It is the analogue pf the linear energy transfer (LET) or stopping power for ionizing events."

The NIEL is defined for both charged and uncharged particles. For uncharged particles, NIEL is equal to the microscopic displacement kerma factor multiplied by the factor N_A/A_L. For silicon, this conversion between microscopic displacement kerma factor (given in units of MeV·-b) and the NIEL (in units of keV·cm^2/g) is 0.02144 [keV·cm^2/g]/[MeV·b]. For charged particles it is equal to the displacement augmented cema multiplied by the factor N_A/A_L.

4.5 1-MeV(Si) Equivalent Neutron Fluence

Per the guidance in ASTM E722-09e1, Standard Practice for Characterizing Neutron Energy Fluence Spectra in terms of an Equivalent Monoenergetic Neutron Fluence for Radiation-Hardness Testing of Electronics, the reference 1-MeV(Si) displacement kerma is defined to be a community standard value of 95 MeV·mbarn. ASTM E722 also provides a detailed 640-group tabulation of the neutron-induced damage factor. In the case of silicon, this damage factor is identical to the microscopic displacement kerma factor for silicon. Thus, the 1-MeV(Si) neutron damage equivalent fluence is obtained by dividing the appropriate spectrum-averaged microscopic displacement kerma factor, obtained by folding the response from E722 with the given neutron energy spectrum, by the reference 1-MeV value of 95 MeV-mbarn.

The determination of a reference 1-MeV(Si) displacement kerma [Da98, Gr03] is difficult since this energy is in the middle of a resonance in the cross section. The reference value was determined to be 95 MeV·mbarn +/- 4 MeV·mbarn [E722] by fitting, over the energy region from 0.01 MeV to 15 MeV, the ASTM E722 displacement kerma data to a simple smooth function form [Na72, Me66, Me65, Me86]:

$$\kappa_{Si}^{dpa}(E) = A \cdot E\left(1 - e^{-B/E}\right) \qquad \text{Eqn. 51}$$

This fit yielded the parameters A = 1.02 MeV^{-1} and B = 3.1 MeV [Me86].

4.6 1-MeV(GaAs) Equivalent Neutron Fluence

Reference [La08] observes that:

> "The comparison of NIEL with experiment cannot be done directly, due to the fact that another step in the chronological order of the production of permanent degradation is missing from the picture illustrated here. NIEL refers to the energy channeled into atomic displacements, i.e., to a number of vacancies and interstitials. In the semiconductors of interest (e.g. Si, Ge, GaAs, other) these defects have a high mobility and could interact mutually or with other defects and impurities in the lattice, producing "stable" degradation, which is measured. It depends on the number of vacancies and interstitials, but also on the concentrations of defects and impurities, on temperature, in a rather complicated manner. Only the generation rate of primary defects scales with NIEL …"
>
> "So, a possible scaling of the degradation produced by irradiation depends both on NIEL and on the evolution of primary defects."

Consistent with the above observation, standard ASTM E722, which provides a community recommendation on characterizing the energy-dependence of the damage in some electronic materials, deviates from the NIEL or displacement kerma in when it specifies a damage factor for the 1-MeV(GaAs) metric. This damage factor for GaAs is not identical to the microscopic displacement kerma factor. The reason for this has been attributed to a thermal spike in cluster damage and the ability of the cluster damage in GaAs to recrystallize at room temperature [Ben00]. The range of defects in GaAs includes antisite atom replacements that are not seen in the case of silicon [Mat95].

The 1-MeV(GaAs) neutron damage equivalent fluence is obtained by dividing the appropriate spectrum-averaged damage factor, obtained by folding the response from E722 with the given neutron energy spectrum, by the reference 1-MeV value of 70 MeV·mbarn.

5. METRICS AVAILABLE FROM CODES

The following subsections address codes that can provide numerical values for the various damage metrics addressed in the above sections for various incident particles and on various types of lattices. NJOY is addressed as the main tool used to represent damage from neutrons. WinNIEL is addressed as the most commonly quoted tool for representing damage from charged particles.

At this time, no code is cited for the treatment of displacement damage induced by high energy electrons[4]. Various tabulations of electron damage metrics are, however, available [Oen73].

Note also that no code is addressed below that treats high energy photon displacements, but high energy photons can also induce displacements through their secondary electron production [Go89, Ak01].

5.1 NJOY - Neutron Displacement Kerma

NJOY is the standard computational tool used to compute the neutron-induced displacement kerma. This code is used to process the nuclear data as represented in standard community ENDF-format files [ENDF102, ENDF201]. The latest NJOY version is NJOY-2012 [NJ2012, Mc84].

Some analyses have used a modified formalism based on the NJOY implementation of the Robinson formalism to address an ion, of a given isotopic mass, incident on and traversing lattice atoms representing the mass of the element rather than that of a specific isotope. This involves using, for the lattice atomic weight, the elemental weight rather than the atomic weight of the incident isotope, e.g. for silicon, use an incident ^{28}Si atom with atomic weight[5] of 27.97692664 amu (mass excess -21.4927 MeV), but a lattice atom weight of 28.085 amu, representing the element ^{nat}Si,.

NJOY uses the original Kinchin-Pease model with a step threshold in computing the damage energy. For recoil atoms whose energy is less than the displacement threshold energy, the atom is not capable of inducing lattice defects and this energy is not included in the displacement damage energy. Some analysis uses a modified version of NJOY that implements the NRT threshold treatment, which was described in Section 3.9.2, and can report quantities in units of displacements per atom.

[4] Low energy electrons cannot deposit energy into the lattice. The lower bound for electrons to be capable of displacing lattice atoms varies with the displacement threshold energy for the crystalline material. For silicon the lower bound for an electron capable of displacing lattice atoms is about ~0.37 MeV [Oen73, Oen67].

[5] The recommended process to determine the isotopic weights is to convert the mass excess, as reported in Reference [Tu11], into an atomic weight using 1 amu = 931.494013 MeV. For ^{28}Si this gives 28 - 21.4927/931.494013 = 27.97692664 amu.

Robinson has noted that there is an inconsistency in the treatment of this energy partition and the use of the displacement threshold energy [Ro82, Ro94]. While recoil atoms with an energy less than the displacement threshold energy are incapable of causing lattice defects, this energy does not go into ionization either but goes into the general category of lattice vibrations. Robinson notes that this discrepancy does not change the energy-dependent shape of the partition function but does result is a small change in magnitude of the damage energy. In reference [Ro94] Robinson summaries his previous work addressing the damage energy and the Kinchin-Pease formalism where $L = 2E_d/\kappa$ and κ=0.8, by saying:

> "However, the ansatz has improperly discounted electronic energy losses that occur for E < L. Moreover, $v(L) = \hat{L}/L < 1$, which contradicts a basic idea in the model. Since low-energy
>
> electronic losses occur only after the number of defects is already determined, they must be restored to the damage energy.
>
> …
>
> where $\hat{L}$ is the damage energy associated with the energy L."

The recommended tabulation for neutron microscopic displacement kerma factor can be found in latest version of the ASTM E722 standard, E722-09e1. These values are produced for silicon using the NJOY code with a displacement threshold energy of 25 eV and using the ^{28}Si ENDF/B-VI.8 cross section. Results produced using this cross section are similar to that when one uses other evaluated data sets [JENDL, JEF].

The latest 2013 ASTM book of standards for silicon microscopic displacement kerma factors, i.e. E722-09e1, are identical to those found in the 1994 version of the standard, i.e. E722-94. Nuclear data files have been updated since 1994. The latest U.S. Evaluated Nuclear Data File cross sections are found in the ENDF/B-VII.1 library [Ch11] and in the latest natural abundance data is found in Reference [Tu11]. Figure 15 compares the ASTM E722-94 recommended values for the silicon displacement kerma with that obtained by using the latest ENDF/B-VII.1 cross sections and with some historical analysis at high neutron energies [Vasil, Ko92, Hu93]. This most recent analysis uses:

- NJOY-2012 code
- ENDF/B-VII.1 cross sections
- Robinson fit to the LSS damage partition function
- E_d = 20.5 eV
- Silicon isotopes combined using their natural abundances, as shown in Table 2.

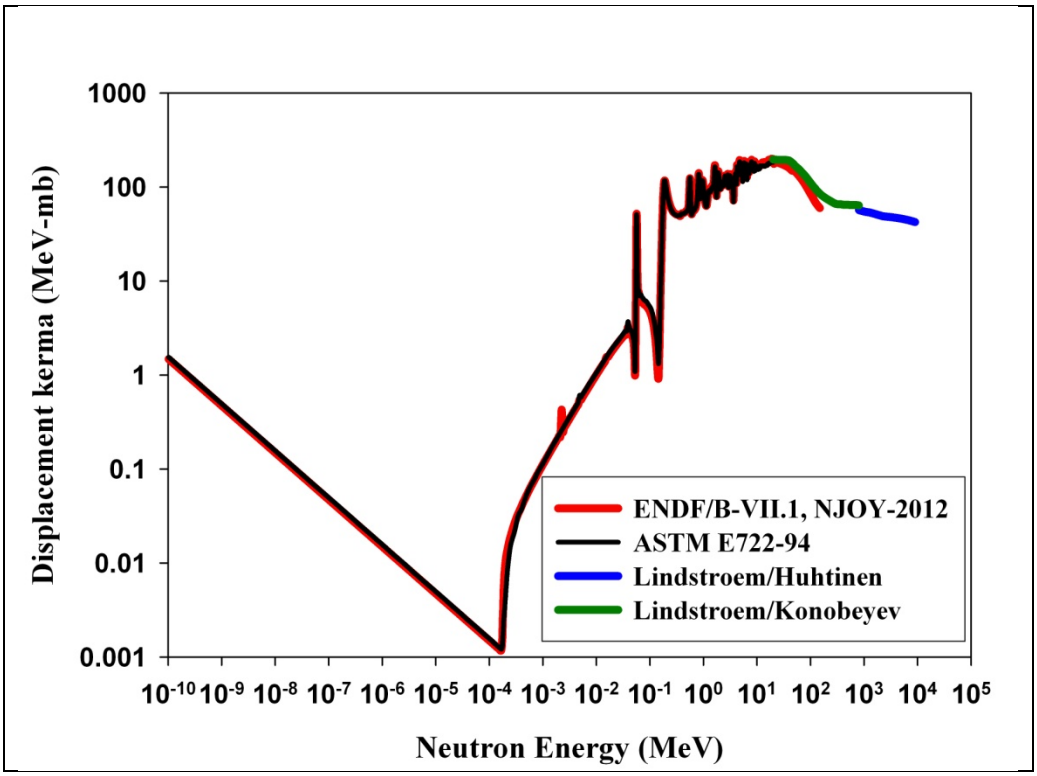

Figure 15: Comparison of Available Tabulations of the Silicon Displacement Kerma

The ENDF/B-VII.1 silicon displacement kerma is not significantly different from the values seen in the previous literature. Figures 16 and 17 display the ratio of the ENDF/B-VII displacement kerma and the ASTM E722-94 recommended displacement kerma. The difference is seen to, in general, be less than 10%. This difference is, in large part, due to the ASTM recommended value being derived from a pure ^{28}Si evaluation rather than an isotopic mixture that was used in processing the latest ENDF/B-VII cross sections. Some features that can be seen in the Figure 16 displacement kerma ratio include:

- There is a particularly noticeable spike in the kerma ratio at 2.25 keV. This is due to a resonance seen in the ^{30}Si isotope. Due to the isotopic mixtures, this resonance appears in the elemental ENDF/B-VII displacement kerma but not in the ASTM ^{28}Si displacement kerma.
- There is a spike in the ENDF/B-VII-to-ASTM displacement kerma ratio near the neutron energy where the elastic scattering reaction can first produce a recoil lattice atom with enough energy to displace atoms, e.g. ~130 eV. The ENDF/B-VII silicon elastic scattering was processed using a displacement threshold energy of 20.5 eV as compared to the ASTM displacement kerma that used a displacement threshold energy of 25 eV.

Figure 17 shows that, in the vicinity of 1-MeV, the neutron displacement kerma has only changed from the older ASTM E722-94 values by about 1%, thus there is no strong indication of a need to change the reference value used in conjunction with this updated curve.

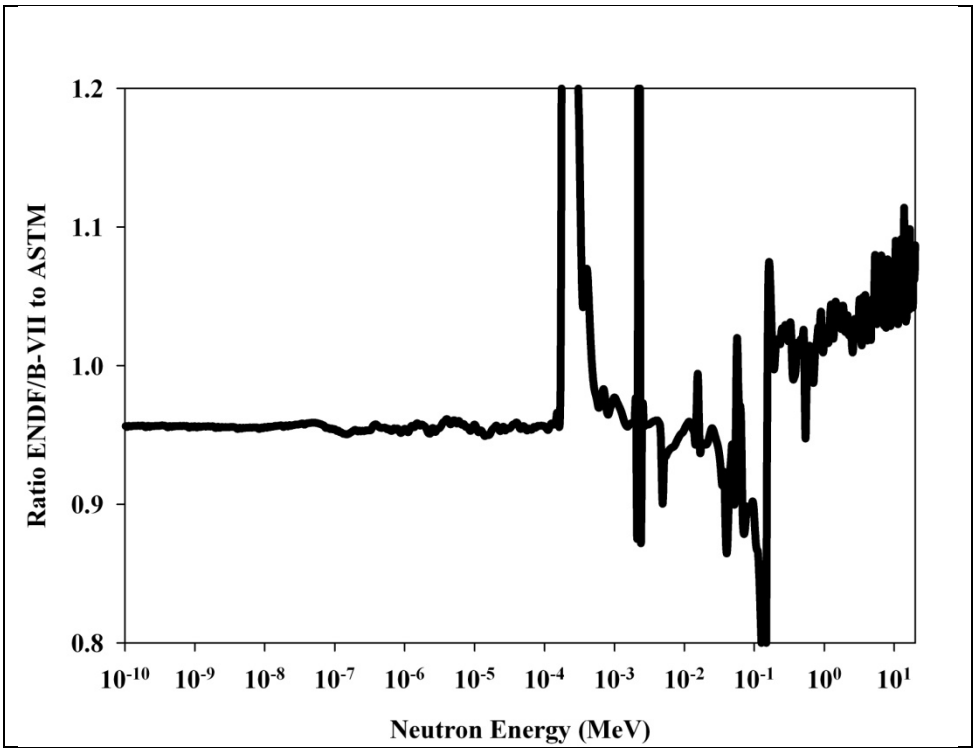

Figure 16: Ratio of ASTM E722-94 and the Latest NJOY-2012 Processed ENDF/B-VII.1 Silicon Displacement Kerma

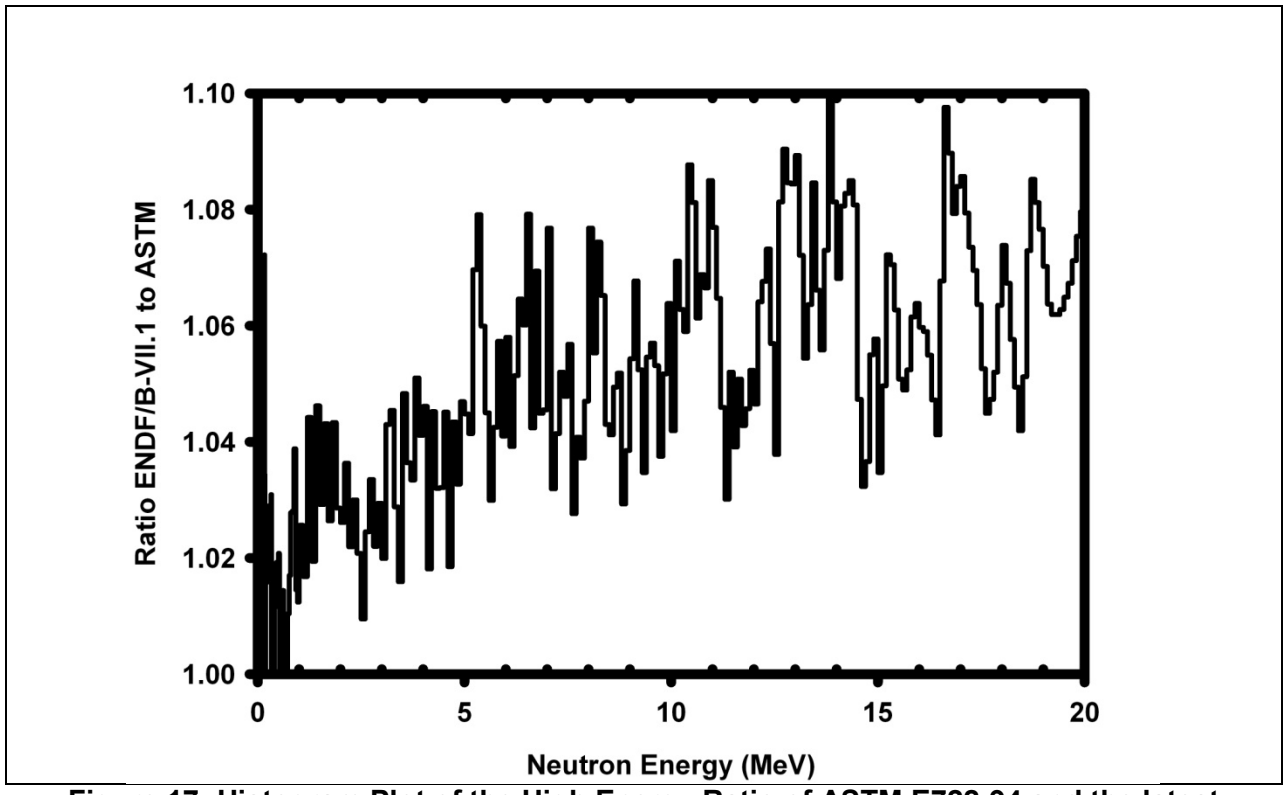

Figure 17: Histogram Plot of the High Energy Ratio of ASTM E722-94 and the latest NJOY-2012 processed ENDF/B-VII.1 Silicon Displacement Kerma

Table 2: Nuclear Data used in the Determination of the ^{nat}Si Displacement Kerma Factor

Isotope	ENDF/B-VII.1 MAT Designator	Natural Abundance (%)	Mass Excess (MeV)
^{28}Si	1425	92.223 (19)	-21.4927
^{29}Si	1428	4.685 (8)	-21.8950
^{30}Si	1431	3.092 (11)	-24.4329
Mass excess correction applied using 1 amu = 931.494013 MeV Data from Reference [Tu11]			

Table 3 provides a tabulation of the ENDF/B-VII.1 ^{nat}Si displacement kerma in units of MeV·mbarn and based on an E_d = 20.5 eV. The number of digits presented in the table for the displacement kerma does not indicate an accuracy, but, rather, are include to support traceability of the calculation with the nuclear data and processing code.

Table 3: ^{nat}Si Neutron Displacement Kerma

Bin Number	Lower Energy Bound (MeV)	Upper Energy Bound (MeV)	Energy Mid-point (MeV)	Displacement Kerma (MeV-mbarn)
1	1.4900E+02	1.5000E+02	1.4950E+02	5.982537E+01
2	1.4800E+02	1.4900E+02	1.4850E+02	6.008900E+01
3	1.4700E+02	1.4800E+02	1.4750E+02	6.036161E+01
4	1.4600E+02	1.4700E+02	1.4650E+02	6.063729E+01
5	1.4500E+02	1.4600E+02	1.4550E+02	6.092204E+01
6	1.4400E+02	1.4500E+02	1.4450E+02	6.121172E+01
7	1.4300E+02	1.4400E+02	1.4350E+02	6.151157E+01
8	1.4200E+02	1.4300E+02	1.4250E+02	6.181738E+01
9	1.4100E+02	1.4200E+02	1.4150E+02	6.213433E+01
10	1.4000E+02	1.4100E+02	1.4050E+02	6.245731E+01
11	1.3900E+02	1.4000E+02	1.3950E+02	6.277704E+01
12	1.3800E+02	1.3900E+02	1.3850E+02	6.309329E+01
13	1.3700E+02	1.3800E+02	1.3750E+02	6.341950E+01
14	1.3600E+02	1.3700E+02	1.3650E+02	6.374981E+01
15	1.3500E+02	1.3600E+02	1.3550E+02	6.408916E+01
16	1.3400E+02	1.3500E+02	1.3450E+02	6.443452E+01
17	1.3300E+02	1.3400E+02	1.3350E+02	6.478899E+01
18	1.3200E+02	1.3300E+02	1.3250E+02	6.514942E+01
19	1.3100E+02	1.3200E+02	1.3150E+02	6.552091E+01
20	1.3000E+02	1.3100E+02	1.3050E+02	6.589751E+01
21	1.2900E+02	1.3000E+02	1.2950E+02	6.630223E+01
22	1.2800E+02	1.2900E+02	1.2850E+02	6.672099E+01
23	1.2700E+02	1.2800E+02	1.2750E+02	6.714791E+01
24	1.2600E+02	1.2700E+02	1.2650E+02	6.757982E+01
25	1.2500E+02	1.2600E+02	1.2550E+02	6.802268E+01
26	1.2400E+02	1.2500E+02	1.2450E+02	6.847066E+01
27	1.2300E+02	1.2400E+02	1.2350E+02	6.893172E+01
28	1.2200E+02	1.2300E+02	1.2250E+02	6.939970E+01
29	1.2100E+02	1.2200E+02	1.2150E+02	6.988194E+01
30	1.2000E+02	1.2100E+02	1.2050E+02	7.037225E+01
31	1.1900E+02	1.2000E+02	1.1950E+02	7.095439E+01
32	1.1800E+02	1.1900E+02	1.1850E+02	7.158205E+01
33	1.1700E+02	1.1800E+02	1.1750E+02	7.222276E+01
34	1.1600E+02	1.1700E+02	1.1650E+02	7.287045E+01
35	1.1500E+02	1.1600E+02	1.1550E+02	7.353226E+01
36	1.1400E+02	1.1500E+02	1.1450E+02	7.420107E+01
37	1.1300E+02	1.1400E+02	1.1350E+02	7.488583E+01
38	1.1200E+02	1.1300E+02	1.1250E+02	7.557767E+01
39	1.1100E+02	1.1200E+02	1.1150E+02	7.628654E+01
40	1.1000E+02	1.1100E+02	1.1050E+02	7.700248E+01
41	1.0900E+02	1.1000E+02	1.0950E+02	7.771273E+01
42	1.0800E+02	1.0900E+02	1.0850E+02	7.842105E+01

43	1.0700E+02	1.0800E+02	1.0750E+02	7.914336E+01
44	1.0600E+02	1.0700E+02	1.0650E+02	7.987173E+01
45	1.0500E+02	1.0600E+02	1.0550E+02	8.061710E+01
46	1.0400E+02	1.0500E+02	1.0450E+02	8.136951E+01
47	1.0300E+02	1.0400E+02	1.0350E+02	8.214204E+01
48	1.0200E+02	1.0300E+02	1.0250E+02	8.292448E+01
49	1.0100E+02	1.0200E+02	1.0150E+02	8.373005E+01
50	1.0000E+02	1.0100E+02	1.0050E+02	8.454664E+01
51	9.9000E+01	1.0000E+02	9.9500E+01	8.538785E+01
52	9.8000E+01	9.9000E+01	9.8500E+01	8.625471E+01
53	9.7000E+01	9.8000E+01	9.7500E+01	8.714066E+01
54	9.6000E+01	9.7000E+01	9.6500E+01	8.804468E+01
55	9.5000E+01	9.6000E+01	9.5500E+01	8.896772E+01
56	9.4000E+01	9.5000E+01	9.4500E+01	8.990762E+01
57	9.3000E+01	9.4000E+01	9.3500E+01	9.086671E+01
58	9.2000E+01	9.3000E+01	9.2500E+01	9.184360E+01
59	9.1000E+01	9.2000E+01	9.1500E+01	9.283885E+01
60	9.0000E+01	9.1000E+01	9.0500E+01	9.385116E+01
61	8.9000E+01	9.0000E+01	8.9500E+01	9.490298E+01
62	8.8000E+01	8.9000E+01	8.8500E+01	9.596648E+01
63	8.7000E+01	8.8000E+01	8.7500E+01	9.702551E+01
64	8.6000E+01	8.7000E+01	8.6500E+01	9.810269E+01
65	8.5000E+01	8.6000E+01	8.5500E+01	9.921571E+01
66	8.4000E+01	8.5000E+01	8.4500E+01	1.003709E+02
67	8.3000E+01	8.4000E+01	8.3500E+01	1.015689E+02
68	8.2000E+01	8.3000E+01	8.2500E+01	1.028077E+02
69	8.1000E+01	8.2000E+01	8.1500E+01	1.040661E+02
70	8.0000E+01	8.1000E+01	8.0500E+01	1.053153E+02
71	7.9000E+01	8.0000E+01	7.9500E+01	1.065353E+02
72	7.8000E+01	7.9000E+01	7.8500E+01	1.077461E+02
73	7.7000E+01	7.8000E+01	7.7500E+01	1.089672E+02
74	7.6000E+01	7.7000E+01	7.6500E+01	1.102083E+02
75	7.5000E+01	7.6000E+01	7.5500E+01	1.114777E+02
76	7.4000E+01	7.5000E+01	7.4500E+01	1.127864E+02
77	7.3000E+01	7.4000E+01	7.3500E+01	1.141252E+02
78	7.2000E+01	7.3000E+01	7.2500E+01	1.154930E+02
79	7.1000E+01	7.2000E+01	7.1500E+01	1.168605E+02
80	7.0000E+01	7.1000E+01	7.0500E+01	1.182674E+02
81	6.9000E+01	7.0000E+01	6.9500E+01	1.196185E+02
82	6.8000E+01	6.9000E+01	6.8500E+01	1.209333E+02
83	6.7000E+01	6.8000E+01	6.7500E+01	1.222469E+02
84	6.6000E+01	6.7000E+01	6.6500E+01	1.235606E+02
85	6.5000E+01	6.6000E+01	6.5500E+01	1.248857E+02
86	6.4000E+01	6.5000E+01	6.4500E+01	1.262834E+02
87	6.3000E+01	6.4000E+01	6.3500E+01	1.277037E+02

88	6.2000E+01	6.3000E+01	6.2500E+01	1.291443E+02
89	6.1000E+01	6.2000E+01	6.1500E+01	1.306414E+02
90	6.0000E+01	6.1000E+01	6.0500E+01	1.321393E+02
91	5.9000E+01	6.0000E+01	5.9500E+01	1.336983E+02
92	5.8000E+01	5.9000E+01	5.8500E+01	1.352675E+02
93	5.7000E+01	5.8000E+01	5.7500E+01	1.368560E+02
94	5.6000E+01	5.7000E+01	5.6500E+01	1.384458E+02
95	5.5000E+01	5.6000E+01	5.5500E+01	1.400639E+02
96	5.4000E+01	5.5000E+01	5.4500E+01	1.416622E+02
97	5.3000E+01	5.4000E+01	5.3500E+01	1.432293E+02
98	5.2000E+01	5.3000E+01	5.2500E+01	1.447487E+02
99	5.1000E+01	5.2000E+01	5.1500E+01	1.462459E+02
100	5.0000E+01	5.1000E+01	5.0500E+01	1.477550E+02
101	4.9000E+01	5.0000E+01	4.9500E+01	1.484863E+02
102	4.8000E+01	4.9000E+01	4.8500E+01	1.486630E+02
103	4.7000E+01	4.8000E+01	4.7500E+01	1.488713E+02
104	4.6000E+01	4.7000E+01	4.6500E+01	1.491205E+02
105	4.5000E+01	4.6000E+01	4.5500E+01	1.494120E+02
106	4.4000E+01	4.5000E+01	4.4500E+01	1.506491E+02
107	4.3000E+01	4.4000E+01	4.3500E+01	1.526150E+02
108	4.2000E+01	4.3000E+01	4.2500E+01	1.546139E+02
109	4.1000E+01	4.2000E+01	4.1500E+01	1.566223E+02
110	4.0000E+01	4.1000E+01	4.0500E+01	1.585304E+02
111	3.9000E+01	4.0000E+01	3.9500E+01	1.603260E+02
112	3.8000E+01	3.9000E+01	3.8500E+01	1.620434E+02
113	3.7000E+01	3.8000E+01	3.7500E+01	1.636787E+02
114	3.6000E+01	3.7000E+01	3.6500E+01	1.652546E+02
115	3.5000E+01	3.6000E+01	3.5500E+01	1.667502E+02
116	3.4000E+01	3.5000E+01	3.4500E+01	1.682129E+02
117	3.3000E+01	3.4000E+01	3.3500E+01	1.696805E+02
118	3.2000E+01	3.3000E+01	3.2500E+01	1.710776E+02
119	3.1000E+01	3.2000E+01	3.1500E+01	1.724142E+02
120	3.0000E+01	3.1000E+01	3.0500E+01	1.737391E+02
121	2.9000E+01	3.0000E+01	2.9500E+01	1.751022E+02
122	2.8000E+01	2.9000E+01	2.8500E+01	1.765111E+02
123	2.7000E+01	2.8000E+01	2.7500E+01	1.778196E+02
124	2.6000E+01	2.7000E+01	2.6500E+01	1.790362E+02
125	2.5000E+01	2.6000E+01	2.5500E+01	1.801838E+02
126	2.4000E+01	2.5000E+01	2.4500E+01	1.812437E+02
127	2.3000E+01	2.4000E+01	2.3500E+01	1.819478E+02
128	2.2000E+01	2.3000E+01	2.2500E+01	1.823571E+02
129	2.1000E+01	2.2000E+01	2.1500E+01	1.808784E+02
130	2.0000E+01	2.1000E+01	2.0500E+01	1.777125E+02
131	1.9900E+01	2.0000E+01	1.9950E+01	1.974223E+02
132	1.9800E+01	1.9900E+01	1.9850E+01	1.967937E+02

133	1.9700E+01	1.9800E+01	1.9750E+01	1.961647E+02
134	1.9600E+01	1.9700E+01	1.9650E+01	1.955857E+02
135	1.9500E+01	1.9600E+01	1.9550E+01	1.952768E+02
136	1.9400E+01	1.9500E+01	1.9450E+01	1.950267E+02
137	1.9300E+01	1.9400E+01	1.9350E+01	1.949968E+02
138	1.9200E+01	1.9300E+01	1.9250E+01	1.951260E+02
139	1.9100E+01	1.9200E+01	1.9150E+01	1.955842E+02
140	1.9000E+01	1.9100E+01	1.9050E+01	1.969098E+02
141	1.8900E+01	1.9000E+01	1.8950E+01	1.982156E+02
142	1.8800E+01	1.8900E+01	1.8850E+01	1.991628E+02
143	1.8700E+01	1.8800E+01	1.8750E+01	1.999799E+02
144	1.8600E+01	1.8700E+01	1.8650E+01	1.978047E+02
145	1.8500E+01	1.8600E+01	1.8550E+01	1.938940E+02
146	1.8400E+01	1.8500E+01	1.8450E+01	1.920378E+02
147	1.8300E+01	1.8400E+01	1.8350E+01	1.930547E+02
148	1.8200E+01	1.8300E+01	1.8250E+01	1.941904E+02
149	1.8100E+01	1.8200E+01	1.8150E+01	1.956167E+02
150	1.8000E+01	1.8100E+01	1.8050E+01	1.964416E+02
151	1.7900E+01	1.8000E+01	1.7950E+01	1.941766E+02
152	1.7800E+01	1.7900E+01	1.7850E+01	1.917115E+02
153	1.7700E+01	1.7800E+01	1.7750E+01	1.905113E+02
154	1.7600E+01	1.7700E+01	1.7650E+01	1.897319E+02
155	1.7500E+01	1.7600E+01	1.7550E+01	1.907675E+02
156	1.7400E+01	1.7500E+01	1.7450E+01	1.921653E+02
157	1.7300E+01	1.7400E+01	1.7350E+01	1.923810E+02
158	1.7200E+01	1.7300E+01	1.7250E+01	1.922374E+02
159	1.7100E+01	1.7200E+01	1.7150E+01	1.924440E+02
160	1.7000E+01	1.7100E+01	1.7050E+01	1.926999E+02
161	1.6900E+01	1.7000E+01	1.6950E+01	1.921279E+02
162	1.6800E+01	1.6900E+01	1.6850E+01	1.915772E+02
163	1.6700E+01	1.6800E+01	1.6750E+01	1.937092E+02
164	1.6600E+01	1.6700E+01	1.6650E+01	1.953922E+02
165	1.6500E+01	1.6600E+01	1.6550E+01	1.903341E+02
166	1.6400E+01	1.6500E+01	1.6450E+01	1.856649E+02
167	1.6300E+01	1.6400E+01	1.6350E+01	1.865918E+02
168	1.6200E+01	1.6300E+01	1.6250E+01	1.877974E+02
169	1.6100E+01	1.6200E+01	1.6150E+01	1.883864E+02
170	1.6000E+01	1.6100E+01	1.6050E+01	1.883452E+02
171	1.5900E+01	1.6000E+01	1.5950E+01	1.875458E+02
172	1.5800E+01	1.5900E+01	1.5850E+01	1.843038E+02
173	1.5700E+01	1.5800E+01	1.5750E+01	1.803025E+02
174	1.5600E+01	1.5700E+01	1.5650E+01	1.792159E+02
175	1.5500E+01	1.5600E+01	1.5550E+01	1.793850E+02
176	1.5400E+01	1.5500E+01	1.5450E+01	1.812501E+02
177	1.5300E+01	1.5400E+01	1.5350E+01	1.824167E+02

178	1.5200E+01	1.5300E+01	1.5250E+01	1.825359E+02
179	1.5100E+01	1.5200E+01	1.5150E+01	1.785266E+02
180	1.5000E+01	1.5100E+01	1.5050E+01	1.758240E+02
181	1.4900E+01	1.5000E+01	1.4950E+01	1.795943E+02
182	1.4800E+01	1.4900E+01	1.4850E+01	1.789953E+02
183	1.4700E+01	1.4800E+01	1.4750E+01	1.757235E+02
184	1.4600E+01	1.4700E+01	1.4650E+01	1.748468E+02
185	1.4500E+01	1.4600E+01	1.4550E+01	1.772119E+02
186	1.4400E+01	1.4500E+01	1.4450E+01	1.823635E+02
187	1.4300E+01	1.4400E+01	1.4350E+01	1.822088E+02
188	1.4200E+01	1.4300E+01	1.4250E+01	1.809770E+02
189	1.4100E+01	1.4200E+01	1.4150E+01	1.797454E+02
190	1.4000E+01	1.4100E+01	1.4050E+01	1.768178E+02
191	1.3900E+01	1.4000E+01	1.3950E+01	1.788456E+02
192	1.3800E+01	1.3900E+01	1.3850E+01	1.847664E+02
193	1.3700E+01	1.3800E+01	1.3750E+01	1.784289E+02
194	1.3600E+01	1.3700E+01	1.3650E+01	1.760411E+02
195	1.3500E+01	1.3600E+01	1.3550E+01	1.782104E+02
196	1.3400E+01	1.3500E+01	1.3450E+01	1.816978E+02
197	1.3300E+01	1.3400E+01	1.3350E+01	1.785120E+02
198	1.3200E+01	1.3300E+01	1.3250E+01	1.772619E+02
199	1.3100E+01	1.3200E+01	1.3150E+01	1.805299E+02
200	1.3000E+01	1.3100E+01	1.3050E+01	1.837276E+02
201	1.2900E+01	1.3000E+01	1.2950E+01	1.828576E+02
202	1.2800E+01	1.2900E+01	1.2850E+01	1.825162E+02
203	1.2700E+01	1.2800E+01	1.2750E+01	1.831141E+02
204	1.2600E+01	1.2700E+01	1.2650E+01	1.812270E+02
205	1.2500E+01	1.2600E+01	1.2550E+01	1.735857E+02
206	1.2400E+01	1.2500E+01	1.2450E+01	1.767395E+02
207	1.2300E+01	1.2400E+01	1.2350E+01	1.797322E+02
208	1.2200E+01	1.2300E+01	1.2250E+01	1.790482E+02
209	1.2100E+01	1.2200E+01	1.2150E+01	1.787140E+02
210	1.2000E+01	1.2100E+01	1.2050E+01	1.759861E+02
211	1.1900E+01	1.2000E+01	1.1950E+01	1.743238E+02
212	1.1800E+01	1.1900E+01	1.1850E+01	1.730297E+02
213	1.1700E+01	1.1800E+01	1.1750E+01	1.727131E+02
214	1.1600E+01	1.1700E+01	1.1650E+01	1.742102E+02
215	1.1500E+01	1.1600E+01	1.1550E+01	1.752101E+02
216	1.1400E+01	1.1500E+01	1.1450E+01	1.739761E+02
217	1.1300E+01	1.1400E+01	1.1350E+01	1.710272E+02
218	1.1200E+01	1.1300E+01	1.1250E+01	1.668493E+02
219	1.1100E+01	1.1200E+01	1.1150E+01	1.656722E+02
220	1.1000E+01	1.1100E+01	1.1050E+01	1.709562E+02
221	1.0900E+01	1.1000E+01	1.0950E+01	1.736557E+02
222	1.0800E+01	1.0900E+01	1.0850E+01	1.737472E+02

223	1.0700E+01	1.0800E+01	1.0750E+01	1.699377E+02
224	1.0600E+01	1.0700E+01	1.0650E+01	1.650493E+02
225	1.0500E+01	1.0600E+01	1.0550E+01	1.671501E+02
226	1.0400E+01	1.0500E+01	1.0450E+01	1.683353E+02
227	1.0300E+01	1.0400E+01	1.0350E+01	1.743913E+02
228	1.0200E+01	1.0300E+01	1.0250E+01	1.736199E+02
229	1.0100E+01	1.0200E+01	1.0150E+01	1.752688E+02
230	1.0000E+01	1.0100E+01	1.0050E+01	1.731668E+02
231	9.9000E+00	1.0000E+01	9.9500E+00	1.749790E+02
232	9.8000E+00	9.9000E+00	9.8500E+00	1.725378E+02
233	9.7000E+00	9.8000E+00	9.7500E+00	1.680329E+02
234	9.6000E+00	9.7000E+00	9.6500E+00	1.643838E+02
235	9.5000E+00	9.6000E+00	9.5500E+00	1.737880E+02
236	9.4000E+00	9.5000E+00	9.4500E+00	1.790983E+02
237	9.3000E+00	9.4000E+00	9.3500E+00	1.719788E+02
238	9.2000E+00	9.3000E+00	9.2500E+00	1.585817E+02
239	9.1000E+00	9.2000E+00	9.1500E+00	1.642940E+02
240	9.0000E+00	9.1000E+00	9.0500E+00	1.840511E+02
241	8.9000E+00	9.0000E+00	8.9500E+00	1.844116E+02
242	8.8000E+00	8.9000E+00	8.8500E+00	1.649178E+02
243	8.7000E+00	8.8000E+00	8.7500E+00	1.543472E+02
244	8.6000E+00	8.7000E+00	8.6500E+00	1.719501E+02
245	8.5000E+00	8.6000E+00	8.5500E+00	1.726602E+02
246	8.4000E+00	8.5000E+00	8.4500E+00	1.737737E+02
247	8.3000E+00	8.4000E+00	8.3500E+00	1.725798E+02
248	8.2000E+00	8.3000E+00	8.2500E+00	1.702067E+02
249	8.1000E+00	8.2000E+00	8.1500E+00	1.629746E+02
250	8.0000E+00	8.1000E+00	8.0500E+00	1.776760E+02
251	7.9000E+00	8.0000E+00	7.9500E+00	1.951620E+02
252	7.8000E+00	7.9000E+00	7.8500E+00	1.818550E+02
253	7.7000E+00	7.8000E+00	7.7500E+00	1.819305E+02
254	7.6000E+00	7.7000E+00	7.6500E+00	1.750185E+02
255	7.5000E+00	7.6000E+00	7.5500E+00	1.721660E+02
256	7.4000E+00	7.5000E+00	7.4500E+00	1.750415E+02
257	7.3000E+00	7.4000E+00	7.3500E+00	1.771959E+02
258	7.2000E+00	7.3000E+00	7.2500E+00	1.762695E+02
259	7.1000E+00	7.2000E+00	7.1500E+00	1.436002E+02
260	7.0000E+00	7.1000E+00	7.0500E+00	1.734795E+02
261	6.9000E+00	7.0000E+00	6.9500E+00	1.482196E+02
262	6.8000E+00	6.9000E+00	6.8500E+00	1.534783E+02
263	6.7000E+00	6.8000E+00	6.7500E+00	1.735103E+02
264	6.6000E+00	6.7000E+00	6.6500E+00	1.573224E+02
265	6.5000E+00	6.6000E+00	6.5500E+00	1.287192E+02
266	6.4000E+00	6.5000E+00	6.4500E+00	1.476404E+02
267	6.3000E+00	6.4000E+00	6.3500E+00	1.597855E+02

268	6.2000E+00	6.3000E+00	6.2500E+00	1.843861E+02
269	6.1000E+00	6.2000E+00	6.1500E+00	1.327218E+02
270	6.0000E+00	6.1000E+00	6.0500E+00	1.618680E+02
271	5.9000E+00	6.0000E+00	5.9500E+00	1.427187E+02
272	5.8000E+00	5.9000E+00	5.8500E+00	1.741425E+02
273	5.7000E+00	5.8000E+00	5.7500E+00	1.877007E+02
274	5.6000E+00	5.7000E+00	5.6500E+00	1.566230E+02
275	5.5000E+00	5.6000E+00	5.5500E+00	1.521489E+02
276	5.4000E+00	5.5000E+00	5.4500E+00	1.239832E+02
277	5.3000E+00	5.4000E+00	5.3500E+00	1.296535E+02
278	5.2000E+00	5.3000E+00	5.2500E+00	1.558386E+02
279	5.1000E+00	5.2000E+00	5.1500E+00	1.773568E+02
280	5.0000E+00	5.1000E+00	5.0500E+00	1.558377E+02
281	4.9000E+00	5.0000E+00	4.9500E+00	1.523304E+02
282	4.8000E+00	4.9000E+00	4.8500E+00	1.659307E+02
283	4.7000E+00	4.8000E+00	4.7500E+00	1.936596E+02
284	4.6000E+00	4.7000E+00	4.6500E+00	1.615820E+02
285	4.5000E+00	4.6000E+00	4.5500E+00	1.446275E+02
286	4.4000E+00	4.5000E+00	4.4500E+00	1.454466E+02
287	4.3000E+00	4.4000E+00	4.3500E+00	1.391803E+02
288	4.2000E+00	4.3000E+00	4.2500E+00	1.718335E+02
289	4.1000E+00	4.2000E+00	4.1500E+00	1.106764E+02
290	4.0000E+00	4.1000E+00	4.0500E+00	1.377047E+02
291	3.9000E+00	4.0000E+00	3.9500E+00	1.398655E+02
292	3.8000E+00	3.9000E+00	3.8500E+00	1.143880E+02
293	3.7000E+00	3.8000E+00	3.7500E+00	1.189786E+02
294	3.6000E+00	3.7000E+00	3.6500E+00	7.205235E+01
295	3.5000E+00	3.6000E+00	3.5500E+00	1.166491E+02
296	3.4000E+00	3.5000E+00	3.4500E+00	1.209489E+02
297	3.3000E+00	3.4000E+00	3.3500E+00	1.171509E+02
298	3.2000E+00	3.3000E+00	3.2500E+00	1.233782E+02
299	3.1000E+00	3.2000E+00	3.1500E+00	1.371566E+02
300	3.0000E+00	3.1000E+00	3.0500E+00	1.225885E+02
301	2.9000E+00	3.0000E+00	2.9500E+00	1.017558E+02
302	2.8000E+00	2.9000E+00	2.8500E+00	1.380089E+02
303	2.7000E+00	2.8000E+00	2.7500E+00	1.104907E+02
304	2.6000E+00	2.7000E+00	2.6500E+00	1.185021E+02
305	2.5000E+00	2.6000E+00	2.5500E+00	1.324304E+02
306	2.4000E+00	2.5000E+00	2.4500E+00	1.213907E+02
307	2.3000E+00	2.4000E+00	2.3500E+00	1.059031E+02
308	2.2000E+00	2.3000E+00	2.2500E+00	1.077988E+02
309	2.1000E+00	2.2000E+00	2.1500E+00	1.108041E+02
310	2.0000E+00	2.1000E+00	2.0500E+00	9.770454E+01
311	1.9000E+00	2.0000E+00	1.9500E+00	1.330953E+02
312	1.8000E+00	1.9000E+00	1.8500E+00	1.348081E+02

313	1.7000E+00	1.8000E+00	1.7500E+00	8.041240E+01
314	1.6000E+00	1.7000E+00	1.6500E+00	1.700470E+02
315	1.5000E+00	1.6000E+00	1.5500E+00	1.090791E+02
316	1.4000E+00	1.5000E+00	1.4500E+00	1.035514E+02
317	1.3000E+00	1.4000E+00	1.3500E+00	9.048161E+01
318	1.2000E+00	1.3000E+00	1.2500E+00	9.292444E+01
319	1.1000E+00	1.2000E+00	1.1500E+00	6.372608E+01
320	1.0000E+00	1.1000E+00	1.0500E+00	7.763185E+01
321	9.6000E-01	1.0000E+00	9.8000E-01	1.131754E+02
322	9.2000E-01	9.6000E-01	9.4000E-01	1.131017E+02
323	8.8000E-01	9.2000E-01	9.0000E-01	9.118594E+01
324	8.4000E-01	8.8000E-01	8.6000E-01	8.053426E+01
325	8.0000E-01	8.4000E-01	8.2000E-01	1.406037E+02
326	7.6000E-01	8.0000E-01	7.8000E-01	8.943636E+01
327	7.2000E-01	7.6000E-01	7.4000E-01	6.524542E+01
328	6.9000E-01	7.2000E-01	7.0500E-01	5.860863E+01
329	6.6000E-01	6.9000E-01	6.7500E-01	5.631161E+01
330	6.3000E-01	6.6000E-01	6.4500E-01	5.497674E+01
331	6.0000E-01	6.3000E-01	6.1500E-01	5.337400E+01
332	5.7500E-01	6.0000E-01	5.8750E-01	5.845961E+01
333	5.5000E-01	5.7500E-01	5.6250E-01	1.238521E+02
334	5.2500E-01	5.5000E-01	5.3750E-01	7.387514E+01
335	5.0000E-01	5.2500E-01	5.1250E-01	5.861309E+01
336	4.7500E-01	5.0000E-01	4.8750E-01	5.610784E+01
337	4.5000E-01	4.7500E-01	4.6250E-01	5.453479E+01
338	4.2500E-01	4.5000E-01	4.3750E-01	5.326508E+01
339	4.0000E-01	4.2500E-01	4.1250E-01	5.275325E+01
340	3.8000E-01	4.0000E-01	3.9000E-01	5.195346E+01
341	3.6000E-01	3.8000E-01	3.7000E-01	4.929888E+01
342	3.4000E-01	3.6000E-01	3.5000E-01	4.988140E+01
343	3.2000E-01	3.4000E-01	3.3000E-01	5.080230E+01
344	3.0000E-01	3.2000E-01	3.1000E-01	5.115308E+01
345	2.8000E-01	3.0000E-01	2.9000E-01	5.263600E+01
346	2.7000E-01	2.8000E-01	2.7500E-01	5.408311E+01
347	2.5500E-01	2.7000E-01	2.6250E-01	5.621729E+01
348	2.4000E-01	2.5500E-01	2.4750E-01	6.002709E+01
349	2.3000E-01	2.4000E-01	2.3500E-01	6.508627E+01
350	2.2000E-01	2.3000E-01	2.2500E-01	7.103450E+01
351	2.1000E-01	2.2000E-01	2.1500E-01	8.003430E+01
352	2.0000E-01	2.1000E-01	2.0500E-01	9.342780E+01
353	1.9000E-01	2.0000E-01	1.9500E-01	1.112661E+02
354	1.8000E-01	1.9000E-01	1.8500E-01	1.143433E+02
355	1.7000E-01	1.8000E-01	1.7500E-01	6.670408E+01
356	1.6000E-01	1.7000E-01	1.6500E-01	2.042371E+01
357	1.5000E-01	1.6000E-01	1.5500E-01	4.389965E+00

358	1.4250E-01	1.5000E-01	1.4625E-01	1.001896E+00
359	1.3500E-01	1.4250E-01	1.3875E-01	1.144801E+00
360	1.2750E-01	1.3500E-01	1.3125E-01	1.886640E+00
361	1.2000E-01	1.2750E-01	1.2375E-01	2.722165E+00
362	1.1500E-01	1.2000E-01	1.1750E-01	3.374691E+00
363	1.1000E-01	1.1500E-01	1.1250E-01	3.836533E+00
364	1.0500E-01	1.1000E-01	1.0750E-01	4.231811E+00
365	1.0000E-01	1.0500E-01	1.0250E-01	4.577435E+00
366	9.6000E-02	1.0000E-01	9.8000E-02	4.858211E+00
367	9.2000E-02	9.6000E-02	9.4000E-02	5.061763E+00
368	8.8000E-02	9.2000E-02	9.0000E-02	5.239306E+00
369	8.4000E-02	8.8000E-02	8.6000E-02	5.416013E+00
370	8.0000E-02	8.4000E-02	8.2000E-02	5.530739E+00
371	7.6000E-02	8.0000E-02	7.8000E-02	5.667758E+00
372	7.2000E-02	7.6000E-02	7.4000E-02	5.824413E+00
373	6.9000E-02	7.2000E-02	7.0500E-02	6.004439E+00
374	6.6000E-02	6.9000E-02	6.7500E-02	6.452232E+00
375	6.3000E-02	6.6000E-02	6.4500E-02	6.704520E+00
376	6.0000E-02	6.3000E-02	6.150001E-02	7.759747E+00
377	5.7500E-02	6.0000E-02	5.8750E-02	1.131117E+01
378	5.5000E-02	5.7500E-02	5.6250E-02	4.881800E+01
379	5.2500E-02	5.5000E-02	5.3750E-02	1.394853E+00
380	5.0000E-02	5.2500E-02	5.1250E-02	1.665855E+00
381	4.7500E-02	5.0000E-02	4.8750E-02	2.324566E+00
382	4.5000E-02	4.7500E-02	4.6250E-02	2.627535E+00
383	4.2500E-02	4.5000E-02	4.3750E-02	2.766006E+00
384	4.0000E-02	4.2500E-02	4.1250E-02	2.815044E+00
385	3.8000E-02	4.0000E-02	3.9000E-02	3.236911E+00
386	3.6000E-02	3.8000E-02	3.7000E-02	2.761191E+00
387	3.4000E-02	3.6000E-02	3.5000E-02	2.694322E+00
388	3.2000E-02	3.4000E-02	3.3000E-02	2.615048E+00
389	3.0000E-02	3.2000E-02	3.1000E-02	2.523839E+00
390	2.8000E-02	3.0000E-02	2.9000E-02	2.416137E+00
391	2.7000E-02	2.8000E-02	2.7500E-02	2.327857E+00
392	2.5500E-02	2.7000E-02	2.6250E-02	2.251406E+00
393	2.4000E-02	2.5500E-02	2.4750E-02	2.159320E+00
394	2.3000E-02	2.4000E-02	2.3500E-02	2.075862E+00
395	2.2000E-02	2.3000E-02	2.2500E-02	2.006089E+00
396	2.1000E-02	2.2000E-02	2.1500E-02	1.936267E+00
397	2.0000E-02	2.1000E-02	2.0500E-02	1.866401E+00
398	1.9000E-02	2.0000E-02	1.9500E-02	1.793231E+00
399	1.8000E-02	1.9000E-02	1.8500E-02	1.716946E+00
400	1.7000E-02	1.8000E-02	1.7500E-02	1.640070E+00
401	1.6000E-02	1.7000E-02	1.6500E-02	1.560138E+00
402	1.5000E-02	1.6000E-02	1.5500E-02	1.556516E+00

403	1.4250E-02	1.5000E-02	1.4625E-02	1.408101E+00
404	1.3500E-02	1.4250E-02	1.3875E-02	1.344240E+00
405	1.2750E-02	1.3500E-02	1.3125E-02	1.280620E+00
406	1.2000E-02	1.2750E-02	1.2375E-02	1.216535E+00
407	1.1500E-02	1.2000E-02	1.1750E-02	1.161918E+00
408	1.1000E-02	1.1500E-02	1.1250E-02	1.117882E+00
409	1.0500E-02	1.1000E-02	1.0750E-02	1.073083E+00
410	1.0000E-02	1.0500E-02	1.0250E-02	1.028187E+00
411	9.6000E-03	1.0000E-02	9.8000E-03	9.874197E-01
412	9.2000E-03	9.6000E-03	9.4000E-03	9.506696E-01
413	8.8000E-03	9.2000E-03	9.0000E-03	9.139211E-01
414	8.4000E-03	8.8000E-03	8.6000E-03	8.768218E-01
415	8.0000E-03	8.4000E-03	8.2000E-03	8.391631E-01
416	7.6000E-03	8.0000E-03	7.8000E-03	8.014963E-01
417	7.2000E-03	7.6000E-03	7.4000E-03	7.636029E-01
418	6.9000E-03	7.2000E-03	7.0500E-03	7.300621E-01
419	6.6000E-03	6.9000E-03	6.7500E-03	7.012189E-01
420	6.3000E-03	6.6000E-03	6.4500E-03	6.723806E-01
421	6.0000E-03	6.3000E-03	6.1500E-03	6.433160E-01
422	5.7500E-03	6.0000E-03	5.8750E-03	6.163418E-01
423	5.5000E-03	5.7500E-03	5.6250E-03	5.917502E-01
424	5.2500E-03	5.5000E-03	5.3750E-03	5.670536E-01
425	5.0000E-03	5.2500E-03	5.1250E-03	5.426664E-01
426	4.7500E-03	5.0000E-03	4.8750E-03	5.478224E-01
427	4.5000E-03	4.7500E-03	4.6250E-03	4.921758E-01
428	4.2500E-03	4.5000E-03	4.3750E-03	4.669758E-01
429	4.0000E-03	4.2500E-03	4.1250E-03	4.417112E-01
430	3.8000E-03	4.0000E-03	3.9000E-03	4.189391E-01
431	3.6000E-03	3.8000E-03	3.7000E-03	3.985144E-01
432	3.4000E-03	3.6000E-03	3.5000E-03	3.780234E-01
433	3.2000E-03	3.4000E-03	3.3000E-03	3.573080E-01
434	3.0000E-03	3.2000E-03	3.1000E-03	3.365366E-01
435	2.8000E-03	3.0000E-03	2.9000E-03	3.157687E-01
436	2.7000E-03	2.8000E-03	2.7500E-03	3.002674E-01
437	2.5500E-03	2.7000E-03	2.6250E-03	2.870274E-01
438	2.4000E-03	2.5500E-03	2.4750E-03	2.711862E-01
439	2.3000E-03	2.4000E-03	2.3500E-03	2.582637E-01
440	2.2000E-03	2.3000E-03	2.2500E-03	4.285303E-01
441	2.1000E-03	2.2000E-03	2.1500E-03	2.373112E-01
442	2.0000E-03	2.1000E-03	2.0500E-03	2.260708E-01
443	1.9000E-03	2.0000E-03	1.9500E-03	2.153233E-01
444	1.8000E-03	1.9000E-03	1.8500E-03	2.045339E-01
445	1.7000E-03	1.8000E-03	1.7500E-03	1.937540E-01
446	1.6000E-03	1.7000E-03	1.6500E-03	1.829727E-01
447	1.5000E-03	1.6000E-03	1.5500E-03	1.720326E-01

448	1.4250E-03	1.5000E-03	1.4625E-03	1.624055E-01
449	1.3500E-03	1.4250E-03	1.3875E-03	1.541113E-01
450	1.2750E-03	1.3500E-03	1.3125E-03	1.459994E-01
451	1.2000E-03	1.2750E-03	1.2375E-03	1.378551E-01
452	1.1500E-03	1.2000E-03	1.1750E-03	1.309130E-01
453	1.1000E-03	1.1500E-03	1.1250E-03	1.253166E-01
454	1.0500E-03	1.1000E-03	1.0750E-03	1.197011E-01
455	1.0000E-03	1.0500E-03	1.0250E-03	1.140764E-01
456	9.6000E-04	1.0000E-03	9.8000E-04	1.089957E-01
457	9.2000E-04	9.6000E-04	9.4000E-04	1.044395E-01
458	8.8000E-04	9.2000E-04	9.0000E-04	9.987921E-02
459	8.4000E-04	8.8000E-04	8.6000E-04	9.530343E-02
460	8.0000E-04	8.4000E-04	8.2000E-04	9.069958E-02
461	7.6000E-04	8.0000E-04	7.8000E-04	8.607882E-02
462	7.2000E-04	7.6000E-04	7.4000E-04	8.144432E-02
463	6.9000E-04	7.2000E-04	7.0500E-04	7.738508E-02
464	6.6000E-04	6.9000E-04	6.7500E-04	7.388832E-02
465	6.3000E-04	6.6000E-04	6.4500E-04	7.038044E-02
466	6.0000E-04	6.3000E-04	6.1500E-04	6.686015E-02
467	5.7500E-04	6.0000E-04	5.8750E-04	6.361766E-02
468	5.5000E-04	5.7500E-04	5.6250E-04	6.065090E-02
469	5.2500E-04	5.5000E-04	5.3750E-04	5.760463E-02
470	5.0000E-04	5.2500E-04	5.1250E-04	5.454441E-02
471	4.7500E-04	5.0000E-04	4.8750E-04	5.136848E-02
472	4.5000E-04	4.7500E-04	4.6250E-04	4.811422E-02
473	4.2500E-04	4.5000E-04	4.3750E-04	4.506059E-02
474	4.0000E-04	4.2500E-04	4.1250E-04	4.182278E-02
475	3.8000E-04	4.0000E-04	3.9000E-04	3.875193E-02
476	3.6000E-04	3.8000E-04	3.7000E-04	3.631544E-02
477	3.4000E-04	3.6000E-04	3.5000E-04	3.391288E-02
478	3.2000E-04	3.4000E-04	3.3000E-04	3.126043E-02
479	3.0000E-04	3.2000E-04	3.1000E-04	2.849958E-02
480	2.8000E-04	3.0000E-04	2.9000E-04	2.549538E-02
481	2.7000E-04	2.8000E-04	2.7500E-04	2.322776E-02
482	2.5500E-04	2.7000E-04	2.6250E-04	2.124416E-02
483	2.4000E-04	2.5500E-04	2.4750E-04	1.885846E-02
484	2.3000E-04	2.4000E-04	2.3500E-04	1.683389E-02
485	2.2000E-04	2.3000E-04	2.2500E-04	1.509236E-02
486	2.1000E-04	2.2000E-04	2.1500E-04	1.325680E-02
487	2.0000E-04	2.1000E-04	2.0500E-04	1.128237E-02
488	1.9000E-04	2.0000E-04	1.9500E-04	8.452462E-03
489	1.8000E-04	1.9000E-04	1.8500E-04	4.783556E-03
490	1.7000E-04	1.8000E-04	1.7500E-04	1.586685E-03
491	1.6000E-04	1.7000E-04	1.6500E-04	1.167438E-03
492	1.5000E-04	1.6000E-04	1.5500E-04	1.204608E-03

493	1.4250E-04	1.5000E-04	1.4625E-04	1.240012E-03
494	1.3500E-04	1.4250E-04	1.3875E-04	1.272877E-03
495	1.2750E-04	1.3500E-04	1.3125E-04	1.309168E-03
496	1.2000E-04	1.2750E-04	1.2375E-04	1.347998E-03
497	1.1500E-04	1.2000E-04	1.1750E-04	1.383702E-03
498	1.1000E-04	1.1500E-04	1.1250E-04	1.413338E-03
499	1.0500E-04	1.1000E-04	1.0750E-04	1.446982E-03
500	1.0000E-04	1.0500E-04	1.0250E-04	1.481218E-03
501	9.6000E-05	1.0000E-04	9.8000E-05	1.514867E-03
502	9.2000E-05	9.6000E-05	9.4000E-05	1.547929E-03
503	8.8000E-05	9.2000E-05	9.0000E-05	1.580986E-03
504	8.4000E-05	8.8000E-05	8.6000E-05	1.616201E-03
505	8.0000E-05	8.4000E-05	8.2000E-05	1.655033E-03
506	7.6000E-05	8.0000E-05	7.8000E-05	1.697291E-03
507	7.2000E-05	7.6000E-05	7.4000E-05	1.742383E-03
508	6.9000E-05	7.2000E-05	7.0500E-05	1.785130E-03
509	6.6000E-05	6.9000E-05	6.7500E-05	1.824350E-03
510	6.3000E-05	6.6000E-05	6.4500E-05	1.866705E-03
511	6.0000E-05	6.3000E-05	6.1500E-05	1.911406E-03
512	5.7500E-05	6.0000E-05	5.8750E-05	1.956307E-03
513	5.5000E-05	5.7500E-05	5.6250E-05	1.998267E-03
514	5.2500E-05	5.5000E-05	5.3750E-05	2.045805E-03
515	5.0000E-05	5.2500E-05	5.1250E-05	2.094225E-03
516	4.7500E-05	5.0000E-05	4.8750E-05	2.146551E-03
517	4.5000E-05	4.7500E-05	4.6250E-05	2.203487E-03
518	4.2500E-05	4.5000E-05	4.3750E-05	2.266084E-03
519	4.0000E-05	4.2500E-05	4.1250E-05	2.333973E-03
520	3.8000E-05	4.0000E-05	3.9000E-05	2.399704E-03
521	3.6000E-05	3.8000E-05	3.7000E-05	2.464949E-03
522	3.4000E-05	3.6000E-05	3.5000E-05	2.533518E-03
523	3.2000E-05	3.4000E-05	3.3000E-05	2.610886E-03
524	3.0000E-05	3.2000E-05	3.1000E-05	2.692761E-03
525	2.8000E-05	3.0000E-05	2.9000E-05	2.786080E-03
526	2.7000E-05	2.8000E-05	2.7500E-05	2.857781E-03
527	2.5500E-05	2.7000E-05	2.6250E-05	2.929086E-03
528	2.4000E-05	2.5500E-05	2.4750E-05	3.015857E-03
529	2.3000E-05	2.4000E-05	2.3500E-05	3.091072E-03
530	2.2000E-05	2.3000E-05	2.2500E-05	3.159446E-03
531	2.1000E-05	2.2000E-05	2.1500E-05	3.231838E-03
532	2.0000E-05	2.1000E-05	2.0500E-05	3.310186E-03
533	1.9000E-05	2.0000E-05	1.9500E-05	3.395679E-03
534	1.8000E-05	1.9000E-05	1.8500E-05	3.488208E-03
535	1.7000E-05	1.8000E-05	1.7500E-05	3.582607E-03
536	1.6000E-05	1.7000E-05	1.6500E-05	3.689127E-03
537	1.5000E-05	1.6000E-05	1.5500E-05	3.806803E-03

538	1.4250E-05	1.5000E-05	1.4625E-05	3.918904E-03
539	1.3500E-05	1.4250E-05	1.3875E-05	4.023078E-03
540	1.2750E-05	1.3500E-05	1.3125E-05	4.138113E-03
541	1.2000E-05	1.2750E-05	1.2375E-05	4.260872E-03
542	1.1500E-05	1.2000E-05	1.1750E-05	4.374144E-03
543	1.1000E-05	1.1500E-05	1.1250E-05	4.468050E-03
544	1.0500E-05	1.1000E-05	1.0750E-05	4.574474E-03
545	1.0000E-05	1.0500E-05	1.0250E-05	4.682956E-03
546	9.6000E-06	1.0000E-05	9.8000E-06	4.789381E-03
547	9.2000E-06	9.6000E-06	9.4000E-06	4.893946E-03
548	8.8000E-06	9.2000E-06	9.0000E-06	4.998510E-03
549	8.4000E-06	8.8000E-06	8.6000E-06	5.109738E-03
550	8.0000E-06	8.4000E-06	8.2000E-06	5.232397E-03
551	7.6000E-06	8.0000E-06	7.8000E-06	5.366212E-03
552	7.2000E-06	7.6000E-06	7.4000E-06	5.508929E-03
553	6.9000E-06	7.2000E-06	7.0500E-06	5.644404E-03
554	6.6000E-06	6.9000E-06	6.7500E-06	5.768537E-03
555	6.3000E-06	6.6000E-06	6.4500E-06	5.902450E-03
556	6.0000E-06	6.3000E-06	6.1500E-06	6.044184E-03
557	5.7500E-06	6.0000E-06	5.8750E-06	6.186510E-03
558	5.5000E-06	5.7500E-06	5.6250E-06	6.319249E-03
559	5.2500E-06	5.5000E-06	5.3750E-06	6.469495E-03
560	5.0000E-06	5.2500E-06	5.1250E-06	6.622585E-03
561	4.7500E-06	5.0000E-06	4.8750E-06	6.787799E-03
562	4.5000E-06	4.7500E-06	4.6250E-06	6.967975E-03
563	4.2500E-06	4.5000E-06	4.3750E-06	7.165866E-03
564	4.0000E-06	4.2500E-06	4.1250E-06	7.381066E-03
565	3.8000E-06	4.0000E-06	3.9000E-06	7.589120E-03
566	3.6000E-06	3.8000E-06	3.7000E-06	7.795908E-03
567	3.4000E-06	3.6000E-06	3.5000E-06	8.012963E-03
568	3.2000E-06	3.4000E-06	3.3000E-06	8.257901E-03
569	3.0000E-06	3.2000E-06	3.1000E-06	8.517317E-03
570	2.8000E-06	3.0000E-06	2.9000E-06	8.813118E-03
571	2.7000E-06	2.8000E-06	2.7500E-06	9.040438E-03
572	2.5500E-06	2.7000E-06	2.6250E-06	9.265617E-03
573	2.4000E-06	2.5500E-06	2.4750E-06	9.539902E-03
574	2.3000E-06	2.4000E-06	2.3500E-06	9.777302E-03
575	2.2000E-06	2.3000E-06	2.2500E-06	9.993087E-03
576	2.1000E-06	2.2000E-06	2.1500E-06	1.022198E-02
577	2.0000E-06	2.1000E-06	2.0500E-06	1.047045E-02
578	1.9000E-06	2.0000E-06	1.9500E-06	1.074139E-02
579	1.8000E-06	1.9000E-06	1.8500E-06	1.103385E-02
580	1.7000E-06	1.8000E-06	1.7500E-06	1.133219E-02
581	1.6000E-06	1.7000E-06	1.6500E-06	1.166773E-02
582	1.5000E-06	1.6000E-06	1.5500E-06	1.203943E-02

583	1.4250E-06	1.5000E-06	1.4625E-06	1.239454E-02
584	1.3500E-06	1.4250E-06	1.3875E-06	1.272416E-02
585	1.2750E-06	1.3500E-06	1.3125E-06	1.308900E-02
586	1.2000E-06	1.2750E-06	1.2375E-06	1.347740E-02
587	1.1500E-06	1.2000E-06	1.1750E-06	1.383637E-02
588	1.1000E-06	1.1500E-06	1.1250E-06	1.413373E-02
589	1.0500E-06	1.1000E-06	1.0750E-06	1.447118E-02
590	1.0000E-06	1.0500E-06	1.0250E-06	1.481547E-02
591	9.6000E-07	1.0000E-06	9.8000E-07	1.515198E-02
592	9.2000E-07	9.6000E-07	9.4000E-07	1.548165E-02
593	8.8000E-07	9.2000E-07	9.0000E-07	1.581131E-02
594	8.4000E-07	8.8000E-07	8.6000E-07	1.616246E-02
595	8.0000E-07	8.4000E-07	8.2000E-07	1.654791E-02
596	7.6000E-07	8.0000E-07	7.8000E-07	1.697144E-02
597	7.2000E-07	7.6000E-07	7.4000E-07	1.742238E-02
598	6.9000E-07	7.2000E-07	7.0500E-07	1.785178E-02
599	6.6000E-07	6.9000E-07	6.7500E-07	1.824409E-02
600	6.3000E-07	6.6000E-07	6.4500E-07	1.866859E-02
601	6.0000E-07	6.3000E-07	6.1500E-07	1.911752E-02
602	5.7500E-07	6.0000E-07	5.8750E-07	1.956753E-02
603	5.5000E-07	5.7500E-07	5.6250E-07	1.998813E-02
604	5.2500E-07	5.5000E-07	5.3750E-07	2.046260E-02
605	5.0000E-07	5.2500E-07	5.1250E-07	2.094677E-02
606	4.7500E-07	5.0000E-07	4.8750E-07	2.146813E-02
607	4.5000E-07	4.7500E-07	4.6250E-07	2.203446E-02
608	4.2500E-07	4.5000E-07	4.3750E-07	2.265366E-02
609	4.0000E-07	4.2500E-07	4.1250E-07	2.333158E-02
610	3.8000E-07	4.0000E-07	3.9000E-07	2.399477E-02
611	3.6000E-07	3.8000E-07	3.7000E-07	2.463545E-02
612	3.4000E-07	3.6000E-07	3.5000E-07	2.532800E-02
613	3.2000E-07	3.4000E-07	3.3000E-07	2.608315E-02
614	3.0000E-07	3.2000E-07	3.1000E-07	2.691166E-02
615	2.8000E-07	3.0000E-07	2.9000E-07	2.782141E-02
616	2.7000E-07	2.8000E-07	2.7500E-07	2.856286E-02
617	2.5500E-07	2.7000E-07	2.6250E-07	2.923981E-02
618	2.4000E-07	2.5500E-07	2.4750E-07	3.011623E-02
619	2.3000E-07	2.4000E-07	2.3500E-07	3.090363E-02
620	2.2000E-07	2.3000E-07	2.2500E-07	3.158349E-02
621	2.1000E-07	2.2000E-07	2.1500E-07	3.231033E-02
622	2.0000E-07	2.1000E-07	2.0500E-07	3.308987E-02
623	1.9000E-07	2.0000E-07	1.9500E-07	3.393308E-02
624	1.8000E-07	1.9000E-07	1.8500E-07	3.483104E-02
625	1.7000E-07	1.8000E-07	1.7500E-07	3.581313E-02
626	1.6000E-07	1.7000E-07	1.6500E-07	3.688423E-02
627	1.5000E-07	1.6000E-07	1.5500E-07	3.805904E-02

628	1.4250E-07	1.5000E-07	1.4625E-07	3.917710E-02
629	1.3500E-07	1.4250E-07	1.3875E-07	4.022379E-02
630	1.2750E-07	1.3500E-07	1.3125E-07	4.135840E-02
631	1.2000E-07	1.2750E-07	1.2375E-07	4.259292E-02
632	1.1500E-07	1.2000E-07	1.1750E-07	4.370313E-02
633	1.1000E-07	1.1500E-07	1.1250E-07	4.466368E-02
634	1.0500E-07	1.1000E-07	1.0750E-07	4.569173E-02
635	1.0000E-07	1.0500E-07	1.0250E-07	4.679612E-02
636	9.6000E-08	1.0000E-07	9.8000E-08	4.786527E-02
637	9.2000E-08	9.6000E-08	9.4000E-08	4.886697E-02
638	8.8000E-08	9.2000E-08	9.0000E-08	4.993907E-02
639	8.4000E-08	8.8000E-08	8.6000E-08	5.108839E-02
640	8.0000E-08	8.4000E-08	8.2000E-08	5.232287E-02
641	7.6000E-08	8.0000E-08	7.8000E-08	5.365028E-02
642	7.2000E-08	7.6000E-08	7.4000E-08	5.508232E-02
643	6.9000E-08	7.2000E-08	7.0500E-08	5.642636E-02
644	6.6000E-08	6.9000E-08	6.7500E-08	5.766764E-02
645	6.3000E-08	6.6000E-08	6.4500E-08	5.899406E-02
646	6.0000E-08	6.3000E-08	6.1500E-08	6.041631E-02
647	5.7500E-08	6.0000E-08	5.8750E-08	6.180925E-02
648	5.5000E-08	5.7500E-08	5.6250E-08	6.316698E-02
649	5.2500E-08	5.5000E-08	5.3750E-08	6.462054E-02
650	5.0000E-08	5.2500E-08	5.1250E-08	6.618267E-02
651	4.7500E-08	5.0000E-08	4.8750E-08	6.786122E-02
652	4.5000E-08	4.7500E-08	4.6250E-08	6.965723E-02
653	4.2500E-08	4.5000E-08	4.3750E-08	7.162239E-02
654	4.0000E-08	4.2500E-08	4.1250E-08	7.376266E-02
655	3.8000E-08	4.0000E-08	3.9000E-08	7.585885E-02
656	3.6000E-08	3.8000E-08	3.7000E-08	7.788274E-02
657	3.4000E-08	3.6000E-08	3.5000E-08	8.008070E-02
658	3.2000E-08	3.4000E-08	3.3000E-08	8.247525E-02
659	3.0000E-08	3.2000E-08	3.1000E-08	8.509391E-02
660	2.8000E-08	3.0000E-08	2.9000E-08	8.797951E-02
661	2.7000E-08	2.8000E-08	2.7500E-08	9.034182E-02
662	2.5500E-08	2.7000E-08	2.6250E-08	9.247034E-02
663	2.4000E-08	2.5500E-08	2.4750E-08	9.522581E-02
664	2.3000E-08	2.4000E-08	2.3500E-08	9.772314E-02
665	2.2000E-08	2.3000E-08	2.2500E-08	9.987204E-02
666	2.1000E-08	2.2000E-08	2.1500E-08	1.021615E-01
667	2.0000E-08	2.1000E-08	2.0500E-08	1.046359E-01
668	1.9000E-08	2.0000E-08	1.9500E-08	1.072865E-01
669	1.8000E-08	1.9000E-08	1.8500E-08	1.101236E-01
670	1.7000E-08	1.8000E-08	1.7500E-08	1.132245E-01
671	1.6000E-08	1.7000E-08	1.6500E-08	1.166087E-01
672	1.5000E-08	1.6000E-08	1.5500E-08	1.203159E-01

673	1.4250E-08	1.5000E-08	1.4625E-08	1.238572E-01
674	1.3500E-08	1.4250E-08	1.3875E-08	1.271636E-01
675	1.2750E-08	1.3500E-08	1.3125E-08	1.307534E-01
676	1.2000E-08	1.2750E-08	1.2375E-08	1.346564E-01
677	1.1500E-08	1.2000E-08	1.1750E-08	1.381875E-01
678	1.1000E-08	1.1500E-08	1.1250E-08	1.412296E-01
679	1.0500E-08	1.1000E-08	1.0750E-08	1.444773E-01
680	1.0000E-08	1.0500E-08	1.0250E-08	1.479692E-01
681	9.6000E-09	1.0000E-08	9.8000E-09	1.513343E-01
682	9.2000E-09	9.6000E-09	9.4000E-09	1.544939E-01
683	8.8000E-09	9.2000E-09	9.0000E-09	1.578786E-01
684	8.4000E-09	8.8000E-09	8.6000E-09	1.615075E-01
685	8.0000E-09	8.4000E-09	8.2000E-09	1.654100E-01
686	7.6000E-09	8.0000E-09	7.8000E-09	1.695969E-01
687	7.2000E-09	7.6000E-09	7.400002E-09	1.741161E-01
688	6.9000E-09	7.2000E-09	7.0500E-09	1.783910E-01
689	6.6000E-09	6.9000E-09	6.7500E-09	1.823136E-01
690	6.3000E-09	6.6000E-09	6.4500E-09	1.865097E-01
691	6.0000E-09	6.3000E-09	6.1500E-09	1.910093E-01
692	5.7500E-09	6.0000E-09	5.8750E-09	1.954305E-01
693	5.5000E-09	5.7500E-09	5.6250E-09	1.997245E-01
694	5.2500E-09	5.5000E-09	5.3750E-09	2.043220E-01
695	5.0000E-09	5.2500E-09	5.1250E-09	2.092620E-01
696	4.7500E-09	5.0000E-09	4.8750E-09	2.145153E-01
697	4.5000E-09	4.7500E-09	4.6250E-09	2.202472E-01
698	4.2500E-09	4.5000E-09	4.3750E-09	2.264489E-01
699	4.0000E-09	4.2500E-09	4.1250E-09	2.332174E-01
700	3.8000E-09	4.0000E-09	3.9000E-09	2.398503E-01
701	3.6000E-09	3.8000E-09	3.7000E-09	2.462570E-01
702	3.4000E-09	3.6000E-09	3.5000E-09	2.532017E-01
703	3.2000E-09	3.4000E-09	3.3000E-09	2.607635E-01
704	3.0000E-09	3.2000E-09	3.1000E-09	2.690486E-01
705	2.8000E-09	3.0000E-09	2.9000E-09	2.781358E-01
706	2.7000E-09	2.8000E-09	2.7500E-09	2.856188E-01
707	2.5500E-09	2.7000E-09	2.6250E-09	2.923387E-01
708	2.4000E-09	2.5500E-09	2.4750E-09	3.010741E-01
709	2.3000E-09	2.4000E-09	2.3500E-09	3.089780E-01
710	2.2000E-09	2.3000E-09	2.2500E-09	3.157665E-01
711	2.1000E-09	2.2000E-09	2.1500E-09	3.230341E-01
712	2.0000E-09	2.1000E-09	2.0500E-09	3.308206E-01
713	1.9000E-09	2.0000E-09	1.9500E-09	3.392524E-01
714	1.8000E-09	1.9000E-09	1.8500E-09	3.482320E-01
715	1.7000E-09	1.8000E-09	1.7500E-09	3.580432E-01
716	1.6000E-09	1.7000E-09	1.6500E-09	3.687250E-01
717	1.5000E-09	1.6000E-09	1.5500E-09	3.804435E-01

718	1.4250E-09	1.5000E-09	1.4625E-09	3.916631E-01
719	1.3500E-09	1.4250E-09	1.3875E-09	4.021197E-01
720	1.2750E-09	1.3500E-09	1.3125E-09	4.134568E-01
721	1.2000E-09	1.2750E-09	1.2375E-09	4.258020E-01
722	1.1500E-09	1.2000E-09	1.1750E-09	4.369826E-01
723	1.1000E-09	1.1500E-09	1.1250E-09	4.465885E-01
724	1.0500E-09	1.1000E-09	1.0750E-09	4.568687E-01
725	1.0000E-09	1.0500E-09	1.0250E-09	4.679121E-01
726	9.6000E-10	1.0000E-09	9.8000E-10	4.785457E-01
727	9.2000E-10	9.6000E-10	9.4000E-10	4.885617E-01
728	8.8000E-10	9.2000E-10	9.0000E-10	4.992629E-01
729	8.4000E-10	8.8000E-10	8.6000E-10	5.107370E-01
730	8.0000E-10	8.4000E-10	8.2000E-10	5.230523E-01
731	7.6000E-10	8.0000E-10	7.8000E-10	5.363069E-01
732	7.2000E-10	7.6000E-10	7.4000E-10	5.506078E-01
733	6.9000E-10	7.2000E-10	7.0500E-10	5.641260E-01
734	6.6000E-10	6.9000E-10	6.7500E-10	5.765295E-01
735	6.3000E-10	6.6000E-10	6.4500E-10	5.897839E-01
736	6.0000E-10	6.3000E-10	6.1500E-10	6.040069E-01
737	5.7500E-10	6.0000E-10	5.8750E-10	6.179947E-01
738	5.5000E-10	5.7500E-10	5.6250E-10	6.315721E-01
739	5.2500E-10	5.5000E-10	5.3750E-10	6.461082E-01
740	5.0000E-10	5.2500E-10	5.1250E-10	6.617193E-01
741	4.7500E-10	5.0000E-10	4.8750E-10	6.783583E-01
742	4.5000E-10	4.7500E-10	4.6250E-10	6.964648E-01
743	4.2500E-10	4.5000E-10	4.3750E-10	7.160863E-01
744	4.0000E-10	4.2500E-10	4.1250E-10	7.374700E-01
745	3.8000E-10	4.0000E-10	3.9000E-10	7.584712E-01
746	3.6000E-10	3.8000E-10	3.7000E-10	7.787098E-01
747	3.4000E-10	3.6000E-10	3.5000E-10	8.006697E-01
748	3.2000E-10	3.4000E-10	3.3000E-10	8.245867E-01
749	3.0000E-10	3.2000E-10	3.1000E-10	8.507917E-01
750	2.8000E-10	3.0000E-10	2.9000E-10	8.795210E-01
751	2.7000E-10	2.8000E-10	2.7500E-10	9.031932E-01
752	2.5500E-10	2.7000E-10	2.6250E-10	9.244294E-01
753	2.4000E-10	2.5500E-10	2.4750E-10	9.520433E-01
754	2.3000E-10	2.4000E-10	2.3500E-10	9.770555E-01
755	2.2000E-10	2.3000E-10	2.2500E-10	9.985254E-01
756	2.1000E-10	2.2000E-10	2.1500E-10	1.021512E+00
757	2.0000E-10	2.1000E-10	2.0500E-10	1.046163E+00
758	1.9000E-10	2.0000E-10	1.9500E-10	1.072772E+00
759	1.8000E-10	1.9000E-10	1.8500E-10	1.101138E+00
760	1.7000E-10	1.8000E-10	1.7500E-10	1.132239E+00
761	1.6000E-10	1.7000E-10	1.6500E-10	1.165989E+00
762	1.5000E-10	1.6000E-10	1.5500E-10	1.203061E+00

763	1.4250E-10	1.5000E-10	1.4625E-10	1.238567E+00
764	1.3500E-10	1.4250E-10	1.3875E-10	1.271631E+00
765	1.2750E-10	1.3500E-10	1.3125E-10	1.307436E+00
766	1.2000E-10	1.2750E-10	1.2375E-10	1.346467E+00
767	1.1500E-10	1.2000E-10	1.1750E-10	1.381874E+00
768	1.1000E-10	1.1500E-10	1.1250E-10	1.412203E+00
769	1.0500E-10	1.1000E-10	1.0750E-10	1.444772E+00
770	1.0000E-10	1.0500E-10	1.0250E-10	1.479691E+00

5.2 WinNIEL - NIEL for Ions

Reference [Xap] noted:

> "Despite the widespread recognition of the NIEL approach there are difficulties that hinder its general use.
>
> …
>
> A solution to this problem would be the availability of a suitable computer program for calculating NIEL for laboratory and space applications.
>
> …
>
> NASA's Space Environments and Effects (SEE) and Living With a Star (LWS) Space Environments Testbed (SET) Programs and the Office of Naval Research (ONR) have sponsored the development of a Windows compatible code for calculating NIEL, called WinNIEL."

The WinNIEL code uses the Zeiger-Biersack-Littmark potential [ZBL] for screened Coulomb calculations at low incident energies (< 50 MeV) and the Mott-Rutherford potential [Ru11], which includes relativistic effects [Mo65], at higher energies. The nuclear elastic and inelastic interactions due to protons and alpha particles are accounted for by utilizing the physics package implemented within the MCNPX code [MCNPX, MCNP, MCNP13a, MCNP13b]. The MCNPX history tape was used to convert the damage energy tally into a NIEL value for nuclear interactions. In elastic events, standard kinematics was used to compute the target recoil energy. In non-elastic events, the high-energy intra-nuclear cascade, pre-equilibrium, and evaporation physics models were used to compute the recoil energies. The MCNPX calculation used the cross sections by Barashenkov and Polanski [Ba94] to estimate the elastic and non-elastic reaction probabilities for protons. These calculations for the proton used a thin target approximation where "thin" is defined as small relative to the continuous slowing down approximation (CSDA) range of the incident proton.

Tabulations of data computed by the WinNIEL code [Xap] are currently the source of the best representations for the NIEL for charged particle irradiations. In order to support the use of this data in radiation effects analysis, the following tables report on the results of Version 2 of the WinNIEL code for incident ions and target materials of interest to the electronics radiation effects community.

In the estimation of the total NIEL, the WinNIEL code considers the sum of the Coulombic and nuclear contributions to the NIEL. For incident proton energies up to ~10 MeV, Coulomb interactions dominate the production of displacement damage in silicon. Above 30 MeV, the nuclear component is a significant part of the NIEL [Bu86].

Table 4: Proton NIEL Values for Various Materials

Energy (MeV)	Total NIEL ($MeV \cdot cm^2/g$)		
	Silicon (E_{th} = 20.5 eV)	Gallium (E_{th} = 10 eV)	Arsenic (E_{th} = 10 eV)
1.000E-004	0.000E+00	0.000E+00	0.000E+00
2.000E-004	1.348E+00	1.760E-01	7.742E-02
3.000E-004	2.838E+00	7.860E-01	6.180E-01
4.000E-004	3.692E+00	1.130E+00	9.234E-01
5.000E-004	4.228E+00	1.370E+00	1.141E+00
6.000E-004	4.513E+00	1.530E+00	1.283E+00
7.000E-004	4.756E+00	1.660E+00	1.410E+00
8.000E-004	4.964E+00	1.730E+00	1.475E+00
9.000E-004	5.003E+00	1.850E+00	1.582E+00
1.000E-003	5.032E+00	1.900E+00	1.633E+00
2.000E-003	4.716E+00	2.060E+00	1.848E+00
3.000E-003	4.300E+00	2.050E+00	1.818E+00
4.000E-003	3.868E+00	1.950E+00	1.746E+00
5.000E-003	3.487E+00	1.860E+00	1.680E+00
6.000E-003	3.246E+00	1.760E+00	1.598E+00
7.000E-003	3.004E+00	1.680E+00	1.526E+00
8.000E-003	2.761E+00	1.600E+00	1.462E+00
9.000E-003	2.600E+00	1.540E+00	1.406E+00
1.000E-002	2.463E+00	1.460E+00	1.356E+00
2.000E-002	1.595E+00	1.040E+00	9.786E-01
3.000E-002	1.201E+00	8.170E-01	7.760E-01
4.000E-002	9.664E-01	6.860E-01	6.459E-01
5.000E-002	8.160E-01	5.910E-01	5.578E-01
6.000E-002	7.110E-01	5.220E-01	4.940E-01
7.000E-002	6.334E-01	4.640E-01	4.455E-01
8.000E-002	5.644E-01	4.240E-01	4.021E-01
9.000E-002	5.177E-01	3.860E-01	3.717E-01
1.000E-001	4.720E-01	3.600E-01	3.420E-01
2.000E-001	2.664E-01	2.080E-01	2.018E-01
3.000E-001	1.866E-01	1.510E-01	1.447E-01
4.000E-001	1.451E-01	1.190E-01	1.141E-01
5.000E-001	1.196E-01	9.890E-02	9.504E-02
6.000E-001	1.006E-01	8.390E-02	8.193E-02
7.000E-001	8.838E-02	7.410E-02	7.132E-02
8.000E-001	7.776E-02	6.560E-02	6.414E-02
9.000E-001	7.065E-02	5.890E-02	5.762E-02
1.000E+000	6.382E-02	5.430E-02	5.233E-02
2.000E+000	3.359E-02	2.940E-02	2.839E-02

3.000E+000	2.288E-02	2.040E-02	1.969E-02
4.000E+000	1.783E-02	1.570E-02	1.523E-02
5.000E+000	1.483E-02	1.280E-02	1.261E-02
6.000E+000	1.310E-02	1.110E-02	1.074E-02
7.000E+000	1.171E-02	9.780E-03	9.573E-03
8.000E+000	1.071E-02	8.810E-03	8.606E-03
9.000E+000	9.944E-03	8.200E-03	7.875E-03
1.000E+001	9.433E-03	7.580E-03	7.269E-03
2.000E+001	6.642E-03	5.400E-03	5.143E-03
3.000E+001	5.573E-03	4.750E-03	4.493E-03
4.000E+001	4.879E-03	4.460E-03	4.263E-03
5.000E+001	4.272E-03	4.130E-03	3.977E-03
6.000E+001	3.880E-03	3.930E-03	3.781E-03
7.000E+001	3.631E-03	3.870E-03	3.702E-03
8.000E+001	3.361E-03	3.780E-03	3.699E-03
9.000E+001	3.138E-03	3.660E-03	3.640E-03
1.000E+002	2.953E-03	3.600E-03	3.569E-03
2.000E+002	1.876E-03	3.200E-03	3.290E-03
3.000E+002	1.614E-03	3.030E-03	3.137E-03
4.000E+002	1.528E-03	3.120E-03	3.261E-03
5.000E+002	1.424E-03	3.170E-03	3.277E-03
6.000E+002	1.412E-03	3.310E-03	3.464E-03
7.000E+002	1.406E-03	3.320E-03	3.548E-03
8.000E+002	1.394E-03	3.370E-03	3.556E-03
9.000E+002	1.355E-03	3.380E-03	3.547E-03
1.000E+003	1.337E-03	3.350E-03	3.579E-03
*Values obtained from a beta version of Version 2 of the WinNIEL Code.			

Table 5: Alpha-particle NIEL Values for Various Materials

Energy (MeV)	Total NIEL ($MeV \cdot cm^2/g$)		
	Silicon (E_{th} = 20.5 eV)	Gallium (E_{th} = 10 eV)	Arsenic (E_{th} = 10 eV)
1.000E-004	1.831E+01	5.043E+00	3.973E+00
2.000E-004	3.415E+01	9.675E+00	8.320E+00
3.000E-004	4.176E+01	1.234E+01	1.068E+01
4.000E-004	4.620E+01	1.408E+01	1.223E+01
5.000E-004	4.900E+01	1.531E+01	1.334E+01
6.000E-004	5.120E+01	1.634E+01	1.427E+01
7.000E-004	5.234E+01	1.722E+01	1.507E+01
8.000E-004	5.322E+01	1.781E+01	1.560E+01
9.000E-004	5.390E+01	1.831E+01	1.606E+01
1.000E-003	5.442E+01	1.874E+01	1.646E+01
2.000E-003	5.345E+01	2.045E+01	1.812E+01
3.000E-003	5.022E+01	2.047E+01	1.836E+01
4.000E-003	4.653E+01	2.015E+01	1.805E+01
5.000E-003	4.371E+01	1.959E+01	1.762E+01
6.000E-003	4.100E+01	1.901E+01	1.716E+01
7.000E-003	3.839E+01	1.845E+01	1.671E+01
8.000E-003	3.639E+01	1.791E+01	1.626E+01
9.000E-003	3.465E+01	1.731E+01	1.584E+01
1.000E-002	3.287E+01	1.683E+01	1.536E+01
2.000E-002	2.265E+01	1.300E+01	1.203E+01
3.000E-002	1.765E+01	1.068E+01	1.000E+01
4.000E-002	1.456E+01	9.142E+00	8.605E+00
5.000E-002	1.248E+01	8.046E+00	7.599E+00
6.000E-002	1.089E+01	7.220E+00	6.799E+00
7.000E-002	9.762E+00	6.534E+00	6.201E+00
8.000E-002	8.795E+00	6.014E+00	5.684E+00
9.000E-002	8.088E+00	5.551E+00	5.285E+00
1.000E-001	7.433E+00	5.192E+00	4.919E+00
2.000E-001	4.255E+00	3.165E+00	3.019E+00
3.000E-001	3.020E+00	2.322E+00	2.222E+00
4.000E-001	2.361E+00	1.855E+00	1.779E+00
5.000E-001	1.951E+00	1.543E+00	1.494E+00
6.000E-001	1.650E+00	1.336E+00	1.284E+00
7.000E-001	1.429E+00	1.172E+00	1.137E+00
8.000E-001	1.278E+00	1.045E+00	1.016E+00
9.000E-001	1.144E+00	9.529E-01	9.181E-01
1.000E+000	1.035E+00	8.695E-01	8.382E-01
2.000E+000	5.457E-01	4.792E-01	4.634E-01
3.000E+000	3.719E-01	3.308E-01	3.242E-01

4.000E+000	2.795E-01	2.562E-01	2.515E-01
5.000E+000	2.273E-01	2.078E-01	2.043E-01
6.000E+000	1.893E-01	1.771E-01	1.721E-01
7.000E+000	1.621E-01	1.529E-01	1.506E-01
8.000E+000	1.441E-01	1.346E-01	1.327E-01
9.000E+000	1.279E-01	1.218E-01	1.185E-01
1.000E+001	1.150E-01	1.100E-01	1.071E-01
2.000E+001	5.859E-02	5.757E-02	5.705E-02
3.000E+001	4.060E-02	4.085E-02	3.983E-02
4.000E+001	3.149E-02	3.272E-02	3.247E-02
5.000E+001	2.648E-02	2.831E-02	2.778E-02
6.000E+001	2.291E-02	2.540E-02	2.498E-02
7.000E+001	2.030E-02	2.310E-02	2.301E-02
8.000E+001	1.842E-02	2.151E-02	2.143E-02
9.000E+001	1.715E-02	2.005E-02	1.989E-02
1.000E+002	1.592E-02	1.911E-02	1.868E-02
2.000E+002	9.610E-03	1.319E-02	1.321E-02
3.000E+002	7.328E-03	1.114E-02	1.115E-02
4.000E+002	6.007E-03	1.024E-02	1.032E-02
5.000E+002	5.220E-03	9.698E-03	9.932E-03
6.000E+002	4.616E-03	9.339E-03	9.728E-03
7.000E+002	4.307E-03	9.014E-03	9.438E-03
8.000E+002	4.065E-03	8.756E-03	9.212E-03
9.000E+002	3.909E-03	8.565E-03	9.002E-03
1.000E+003	3.784E-03	8.404E-03	8.823E-03
*Values obtained from a beta version of Version 2 of the WinNIEL Code.			

Table 6: Primary Knock-on Ion NIEL Values for Various Materials

Energy (MeV)	Total NIEL ($MeV \cdot cm^2/g$)		
	Si in Silicon (E_{th} = 20.5 eV)	Ga in Gallium (E_{th} = 10 eV)	As in Arsenic (E_{th} = 10 eV)
1.000E-004	2.564E+02	1.896E+02	1.846E+02
2.000E-004	4.118E+02	2.992E+02	2.895E+02
3.000E-004	5.167E+02	3.808E+02	3.675E+02
4.000E-004	5.981E+02	4.476E+02	4.314E+02
5.000E-004	6.592E+02	5.055E+02	4.869E+02
6.000E-004	7.153E+02	5.556E+02	5.350E+02
7.000E-004	7.609E+02	6.008E+02	5.783E+02
8.000E-004	8.015E+02	6.420E+02	6.180E+02
9.000E-004	8.379E+02	6.787E+02	6.533E+02
1.000E-003	8.674E+02	7.141E+02	6.875E+02
2.000E-003	1.072E+03	9.684E+02	9.348E+02
3.000E-003	1.178E+03	1.136E+03	1.100E+03
4.000E-003	1.246E+03	1.261E+03	1.224E+03
5.000E-003	1.289E+03	1.359E+03	1.322E+03
6.000E-003	1.318E+03	1.441E+03	1.405E+03
7.000E-003	1.336E+03	1.510E+03	1.476E+03
8.000E-003	1.350E+03	1.568E+03	1.536E+03
9.000E-003	1.358E+03	1.620E+03	1.589E+03
1.000E-002	1.364E+03	1.666E+03	1.637E+03
2.000E-002	1.326E+03	1.938E+03	1.929E+03
3.000E-002	1.248E+03	2.060E+03	2.069E+03
4.000E-002	1.170E+03	2.122E+03	2.146E+03
5.000E-002	1.100E+03	2.153E+03	2.190E+03
6.000E-002	1.036E+03	2.165E+03	2.214E+03
7.000E-002	9.809E+02	2.167E+03	2.226E+03
8.000E-002	9.304E+02	2.161E+03	2.228E+03
9.000E-002	8.867E+02	2.150E+03	2.225E+03
1.000E-001	8.461E+02	2.136E+03	2.218E+03
2.000E-001	5.916E+02	1.934E+03	2.054E+03
3.000E-001	4.611E+02	1.741E+03	1.876E+03
4.000E-001	3.816E+02	1.581E+03	1.720E+03
5.000E-001	3.274E+02	1.450E+03	1.590E+03
6.000E-001	2.871E+02	1.340E+03	1.478E+03
7.000E-001	2.563E+02	1.248E+03	1.383E+03
8.000E-001	2.324E+02	1.169E+03	1.300E+03
9.000E-001	2.124E+02	1.100E+03	1.229E+03
1.000E+000	1.958E+02	1.040E+03	1.165E+03
2.000E+000	1.127E+02	6.870E+02	7.827E+02
3.000E+000	8.064E+01	5.226E+02	6.002E+02

4.000E+000	6.309E+01	4.259E+02	4.915E+02
5.000E+000	5.231E+01	3.613E+02	4.183E+02
6.000E+000	4.462E+01	3.148E+02	3.654E+02
7.000E+000	3.897E+01	2.799E+02	3.255E+02
8.000E+000	3.485E+01	2.523E+02	2.938E+02
9.000E+000	3.140E+01	2.300E+02	2.682E+02
1.000E+001	2.859E+01	2.116E+02	2.470E+02
2.000E+001	1.540E+01	1.206E+02	1.415E+02
3.000E+001	1.071E+01	8.589E+01	1.011E+02
4.000E+001	8.197E+00	6.743E+01	7.950E+01
5.000E+001	6.651E+00	5.572E+01	6.577E+01
6.000E+001	5.668E+00	4.762E+01	5.627E+01
7.000E+001	4.900E+00	4.167E+01	4.928E+01
8.000E+001	4.317E+00	3.721E+01	4.401E+01
9.000E+001	3.859E+00	3.358E+01	3.975E+01
1.000E+002	3.490E+00	3.062E+01	3.627E+01
2.000E+002	1.820E+00	1.666E+01	1.980E+01
3.000E+002	1.249E+00	1.160E+01	1.380E+01
4.000E+002	9.448E-01	8.946E+00	1.066E+01
5.000E+002	7.603E-01	7.307E+00	8.718E+00
6.000E+002	6.366E-01	6.229E+00	7.432E+00
7.000E+002	5.588E-01	5.413E+00	6.463E+00
8.000E+002	4.906E-01	4.791E+00	5.725E+00
9.000E+002	4.373E-01	4.301E+00	5.142E+00
1.000E+003	3.945E-01	3.905E+00	4.670E+00
*Values obtained from a beta version of Version 2 of the WinNIEL Code.			

It should be noted that the values in Tables 4 and 5 agree with those reported by References [Ju01, Ju03, Ju04] for protons and alphas in Ga and As. They differ slightly for the reported value of NIEL in Si due to the use of a value for E_d of 20.5 eV in the WinNIEL calculations reflected in these tables, while Jun's calculations with the WinNIEL code used E_d = 21 eV, which is the WinNIEL default value. Note also that Reference [Ju04] reports the alpha particle energy in units of eV/amu, so a conversion must be made when comparing the NIEL for the tabulated energies.

6. CONTRIBUTIONS TO UNCERTAINTY IN THE DAMAGE METRIC

There are many contributors to the energy-dependent uncertainty of the damage metrics presented here. A detailed covariance matrix for these uncertainty contributors is not yet available, but the list of sources of uncertainty that should be addressed for any application include:

- Knowledge of the neutron source spectrum
- Representation of the neutron recoil spectrum
- Effect from any accompanying gamma environment
    - Interference from potential photon-induced displacement
    - Effect from any potential electron-induced displacement
- Effect of any accompanying ionization on the observed damage
    - Trapped Charge
- Model used for the ion-atom interaction potential
- Knowledge of the displacement threshold energy
- Vacancy-interstitial formation
- Effect of ion channeling in the crystal and modeling of this phenomenon
- Influence of defect evolution on the observed damage mode
- Sampling statistics from the number of defect cascades in the sensitive volume

7. SUMMARY

This report provides a set of consistent definitions for metrics relevant to the modeling of displacement damage in materials. Recommended sources for numerical tabulations of the neutron displacement kerma and the ion non-ionizing energy loss are also provided.

8. REFERENCES

[A170] **ASTM E170, Standard Terminology Relating to Radiation Measurements and Dosimetry**, ASTM International, West Conshohocken, PA, 2013.

[A521] **ASTM E521, Standard Practice for Neutron Radiation Damage Simulation by Charged-Particle Irradiation**, ASTM International, West Conshohocken, PA, 2013.

[A693] **ASTM E693, Standard Practice for Characterizing Neutron Exposures in Iron and Low Alloy Steels in Terms of Displacement Per Atom (DPA)** , ASTM International, West Conshohocken, PA, 2013.

[A722] **ASTM E722, Standard Practice for Characterizing Neutron Fluence Spectra in Terms of an Equivalent Monoenergetic Neutron Fluence for Radiation-Hardness Testing of Electronics**, ASTM International, West Conshohocken, PA, 2013.

[Ak01] A. Akkerman, J. Barak, M.B. Chadwick, J. Levinson, M. Murat, Y. Lifshitz, "Updated NIEL Calculations for Estimating the Damage Induced by Particles and Gamma-rays in Si and GaAs," **Radiation Physics and Chemistry**, Vol. **62**, pp. 301-310, 2001.

[Ak06] A. Akkerman, J. Barak, "New Partition Factor Calculations for Evaluating the Damage of Low Energy Ions in Silicon," **IEEE Transactions on Nuclear Science**, Vol. 53, pp. 3667-3674, December 2006.

[Ba94] V.S. Barashenkov and A. Polanski, "Electronic Guide for Nuclear Cross Sections", **Comm. JINR** E2-94-417, Dubna, 1994.

[Ben00] M.W. Bench, I.M. Robertson, M.A. Kirk, I. Jena, "Production of amphorous zone in GaAs by direct impact of energetic heavy ions," **J. Appl. Phys**., Vol. **87**, pp. 49-56, 2000.

[Bo09] M. J. Boschini, C. Consolandi, M. Gervasi, S. Giani, D. Gransi, V. Ivanchenko, P. G. Rancoita, GEANT4-based Application Development for NIEL: Calculation in the Space Radiation Environment, **Astroparticle, Particle and Space Physics, Detectors and Medical Physics Applications**, Proceedings of the 11th Conference held 5-9 October 2009 in Villa Olmo, Italy, World Scientific Publishing Co., December 14, 2009.

[Bo76] J. C. Bourgoin, P. Ludeau, B. Massarani, "Threshold Energy Determination in Thick Semiconductor Samples," **Revue de Physique Appliquee,** Vol. **11**, pp 279-284, March 1976.

[Bu13] L. Bukonte, F. Djurabekova, J. Samela, K. Nordlund, S. A. Norris, M. J. Azia, "Comparison of Molecular Dynamics and Binary Collision Approximation Simulations for Atom Displacement Analysis", **Nuclear Instruments and Methods in Physics Research B**, Vol. **297,** pp. 23 – 28, 2013.

[Bu86] E.A. Burke, "Energy Dependence of Displacement Damage in Proton Irradiated Silicon", **IEEE Trans. Nucl. Sci.**, Vol. **33**, 1276, 1986.

[Ch11] M.B. Chadwick, et al., "ENDF/B-VII.1 Nuclear Data for Science and Technology: Cross Sections, Covariances, Fission Product Yields and Decay Data," **Nuclear Data Sheets**, Vol. **112**, pp. 2887-2996, 2011.

[Co65] J. Corbett, G. D. Watkins, **Phys. Rev.**, Vol. **138**, A555, 1965.

[Co66] **Electronic Radiation Damage in Semiconductors and Metals**, J.W. Corbett, Academic Press, New York, 1966.

[Da98] M. B. Danjaji, P. J. Griffin, "Uncertainty of Silicon 1-MeV Damage Function," **Proceedings of the 9th International Symposium on Reactor Dosimetry** held in Prague, Czech Republic, 2-6 September 1996, pp. 611-618, 1998.

[De92] R.A.B. Devine, "**Radiation Induced Structural Changes in Amorphous SiO_2: I. Point Defects,**" Jpn. J. Appl. Phys, Vol. **31**, pp. 4411-4421, 1992.

[Do72] D.G. Doran, "Neutron Displacement Cross Sections for Stainless Steel and Tantalum Based on a Lindhard Model", **Nucl. Sci. Eng**., Vol. **49**, 130, 1972.

[ENDF102] ***ENDF-6 Data Formats and Procedures for the Evaluated Nuclear Data File ENDF-VII****,* edited by M. Herman, A. Trkov, Brookhaven National Laboratory, report ENDF-102, Report BNL-9036502009 Rev. 1, July 2010. (see URL: http://www.nndc.bnl.gov/csewg_members/ENDF-102/ENDF-102.pdf)

[ENDF201] ***ENDF/B-VI Summary Documentation****, edited* by P. F. Rose, Brookhaven National Laboratory, report ENDF-201, Report BNL-NCS-1741, 4th Edition, October 1991 Cross Section Evaluation Working Group (CSEWG) is a cooperative effort of the national laboratories, industry, and universities in the United States and Canada, responsible for the production of the U.S. Evaluated Nuclear Data File ENDF/B. (see http://www.nndc.bnl.gov/csewg/).

[Fu03] L. Fukuya, I. Kimura, "Calculation of Gamma Induced Displacement Cross Sections of Iron Considering Positron Contributions and Using Standard Damage Model," **Journal of Nuclear Science and Technology**, Vol. **40**. pp. 423-428, June 2003.

[Gad95] H. Gades, H.M. Urbassek, "Simulation of Ion-Induced Mixing in Metals," **Phys. Rev. B**, Vol. 51, pp 14559, 1995.

[Go89] R. Gold, J.H. Roberts, D.G. Doran, "Determination of Gamma-Ray-Induced Displacement Rates," **Reactor Dosimetry Methods, Applications, and Standardization**, ASTM STP 1001, American Society for Testing and Materials, Philadelphia, 1989.

[Gr03] P. Griffin, M. Danjaji, "Sensitivity of Silicon 1-MeV Damage Function to Cross Section Evaluation," T**ransactions of the American Nuclear Society**, Vol. **73**, pp. 451-453, 1995.

[Gr85] L.R. Greenwood, R.K. Smither, **SPECTER: Neutron Damage Calculations for Materials Irradiation**, Argonne National Laboratory, report ANL/FPP/TM-197, January 1985.

[Hau96] H, Hausmann, A. Pillukat, P. Ehrhart, "Point Defects and Their Reactions in Electron-Irradiated GaAs Investigated by Optical Absorption Spectroscopy," **Phys. Rev. B**, Vol. **54**, pp. 8527, 1996.

[He68] L.F. Hemment, P.R.C. Stevens, **Radiation Effects in Semiconductors**, edited by F. L. Vook, Plenum Press, New York, pp. 290, 1968.

[He70] L.F. Hemment, P.R.C. Stevens, **Atomic Collision Phenomena in Solids**, edited by D. W. Palmer. M. W. Thompson, R. D. Townsend, North-Holland, Amsterdam, pp. 280, 1970.

[He69] P. Hemment, P. Stevens, **J. Appl. Phys**., Vol. **40**, pp. 4893, 1969.

[He93] **Reactor Vessel Irradiation Damage: Absorbed Dose Estimates**, John Helm, Columbia University, published by Electric Power Research Institute, report EP 89-21, second edition, October **18**, 1993.

[Ho08] E. Holmstrom, A. Kuronen, K. Norlund, "Threshold Defect Production in Silicon Determined by Density Functional Theory Molecular Dynamics Simulation," **Phys. Rev. B** Vol. **78**, 2008.

[Hou10] M. Hou, C.J. Ortiz, C.S. Becquart, C. Domain, U. Starkae, A. Debacker, "Microstructure evolution of irradiated tungsten: Crystal effects in He and H implantation as modelled in the Binary Collision Approximation," **Journal of Nuclear Materials**, Vol. **403**, pp. 89-100, 2010.

[Hu93] M. Huhtinen and P.A. Aarnio, **Nuclear Instruments and Methods in Physics A,** Vol. **335**, pp. 580-582, 1993.

[ICRU60] **Fundamental Quantities and Units for Ionizing Radiation**, ICRU Report, 60, International Commission on Radiation Units and Measurements, December 30, 1998.

[ICRU85] **Fundamental Quantities and Units for Ionizing Radiation (Revised)**, ICRU Report, 85, The International Commission on Radiation Units and Measurements, October 2011, Journal of the ICRU Volume **11** No 1, Oxford University Press, 2011.

[JENDL] K. Shibata, O. Iwamoto, T. Nakagawa, N. Iwamoto, A. Ichihara, S. Kunieda, S. Chiba, K. Furutaka, N. Otuka, T. Ohsawa, T. Murata, H. Matsunobu, A. Zukeran, S.

Kamada, and J. Katakura: "JENDL-4.0: A New Library for Nuclear Science and Engineering," **J. Nucl. Sci. Technol. 48**, pp. 1-30, 2011..

[JEF] **The JEF-3.1.1 Nuclear Data Library, JEFF Report 22, Validation Results from JEF-2.2 to JEF-3.1.1**, A. Santamarina, D. Bernard, P. Blaise, M. Coste, A. Courcelle, T.D. Huynh, C. Jouanne, P. Leconte, O. Litaize, S. Mengelle, G. Noguere, J-M. Ruggiere, O. Serot, J. Tommasi, C. Vaglio, J-F. Vidal, Nuclear Energy Agency, Organization for Economic Co-operation and Development, 2009.

[La08] I. Lazanu, S. Lazanu, "Analytical Approximations of the NIEL in Semiconductor Detectors for HEP," **Romanian Reports in Physics**, Vol. **60**, pp. 71-78, 2008.

[La09] S. Lazanu, M.L. Ciurea, I. Lazanu, "Point and Extended Defects in Irradiated Silicon and Consequences for Detectors", **Phys. Status Solidi**, Vol. **C9,** pp. 1974-1978, 2009.

[Leh93] B. Lennartz, D. Braunig, "A Deep-level Transient Spectroscopy Variation for the Determination of Displacement Threshold Energies in GaAs," **J. Appl. Phys**. Vol. **73**, pp. 2781-2785, 1993.

[Li63] J. Lindhard, M. Scharff, H. Schiott, "Range Concepts and Heavy Ion Ranges," **Mat. Phys. Medd. Dan. Vld. Selsk**, Vol. **33**, pp. 1-40, 1963.

[Lof58] J. Loferski, P. Rappaport, "Radiation Damage in Ge and Si Detected by Carrier Lifetime Changes: Damage Thresholds," **Phys. Rev.,** Vol. **111**, pp 432, 1958.

[Ju01] I. Jun, "Effects of Secondary Particles on the Total Dose and the Displacement Damage in Space Proton Environments", **IEEE Trans. Nucl. Sci.,** Vol **48**, 162, 2001.

[Ju03] I. Jun, M.A. Xapsos, S.R. Messenger, E.A. Burke, R.J. Walters, G.P. Summers and T. Jordan, "Proton Nonionizing Energy Loss (NIEL) for Device Applications", **IEEE Trans. Nucl. Sci.**, Vol. **50**, 1924, 2003.

[Ju04] I. Jun, M.A. Xapsos and E.A. Burke, "Alpha Particle Nonionizing Energy Loss (NIEL)", **IEEE Trans. Nucl. Sci**., Vol. **51**, 3207, 2004.

[Ki55] G.H. Kinchin, R.S. Pease, "The Displacement of Atoms in Solids by Radiation", **Reports on Progress in. Physics**, Vol. **18**, pp. 1-51, 1955.

[Ko92] A. Konobeyev, "Neutron displacement cross-sections for structural materials below 800 MeV", **J. Nuclear Mater,** Vol. 186, pp. 117-130, 1992.

[Ma94] **Low Energy Ion-Surface Interaction**, Edited by J.W. Rabalais, chapter by D. Marton, pp 526, Wiley, Chester, 1994.

[Mat95] T. Mattila, R.M. Nieminen, "Direct Antisite Formation in Electron Irradiated GaAs," **Phys. Rev.Lett**., Vol. **74**, pp. 2721, 1995.

[Mc84] R. MacFarlane, “Radiation Damage Calculations with NJOY”, **Journal of Nuclear Materials**, Vol. **122&123**, pp. 1041-1046, 1984.

[MCNP] ***MCNP--A General Monte Carlo Code for Neutron and Photon Transport, Version 3A***, J. Briesmeister (Editor), report LA-7396-M, Los Alamos National Laboratory, Los Alamos, NM, September 1986.

[MCNP13a] Lawrence J. Cox, Scott D. Mathews, MCNP6™ Releaase 1.0: Creating and Testing the Code Distribution, Los Alamos National Laboratory, Los Alamos, New Mexico, report LA-UR-13-24008, May 31, 2013.

[MCNP13b] J.T. Goorley, et al. Initial MCNP6 Release Overview – MCNP6 version 1.0, Los Alamos National Laboratory, Los Alamos, report LA-UR-13-22934, April 24, 2013.

[MCNPX] **MCNPX User’s Manual: Version 2.4.0**, Los Alamos National Laboratory, Sept. 2002.

[Me01] S.R. Messenger, R.J. Walters, E.A. Burke, G.P. Summers and M.A. Xapsos, "NIEL and Damage Correlations for High-Energy Protons in Gallium Arsenide Devices", **IEEE Trans. Nucl. Sci.**, Vol. **48**, 2121, 2001.

[Me03] S.R. Messenger, E.A. Burke, M.A. Xapsos, G.P. Summers, R.J. Walters, I. Jun and T. Jordan, "NIEL for Heavy Ions: An Analytical Approach", **IEEE Trans. Nucl. Sci.,** Vol. **50**, 1919, 2003.

[Me65] G.C. Messenger, “Displacement Damage in Silicon and Germanium Transistors,” **IEEE Transactions in Nuclear Science**, Vol. **12**, Issue 2, pp. 53-74, 1965.

[Me66] G.C. Messenger, “Radiation Effects in Microcircuits,” **IEEE Transactions in Nuclear Science**, Vol. **13,** Issue 6, pp. 141-159, December 1966.

[Me77] K.L. Merkle, W.E. King, “Experimental Determination of the Energy Dependence of Defect Production,” **Journal of Nuclear Materials**, Vol. **117**, pp. 4-11, 1977.

[Me86] G.C. Messenger, M.A. Ash, **The Effects of Radiation on Electronic Systems**, Van Nostrand Reinhold Company, 1986.

[Mi94] L.A. Miller, D.K. Brice, K. Prinja, S.T. Picraux, “Displacement-threshold Energies in Si Calculated by Molecular Dynamics,” **Physics Review B**, Vol. **49**, pp. 16953-16964, June 1994.

[Mo12] F. Mota, C.J. Ortiz, R. Vila, “Primary Displacement Damage Calculation Induced by Neutron and Ion Using Binary Collision Approximation Techniques (MARLOWE code)”, presentation to the First Technical Meeting on Primary Radiation Damage, IAEA Vienna, October 1-4,2012.

[Mo65] N.F. Mott, S.S.W. Massey, **The Theory of Atomic Collisions**, 3rd Edition, Oxford University Press, 1965.

[Mu11] J. Mulroue, D.M. Duffy, "**An ab initio Study of the Effect of Charge Localization on Oxygen Defect Formation and Migration Energies in Magnesium Oxide**," Proc. R. Soc. London, Vol. **A 467**, pp. 2054-2056, 2011.

[Na72] A.L. Nameson, E.A. Wolicki, G.C. Messenger, "Average Silicon Neutron Displacement Kerma Factor at 1 MeV", **IEEE Transactions on Nuclear Science**, **NS-29**, No. 1, pp. 1018-1020, 1972.

[NJ2012] **The NJOY Nuclear Data Processing System, Version 2012**, R.E. MacFarlane, D.W. Muir, R.M. Boicourt, A.C. Kahler, Los Alamos National Laboratory, Los Alamos, NM, LANL report LA-UR-12-27079, December 20, 2012.

[No75] M.J. Norgett. M.T. Robinson, I.M. Torrens, "A Proposed Method of Calculating Displacement Dose Rates," **Nuclear Engineering and Design**, Vol. **33**, pp. 50-54, 1975.

[No97] K. Nordlund, N. Runeberg, D. Sundholm, "Repulsive Interatomic Potentials Calculated Using Hartree-Fock and Density-Functional Theory Methods," **Nuclear Instruments and Methods in Physics Research B**, Vol. 132, pp. 45 – 54, 1997.

[Nor02] J. Nord, K. Nordlund, J. Keinonen, K. Albe, "Molecular Dynamics Study of Defect Formation in GaN Cascades," **Nucl. Instr. Meth. Phys. Res. B**, Vol. **202**, pp. 93 – 99, 2003.

[Nor98a] K. Norlund, M. Ghaly, R.S. Averback, "Mechanisms of Ion Beam Mixing in Metals and Semiconductors," **J. Appl. Physics**, Vol. **83**, pp. 1238-1246, 1998.

[Nor98b] K. Nordlund, L. Wei, Y, Zong, R.S. Averback, "Role of Electron-phonon Coupling on Collision Cascade Development in Ni, Pd, and Pt," **Phys. Rev**. Vol. **B** (Rapid Communications), Vol. **57**, pp. 13965-13968, 1998.

[Od76] G.R. Odette, D.R. Doran, "Neutron-Energy-Dependent Defect Production Cross Sections for Fission and Fusion Applications, **Nuclear Technology**, Vol. **29**, pp. 356-368, June 1976.

[OECD14] **Primary radiation damage in materials – Review of Current Understanding and Proposed New Standard Displacement Damage Model to Incorporate In-Cascade Defect Production Efficiency and Mixing Effects**, draft of pending report prepared by IECD NEA Primary damage group, 2014.

[Oen67] O.S. Oen, "Displacement Cross Sections for Fast Electrons," **Radiation Effects in Semiconductors**, pp. 264-279, 1967.

[Oen73] **Cross Sections for Atomic Displacements**, O. S. Oen, Oak Ridge National laboratory, Oak Ridge, TN, report ORNL-4897, August 1973.

[Pou80] F. Poulin, J.C. Bourgoin, **Revue de Physique Applique**, Vol. **15**, pp. 15, 1980.

[Re93] I. Remec, F. B. Kam, **Neutron Spectra at Different High Flux Isotope Reactor (HFIR) Pressure Vessel Surveillance Locations**, Oak Ridge National Laboratory, report ORNL/TM-12484, NUREG/CR-6117, December 1993.

[Ro68] M. Robinson, **Phil. Mag.**, Vol. **12**, pp. 741, 1965; Vol. **17**, pp. 639, 1968.

[Ro71] M.T. Robinson, The dependence of neutron irradiation damage in solids, R.N.E.S. nuclear fusion reactor conference at Culham Laboratory, September,1969, **Nuclear Fusion Reactors**, pages 364-378, British Nuclear Energy Society, London,1970.

[Ro74] M.T. Robinson, O.M. Torrens, "Computer Simulation of Atomic-Displacement Cascades in Solids in the Binary-Collision Approximation," **Physical Review B**, Vol. **9**, pp. 5008-5024, June 1974.

[Ro75] M. Robinson, "The Theory of Radiation Induced Defect Production," in **Radiation Damage in Metals**, papers presented at a Seminar of the American Society for Metals November 9 and 10 1975, edited by N. L. Peterson and S. D. Hardness, pp 1-27, 1975.

[Ro77] M. Robinson, "The Energy Dependence of Neutron Radiation Damage in Solids," paper 4.3 in the **B.N.E.S. Nuclear Fusion Reactor Conference** at Culham Laboratory, September 1969.

[Ro82] M.T. Robinson, O.S. Oen, **J. Nucl. Mater.** Vol. **10**, pp. 147, 1982.

[Ro83] M. T. Robinson, "Computer simulation of collision cascades in monazite," **Physical Review B**, Vol. **27**, Number 9, pp. 5347-5359, May 1983.

[Ro92] M.T. Robinson, "Computer Simulation Studies of High-Energy Collision Cascades," **Nuclear Instrumentation and Methods in Physics Research** B67, pp. 396-400, 1992.

[Ro94] M.T. Robinson, "Basic Physics of Radiation Damage Production," **Journal of Nuclear Materials**, Vol. **216**, pp. 1 – 28, 1994.

[Ro96] M.T. Robinson, "Binding Energy Effects in Cascade Evolution and Sputtering," **Nuclear Instrumentation and Methods in Physics Research B 115**, pp. 549-553, 1996.

[Ru11] E. Rutherford, "The Scattering of α and β Particles by Latter and the Structure of the Atom," **Philosophical Magazine**, Series 6, Vol. **21**, May 1911.

[Si69] O. Sigmund, "A Note on Integral Equations of the Kinchin-Pease Type," **Radiation Effects**, Vol. **1**, p. 15-18, 1969.

[Smit] F.M. Smits, H.J. Stein, "Energy Dependence of Neutron-Damaged in Silicon Experiments", **Bulletin of APS**, Series 2, Volume **9**, no. 3, pp. 289, March meeting.

[To12] M. Toulemonde, W.J. Weber, G. Li, V. Shuttanandan, P. Kluth, T. Yang, Y, Wang, Y.W. Zhang, "**Synergy of Nuclear and Electronic Energy Losses in Ion-Irradiation Processes: The case of Vitreous Silicon Oxide**," Physical Review, Vol. **B83**, 2011.

[Tu11] **Nuclear Wallet Cards**, J. Tuli, National Nuclear Data Center, Brookhaven National laboratory, Upton, NY, October 2011. (see URL:www.nndc.bnl.gov)

[Vasil] A. Vasilescu (INPE Bucharest), G. Lindstroem (University of Hamurg), Displacement damage in silicon online compilation. http://rd50.web.cern.ch/rd50/NIEL/default.html, updated 15-Aug-11.

[Vit77] N.A. Vitovski, D. Mustafakulov, A.P. Chekmareva, Threshold Energy for the Displacement of Atoms in Semiconductors, **Sov. Phy. Semicond**., Vol. **11**, pp. 1024-1-28, 1977.

[Wen03] E. Wendler, W. Wesch, E. Alves, A.Kamarou, Comparative Study of Radiation Damage in GaN and InGaN by 400 keV Au Implantation, **Nucl. Instru. Meth. Phys. Res. B**, 2003.

[Xap] M.A. Xapsos, E.A. Burke, I. Jun, S.R. Messenger, G. Gee, B. Fodness, J.F. Ziegler, R.. Walters, G.P. Summers, T. Jordan, Space Environment effects: Nonionizing Energy Loss Tool for Space Applications, private communication.

[Xa04] M.A. Xapsos, E.A. Burke, F.F. Badavi, L.W. Townsend, J.W. Wilson and I. Jun, "NIEL Calculations for High-Energy Heavy Ions", **IEEE Trans. Nucl. Sci.,** Vol. **51**, 3251, 2004.

[ZBL85] **The Stopping and Range of Ions in Solids**, J.F. Ziegler, J.P. Biersack and U. Littmark, Pergamon Press, Inc., New York, 1985.

[Zi10] J.F. Ziegler, M.D. Ziegler, J.P Biersack, SRIM – The stopping and range of ions in matter (2010), **Nuclear Instruments and Methods in Physics Research Section B: Beam interactions with materials and Atoms**, Vol. **268**, Issue 11-12, pp. 1818-1823, June 2010.

[Zi99] J.F. Ziegler, The Stopping of Energetic Light Ions in Elemental Matter, J**. Appl. Phys. / Rev. Appl. Phys**. Vol. **85**, pp. 1249-1272, 1999.

[Zin97] S.J. Zinkle, C. Kinoshita, "**Defect Production in Ceramics**," J. Nucl. Mater. Vol. **251**, pp. 200-217, 1997.

[Zin97a] S.J. Zinkle, “Irradiation Spectrum and Ionization-Induced Diffusion Effects in Ceramics,” in I.M. Robertson et al. (Eds.) **Microstructure Evolution During Irradiation**, Materials Research Society, Pittsburgh, pp. 667-678, 1997.

DISTRIBUTION

1 Steve McCready (electronic copy)
Los Alamos National Laboratory
P. O. Box 1663
MS T080
Los Alamos, NM 87545

1 Mary Helen Sparks (electronic copy)
White Sands Missile Range
TEDT-WST-SV-NR
Bldg. 21225
Reactor Physics Branch
Lax Cruces, NM 88002-5158

1 Craig Heimbach (electronic copy)
US Dept. of Commerce – NIST
1 Melmark Ct
Gaithersburg, MD 20878

1 Doug Selby (electronic copy)
Oak Ridge National Laboratory
708 Andover Blvd.
Knoxville, TN 37934

1 John Williams (electronic copy)
University of Arizona
2821 East Helen St.
Tucson, AZ 85716

1	MS0417	David M. Fordham	00243 (electronic copy)
1	MS1146	K. Russell DePriest	01384 (electronic copy)
1	MS1146	Donald King	01384 (electronic copy)
1	MS1146	Edward Parma	01384 (electronic copy)
1	MS1146	Brian Hehr	01384 (electronic copy)
1	MS1146	Patrick J. Griffin	01340 (electronic copy)
1	MS9018	Central Technical Files	08944 (electronic copy)
1	MS0899	Technical Library	09536 (electronic copy)


Sandia National Laboratories